UNIVERSITÀ
DEGLI STUDI DI TRIESTE

dipartimento
di ingegneria
e architettura

A.A. 2020-21

Corso «Materiali Naturali e Biomimetici»

- Biomimetic Materials -

Vanni Lughi

DIA – Department of Engineering and Architecture, University of Trieste

vlughi@units.it

“In materials processing, Nature replaces the massive use of energy (for example high temperatures or harsh chemical reactions) with the **use of information** (which equates with structure at all levels, molecule to ecosystem).

Indeed, most of the exceptional functionality of biological materials is due to their **complex structure**, driven by their chemical composition and morphology derived from DNA. It is here that the most important aspect of biomimetics emerges, and **it has the power to redesign engineering**.”

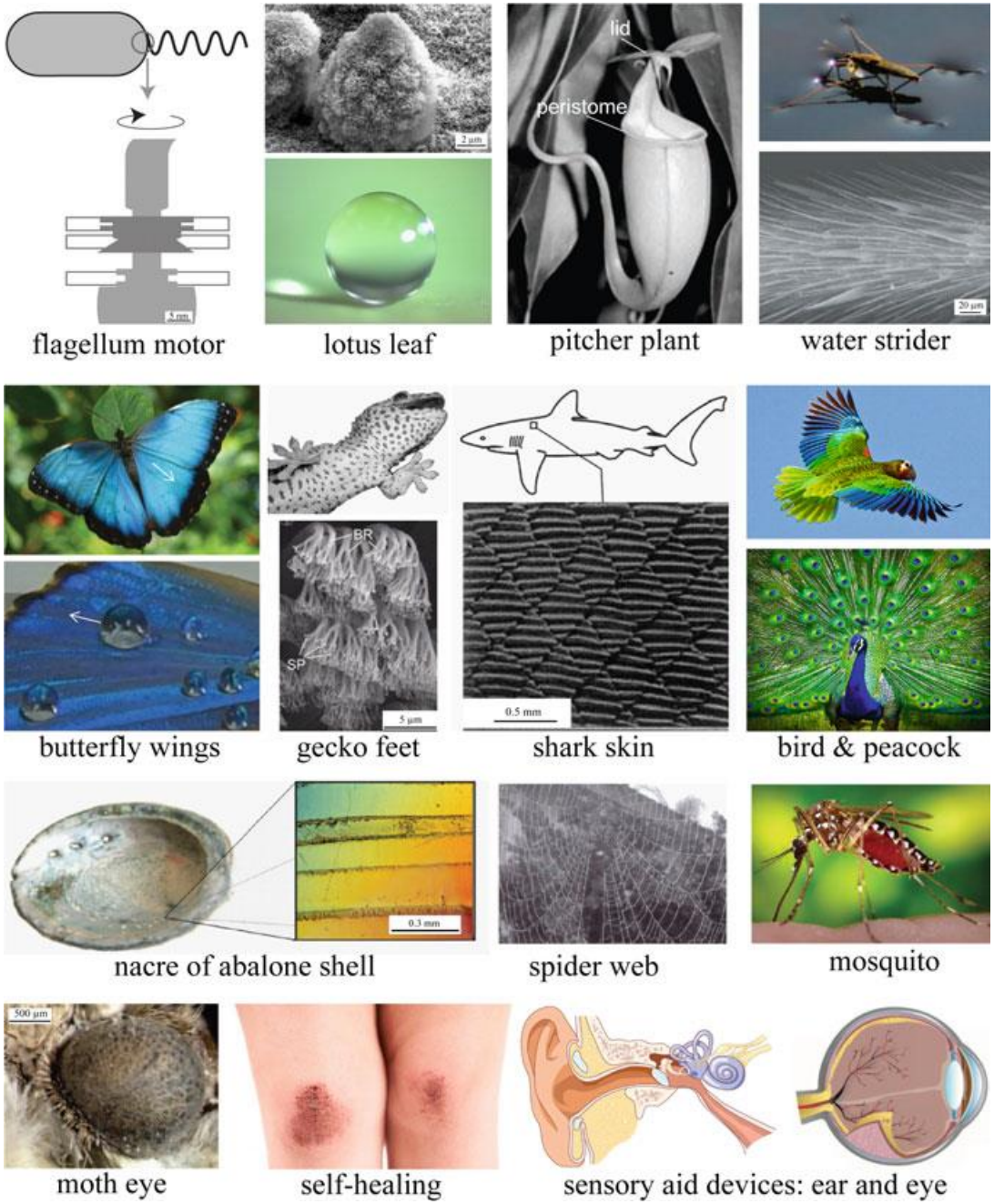
flagellum motor
lotus leaf
lid
peristome
pitcher plant
water strider
butterfly wings
BR
SP
gecko feet
0.5 mm
shark skin
bird & peacock
0.3 mm
nacre of abalone shell
spider web
mosquito
500 μm
moth eye
self-healing
sensory aid devices: ear and eye

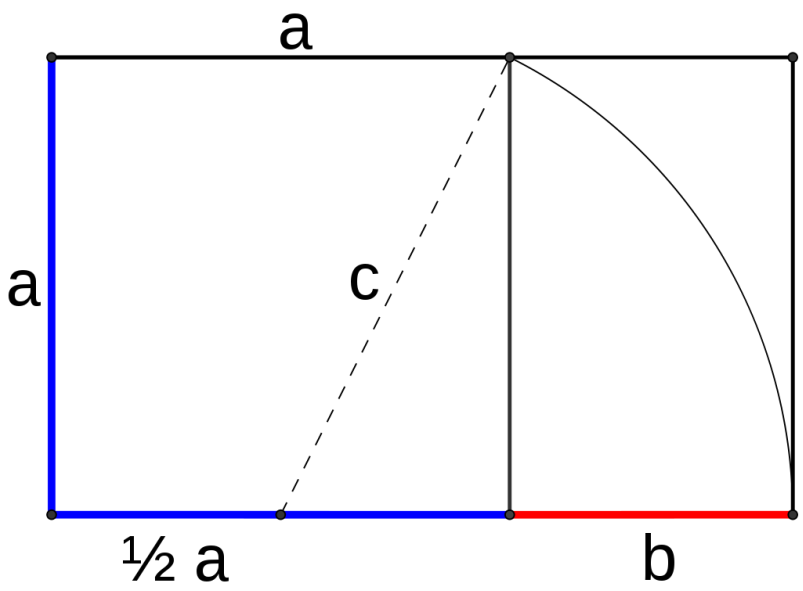
a
a
c
½ a
b

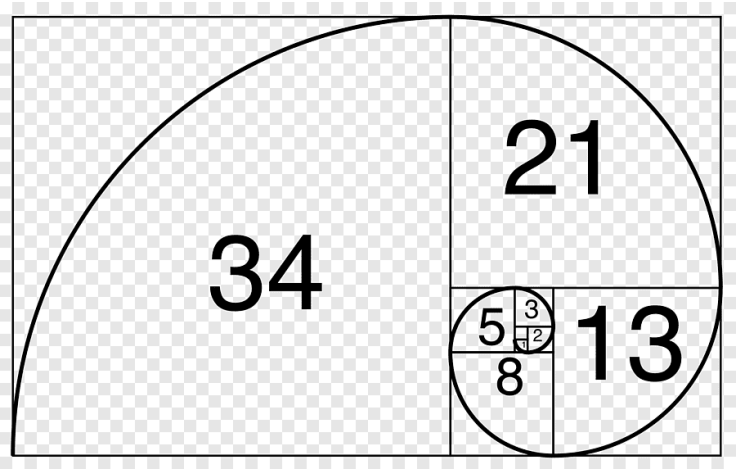
34
21
13
5
3
2
1
8

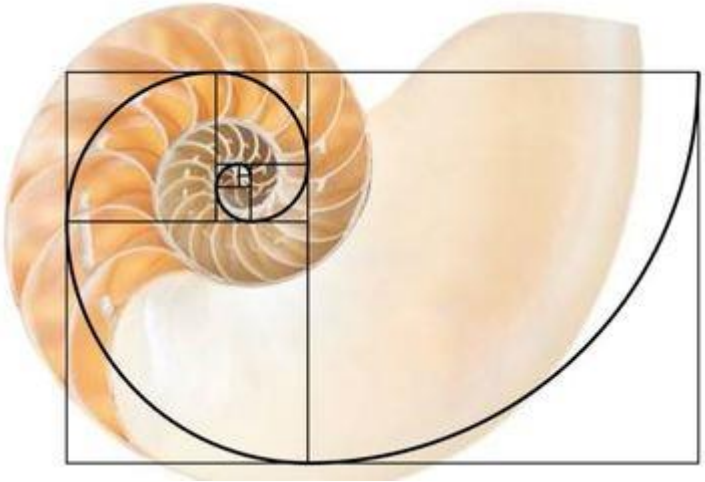

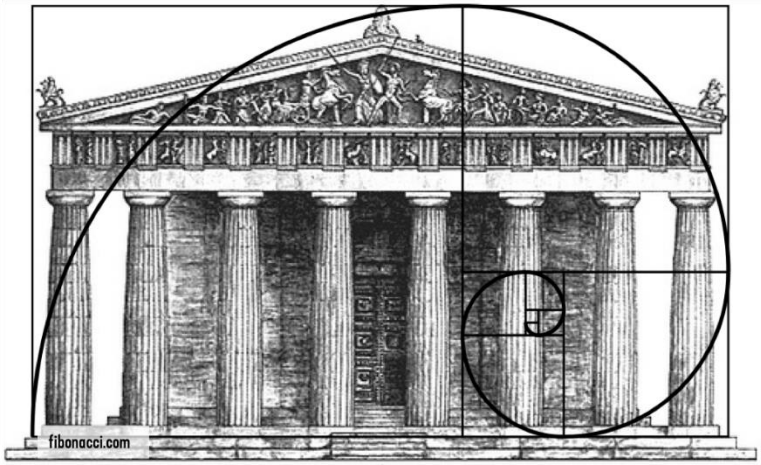
fibonacci.com

Examples of Bioinspiration in Art

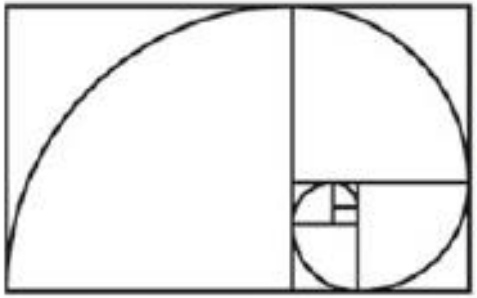

Golden Spiral

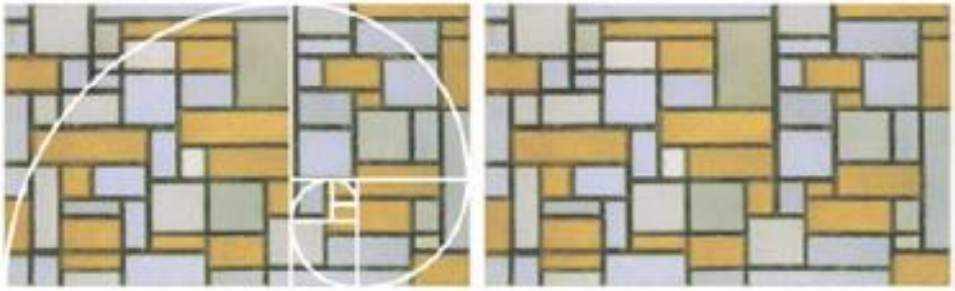

Composition in Gray and Light Brown (Mondrian, 1918)

Interior of Bird Bone

Bone Chair and Bone Armchair (Learman, 2006 & 2008)

Examples of Bioinspiration in Architecture: Plants, Animals, and Replication

Evergreen Forest

Sagrada Familia, Barcelona, Spain (Gaudi, 1882)

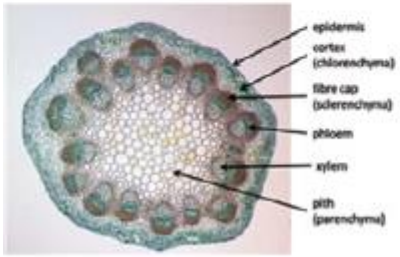

Cross section of a dicot stem

Nakagin Tower, Tokyo (Kurokawa, 1972)

Bird wings unfolding

Solar sensitive wings, Milwaukee Art Museum, Wisconsin (Calatrava, 2001)

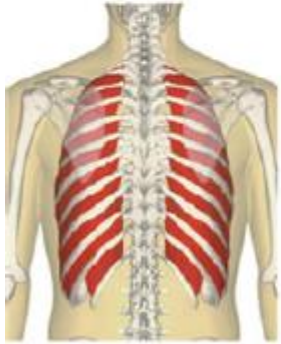

Ribs with intercostal muscles

Rib vaulting, Exeter Cathedral, Exeter UK (architect unknown, 1400)

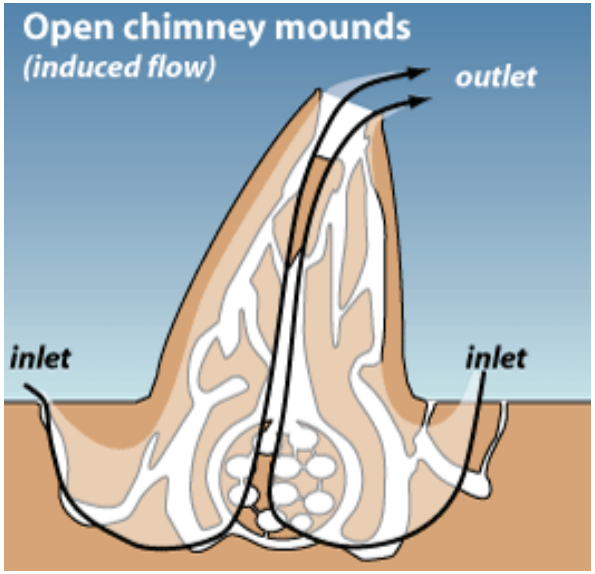
Open chimney mounds
(induced flow)
outlet
inlet
inlet

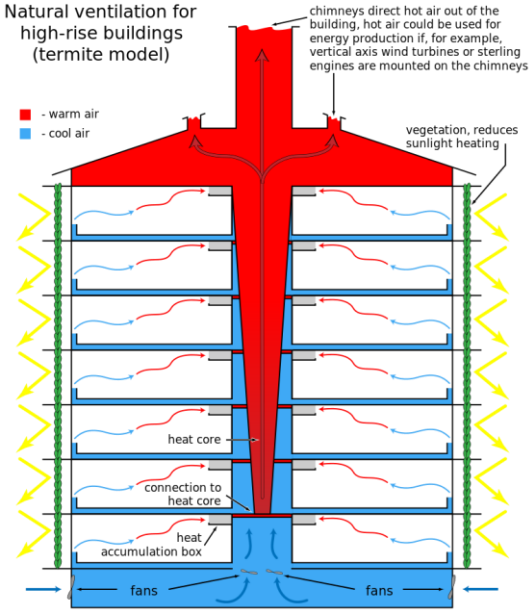
Natural ventilation for high-rise buildings (termite model)
chimneys direct hot air out of the building, hot air could be used for energy production if, for example, vertical axis wind turbines or sterling engines are mounted on the chimneys
- warm air
- cool air
vegetation, reduces sunlight heating
heat core
connection to heat core
heat accumulation box
fans
fans

Toothed gears on hind legs of insect *Issus coleoptratus*

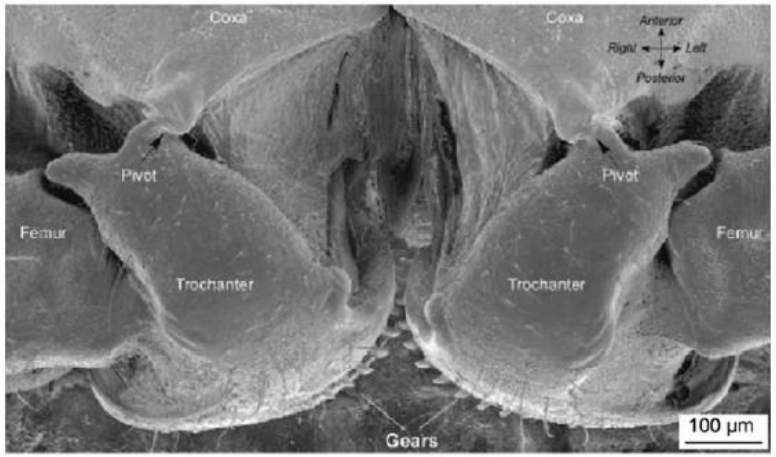

Magnified view of the gears

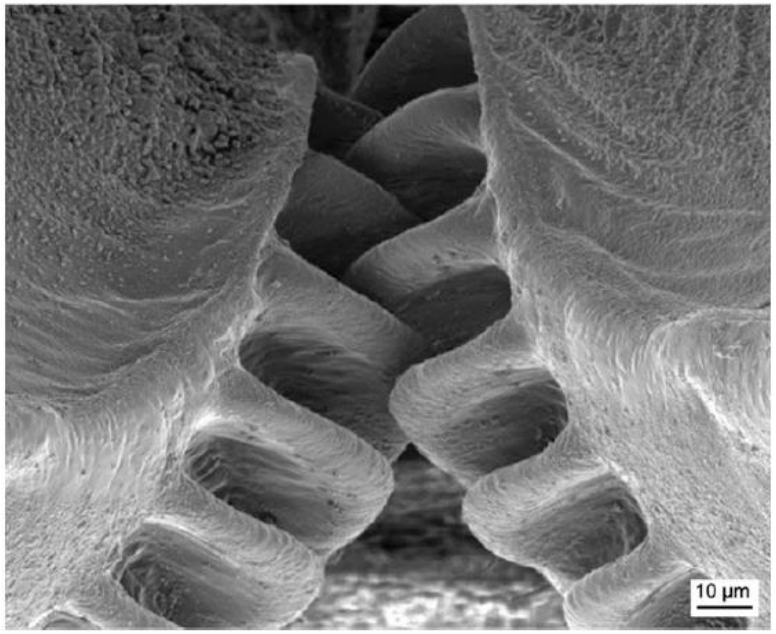

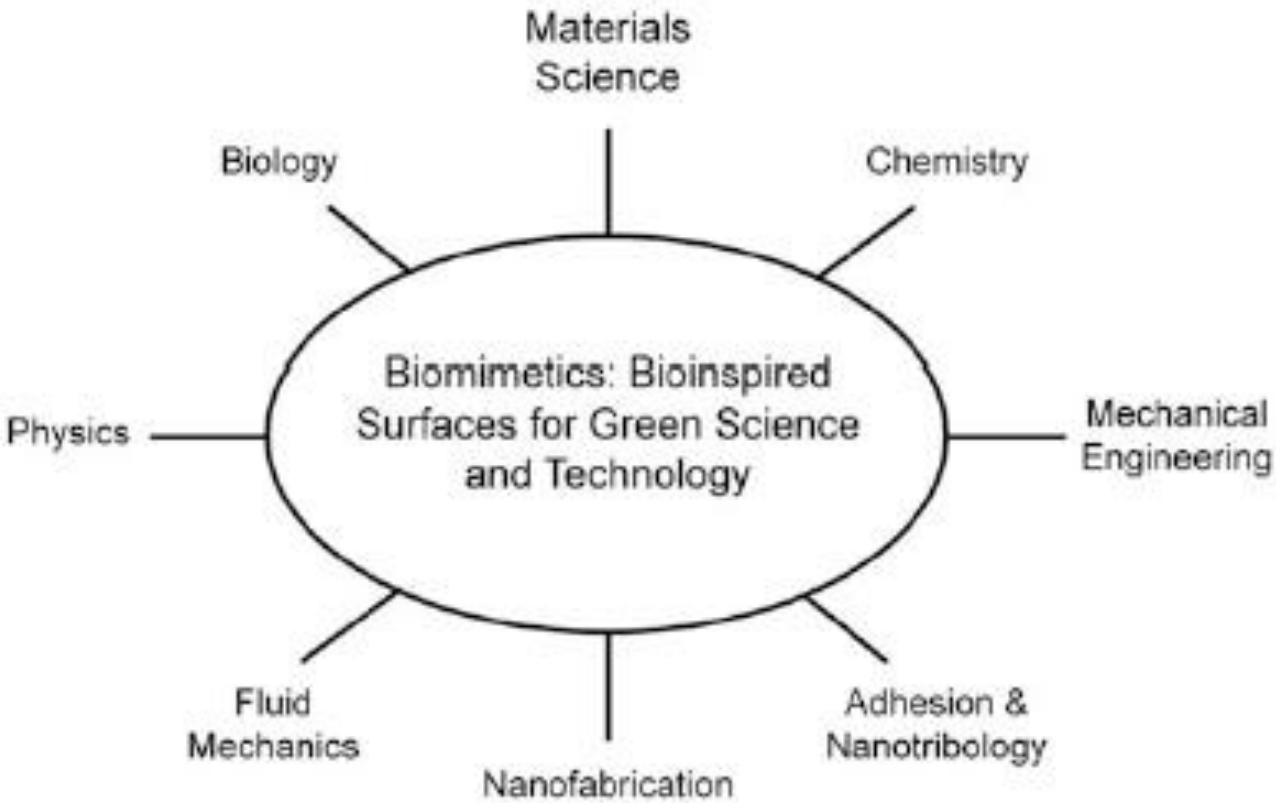
Materials Science
Biology
Chemistry
Biomimetics: Bioinspired Surfaces for Green Science and Technology
Physics
Mechanical Engineering
Fluid Mechanics
Nanofabrication
Adhesion & Nanotribology

Overview of Various Species and Objects from Living Nature and Their Selected Functions

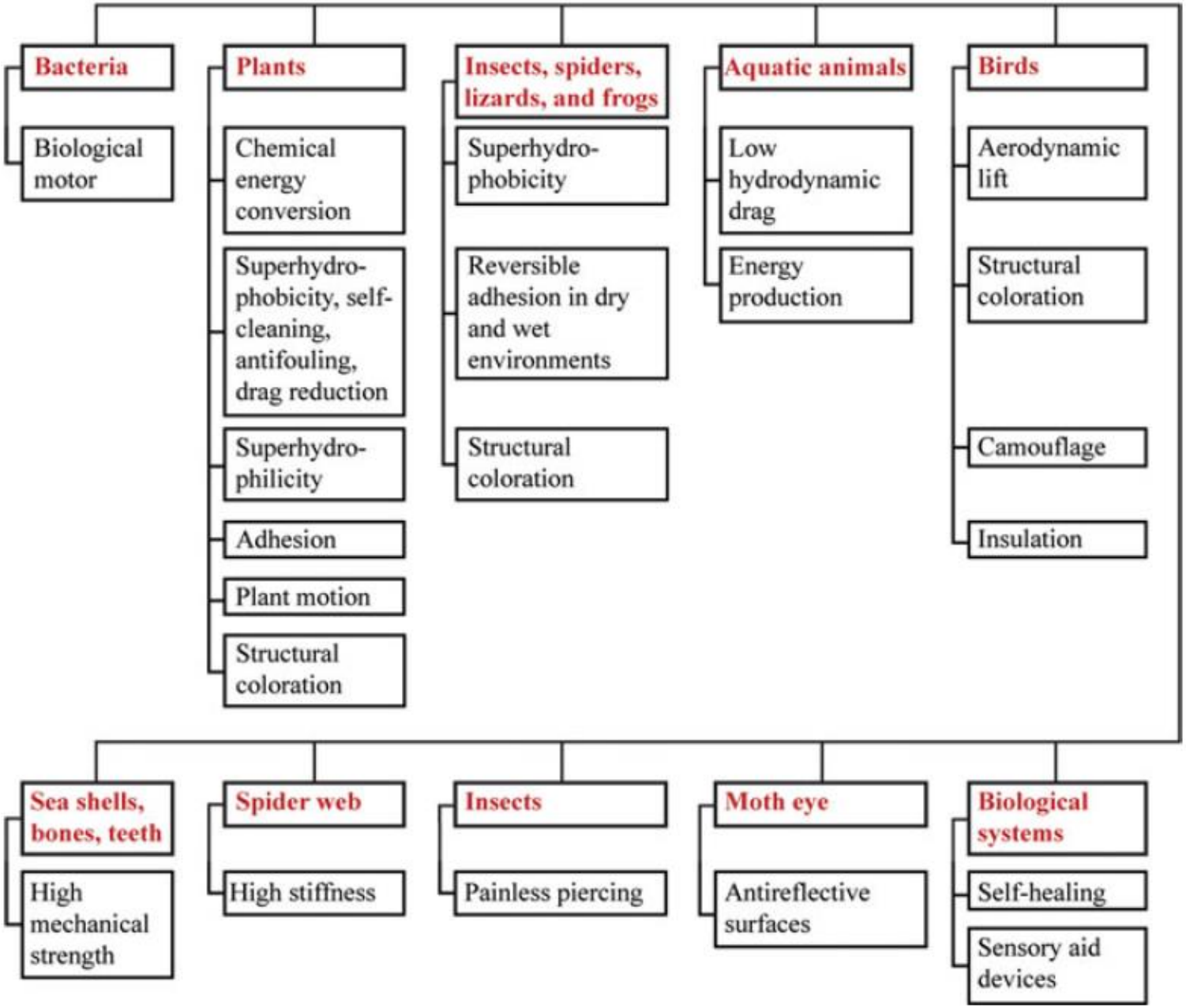

Biomimicry

Natural materials are efficient

Little material and energy are used for complex requirements:

- Mechanical: static and dynamic loads
- Thermal and electrical: insulation, transpiration, sensing, actuation
- Sustainable: recyclable, biodegradable

Mimicking these characteristics is a very promising strategy for engineering

Most natural materials are hybrids and composites

Key role of surfaces!

Building Blocks of Natural Materials

Proteins

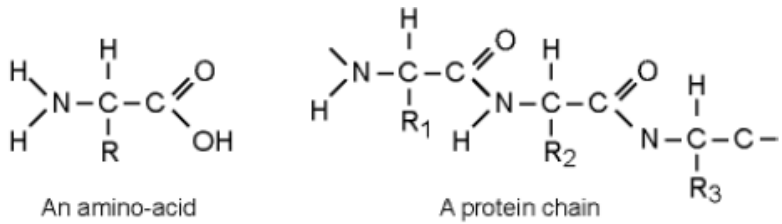

- Natural polymers (collagen, keratin)
- Natural elastomers (elastin, resilin, abductin)

Minerals

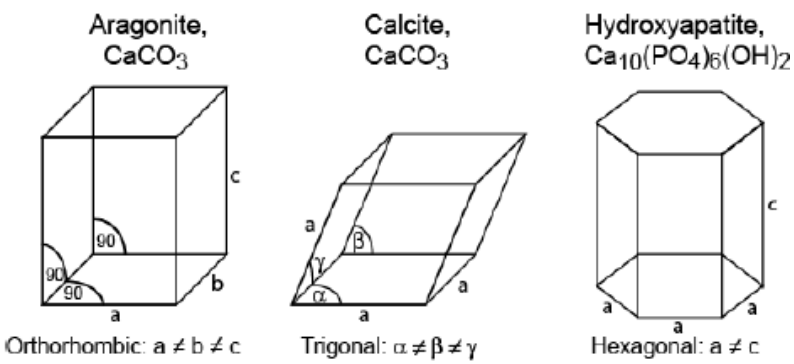

- Also: amorphous bio-silica, SiO_2

Polysaccharides

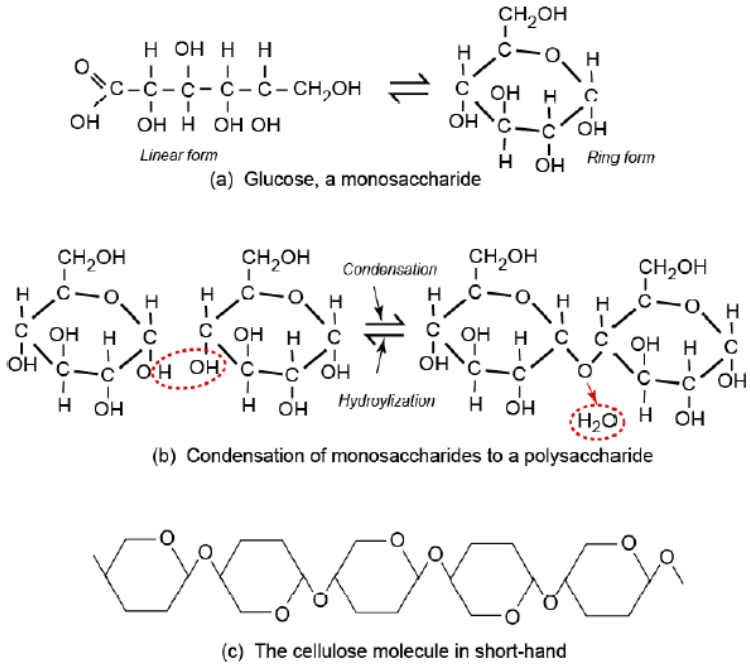

- Starch, glycogen (energy storage)
- Coellulose, lignin, chitin (structural)

Natural Materials

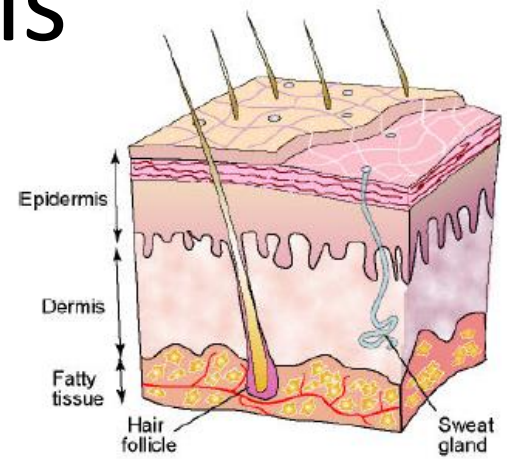

- Soft tissue
- Mineralized tissue
- Woods and wood-like materials
- Natural fibers
- Bio-materials

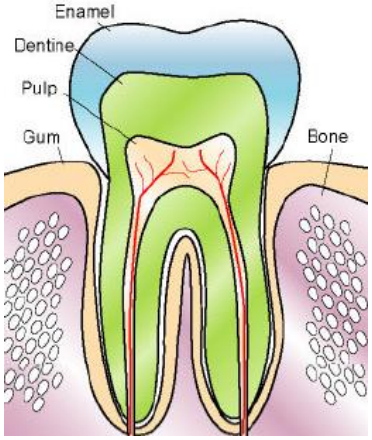

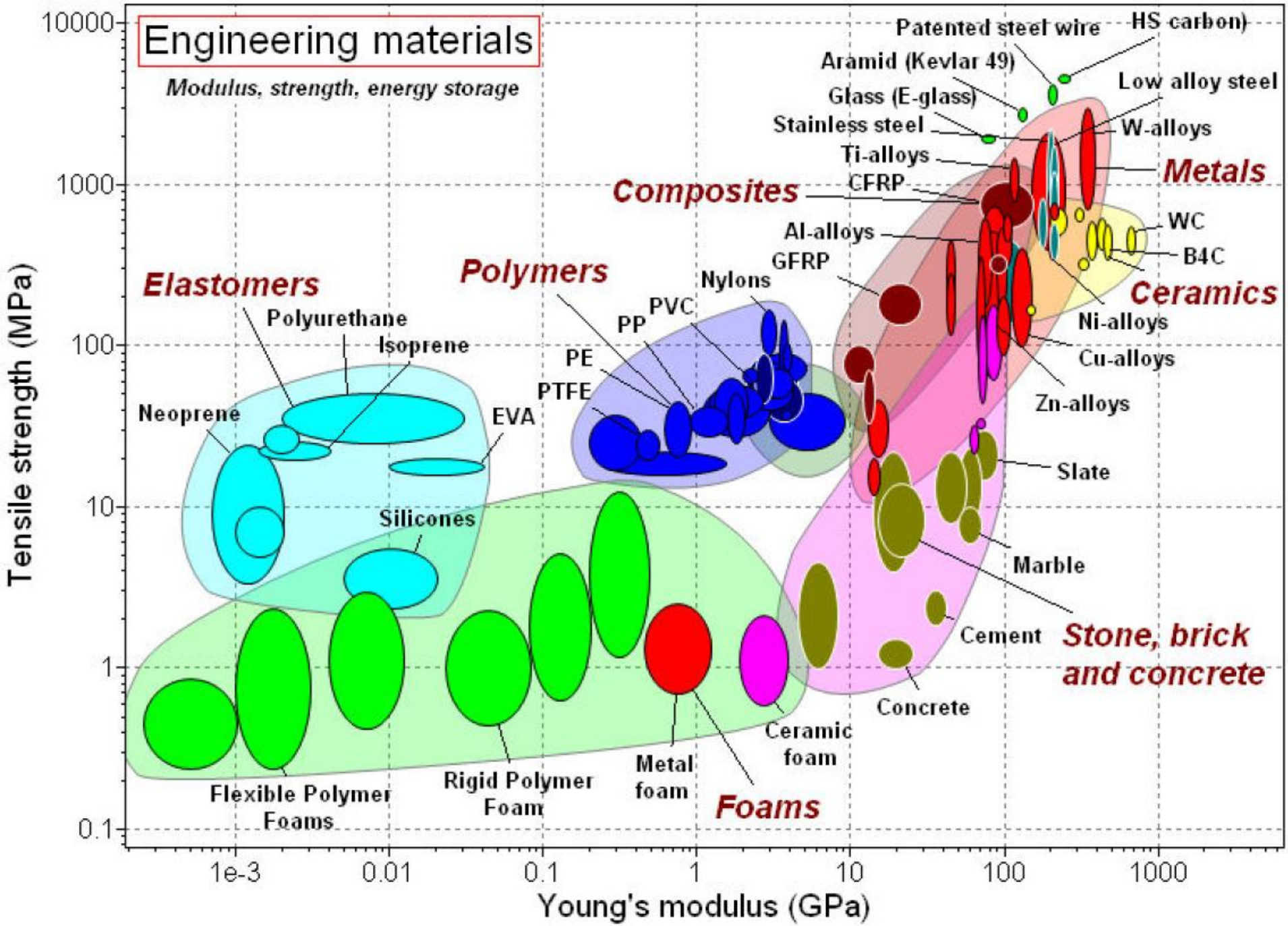
Engineering materials
Modulus, strength, energy storage
Tensile strength (MPa)
Young's modulus (GPa)
10000
1000
100
10
1
0.1
1e-3
0.01
0.1
1
10
100
1000
Patented steel wire
HS carbon)
Aramid (Kevlar 49)
Low alloy steel
Glass (E-glass)
Stainless steel
W-alloys
Ti-alloys
Metals
CFRP
Composites
WC
Al-alloys
B4C
GFRP
Nylons
Ceramics
Elastomers
Polymers
PVC
PP
Ni-alloys
Polyurethane
Isoprene
PE
Cu-alloys
PTFE
Zn-alloys
Neoprene
EVA
Slate
Silicones
Marble
Cement
Stone, brick and concrete
Concrete
Ceramic foam
Metal foam
Rigid Polymer Foam
Flexible Polymer Foams
Foams

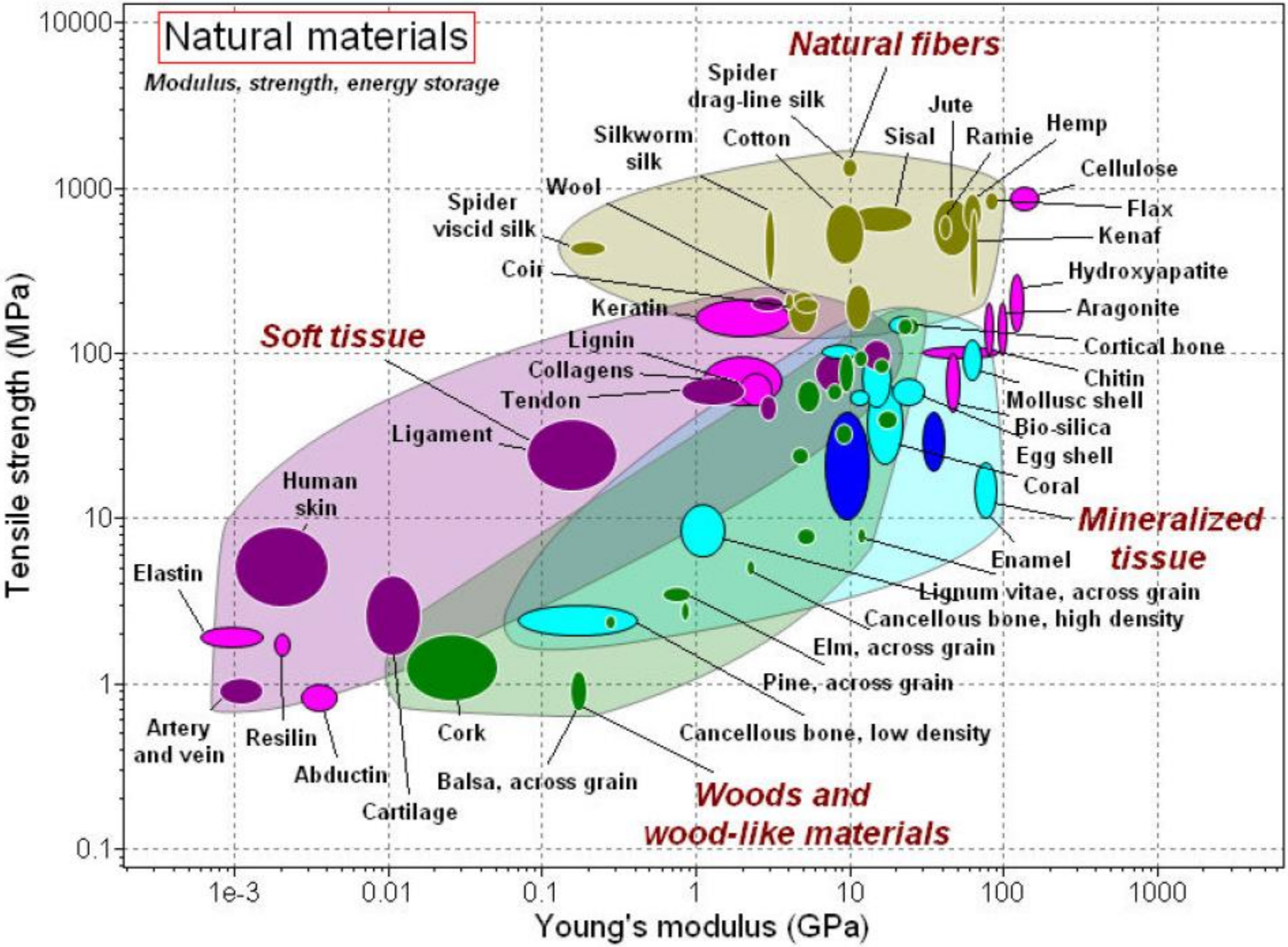
Natural materials
Modulus, strength, energy storage
Natural fibers
Spider drag-line silk
Jute
Hemp
Silkworm silk
Cotton
Sisal
Ramie
Cellulose
Wool
Flax
Spider viscid silk
Kenaf
Coir
Hydroxyapatite
Keratin
Aragonite
Soft tissue
Lignin
Cortical bone
Collagens
Chitin
Tendon
Mollusc shell
Ligament
Bio-silica
Egg shell
Human skin
Coral
Mineralized tissue
Elastin
Enamel
Lignum vitae, across grain
Cancellous bone, high density
Elm, across grain
Pine, across grain
Artery and vein
Resilin
Cork
Cancellous bone, low density
Abductin
Balsa, across grain
Cartilage
Woods and wood-like materials
Tensile strength (MPa)
Young's modulus (GPa)
10000
1000
100
10
1
0.1
1e-3
0.01
0.1
1
10
100
1000

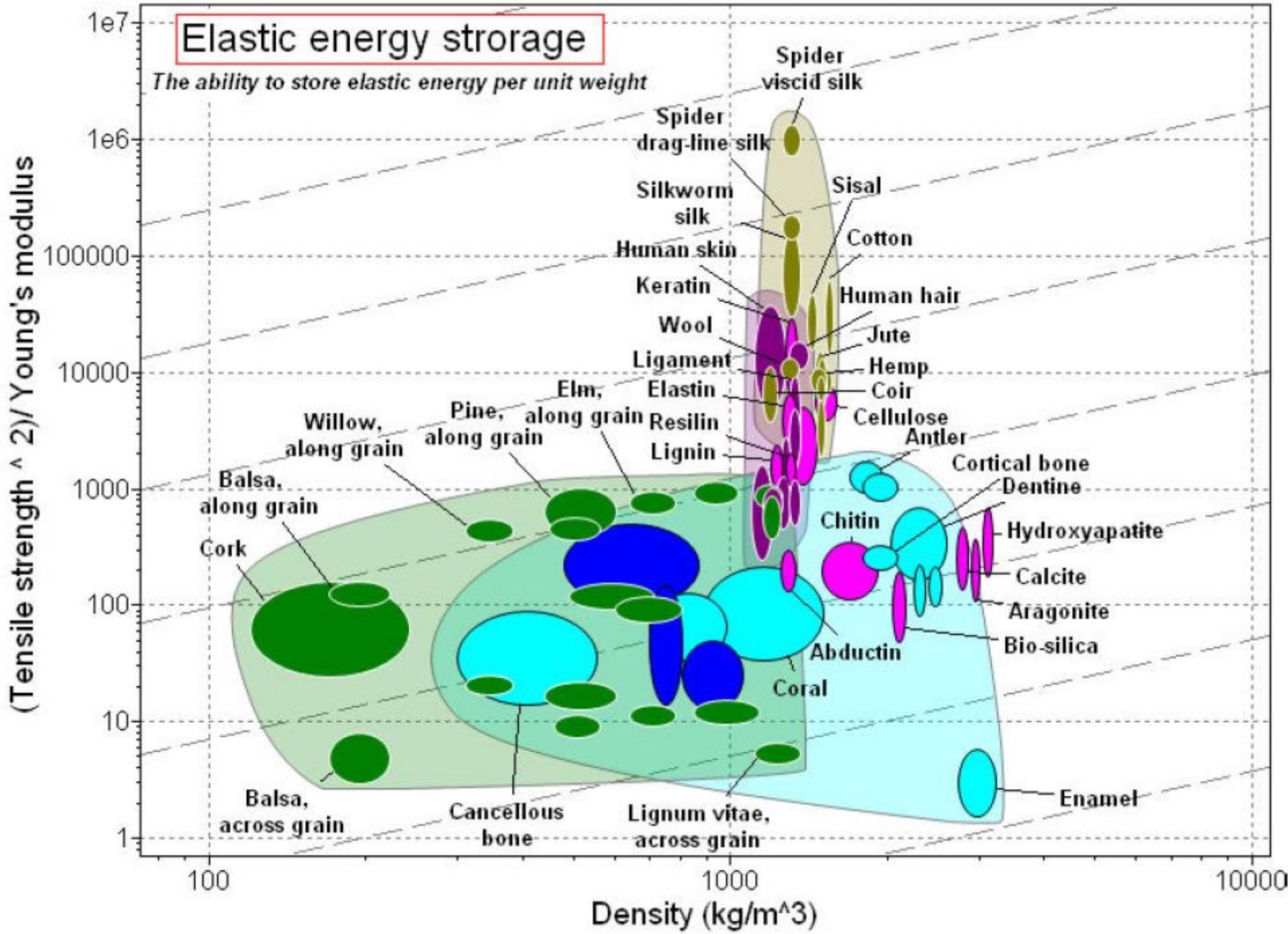
Elastic energy strorage
The ability to store elastic energy per unit weight
(Tensile strength ^ 2)/ Young's modulus
Density (kg/m^3)
1e7
1e6
100000
10000
1000
100
10
1
100
1000
10000
Spider viscid silk
Spider drag-line silk
Silkworm silk
Sisal
Cotton
Human skin
Keratin
Human hair
Wool
Jute
Ligament
Hemp
Elastin
Coir
Elm, along grain
Resilin
Cellulose
Pine, along grain
Willow, along grain
Lignin
Antler
Cortical bone
Balsa, along grain
Dentine
Chitin
Hydroxyapatite
Cork
Calcite
Aragonite
Bio-silica
Abductin
Coral
Balsa, across grain
Cancellous bone
Lignum vitae, across grain
Enamel

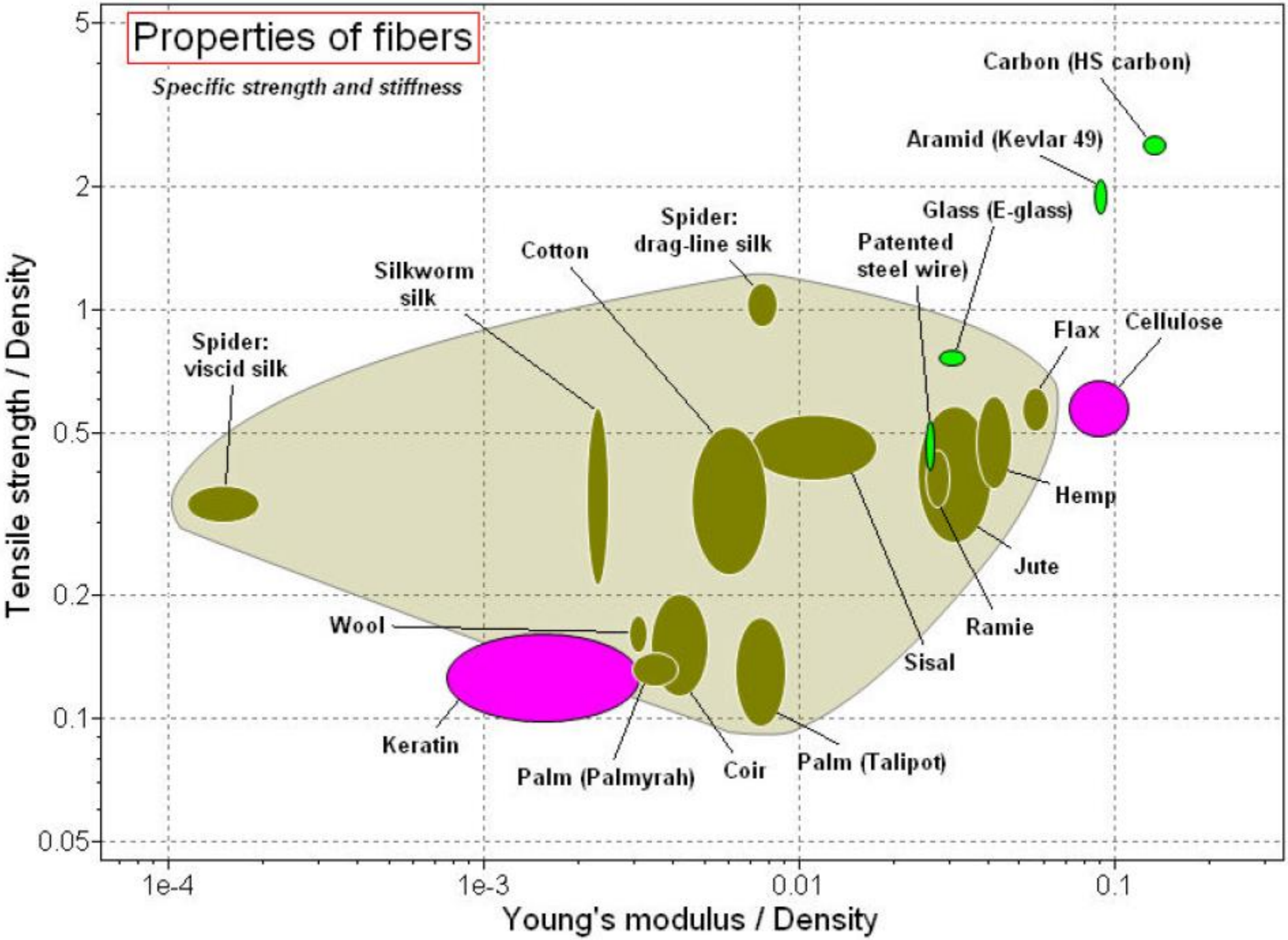
Properties of fibers
Specific strength and stiffness
Carbon (HS carbon)
Aramid (Kevlar 49)
Glass (E-glass)
Spider: drag-line silk
Cotton
Silkworm silk
Patented steel wire)
Spider: viscid silk
Flax
Cellulose
Hemp
Jute
Ramie
Sisal
Wool
Keratin
Palm (Palmyrah)
Coir
Palm (Talipot)
Tensile strength / Density
Young's modulus / Density
5
2
1
0.5
0.2
0.1
0.05
1e-4
1e-3
0.01
0.1

Applications

Objects	Typical materials	Desired properties
(a) *Biomedical applications*		
Biomedical devices, catheters, drainage tubing, micropumps, microvalves, electronic circuits	PDMS, Polystyrene, PMMA	Superoleophobic, self-cleaning, anti-biofouling
(b) *Automotive applications*		
Windshield, window glass, side/rear view mirrors, camera lens (back of car)	Glass	Superoleophobic, self-cleaning, anti-finger touch, antifouling, optically transparent/ antireflective
Display, headlights	PMMA for smart screens for capacitive touch material, Polycarbonate (head lights)	Superoleophobic, self-cleaning, anti-finger touch, antifouling, optically transparent/ antireflective
Dashboard, door liners, seats, carpet, leather	Polyurethane, nylon (dashboard), Polypropylene (door liner), Polyurethane (seats), Leather (natural, synthetic polycarbonate)	Superoleophobic, self-cleaning, anti-finger touch, antifouling
Car body	Painted Steel	Self-cleaning, anti-smudge, low drag
(c) *Smart screens for electronic display*		
Screens	Soda-lime glass, polyethylene terephthalate, polycarbonate	Superoleophobic, self-cleaning, anti-finger touch, antifouling, optically transparent
(d) *Plastic bottles and caps and plastic sheets*		
Bottles	High-density polyethylene, polyethylene terephthalate, polypropylene	Superoleophobic, superhydrophobic
Bottle caps	Polypropylene	Superoleophobic, superhydrophobic
Plastic packaging sheets	Polypropylene, acrylic	Superoleophobic, superhydrophobic, anti-fouling








(reversible) Super-Adhesion

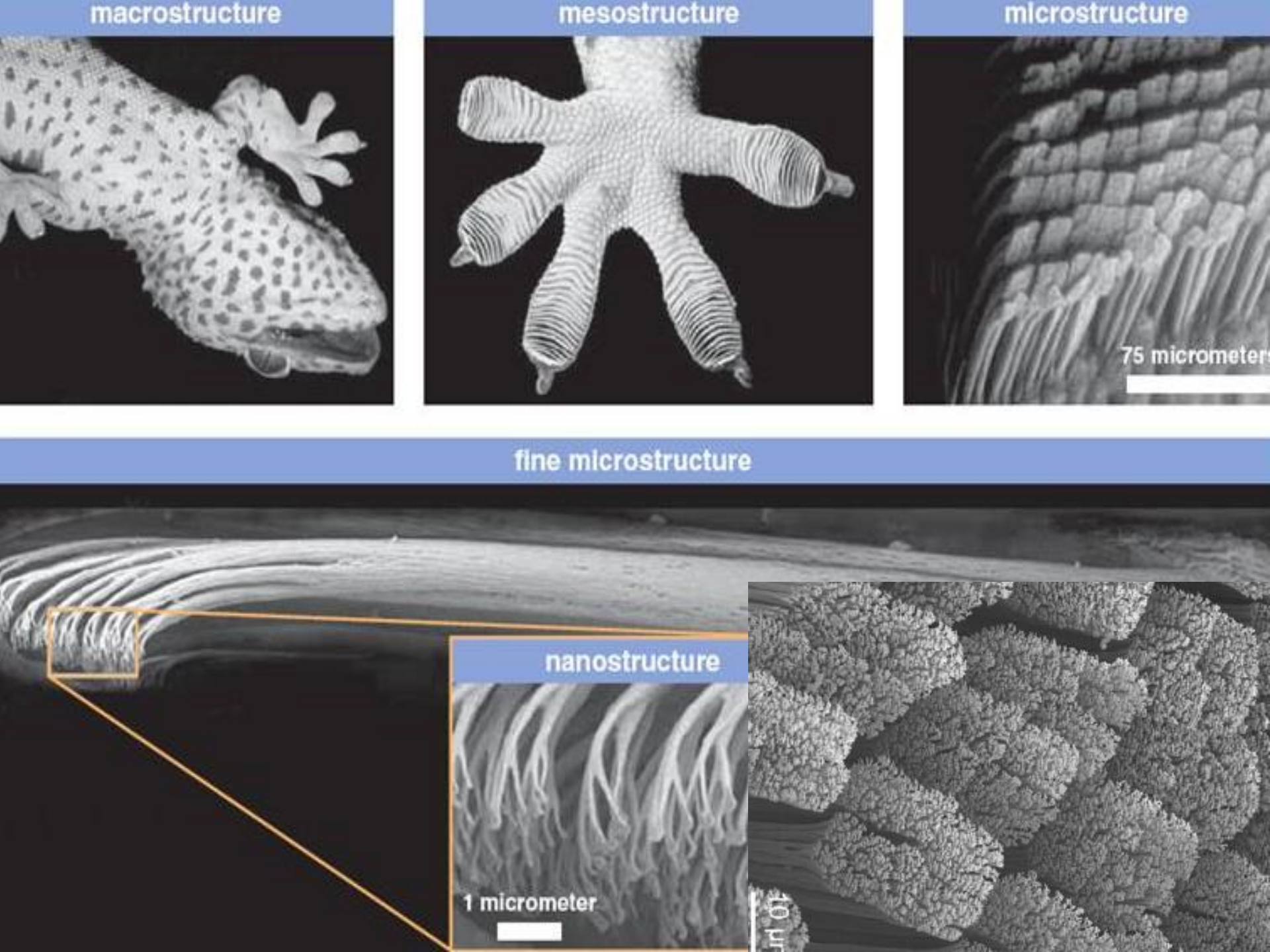
macrostructure
mesostructure
microstructure
75 micrometers
fine microstructure
nanostructure
1 micrometer

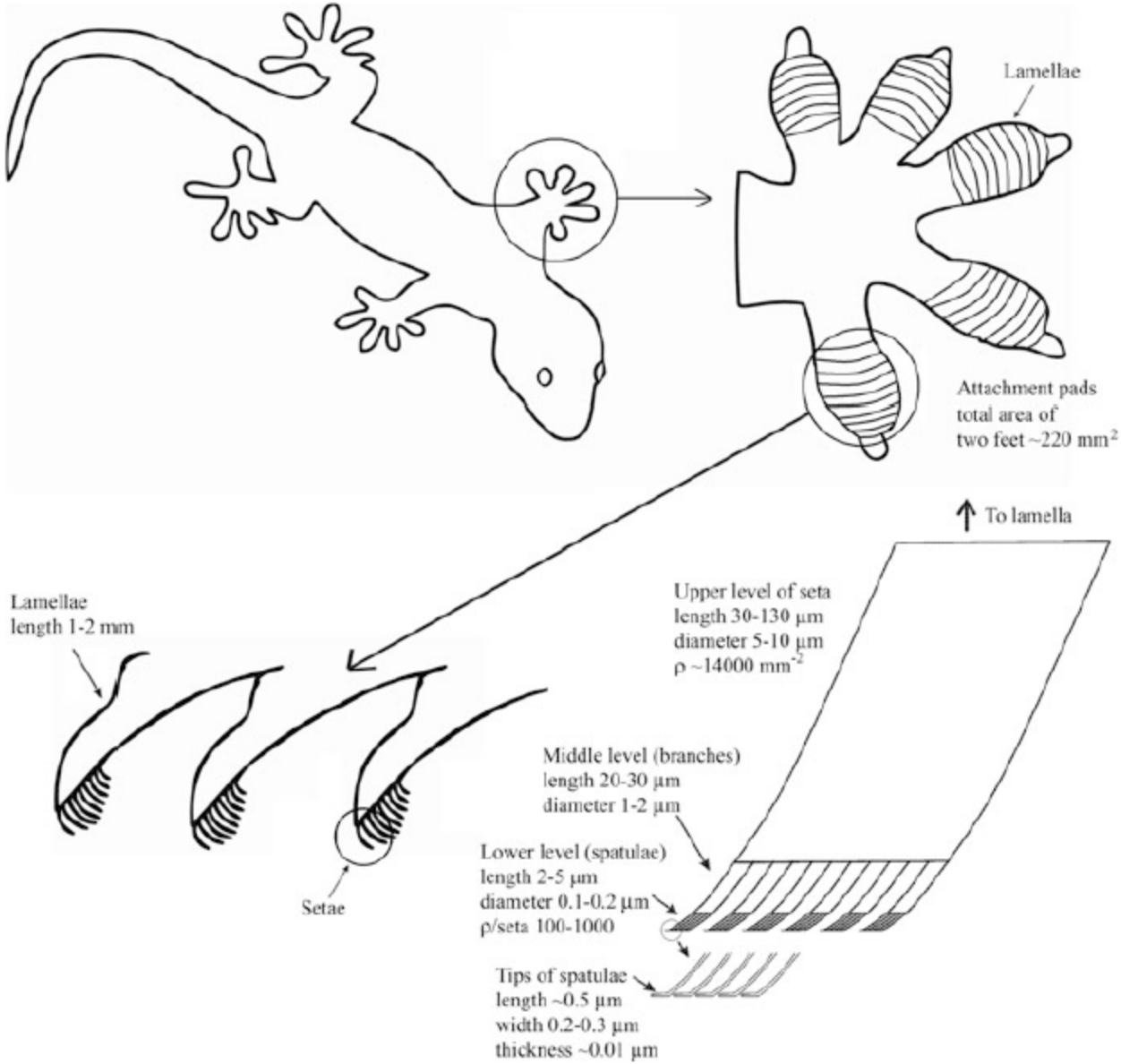
Lamellae
Attachment pads
total area of
two feet ~220 mm²
To lamella
Lamellae
length 1-2 mm
Upper level of seta
length 30-130 µm
diameter 5-10 µm
ρ ~14000 mm⁻²
Middle level (branches)
length 20-30 µm
diameter 1-2 µm
Lower level (spatulae)
length 2-5 µm
diameter 0.1-0.2 µm
ρ/seta 100-1000
Setae
Tips of spatulae
length ~0.5 µm
width 0.2-0.3 µm
thickness ~0.01 µm

Van der Waals forces

$$F_{VdW,sphere} \cong A\frac{R}{12r^2}$$

$A \cong 10^{-19} - 10^{-20}\ J$

Hamaker coefficient

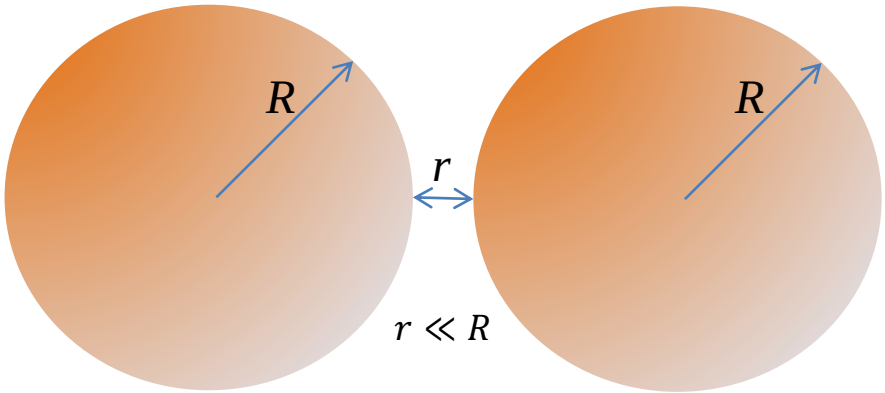

VdW forces between "large" (multimolecular and above) objects:

- Are very small
- Grow with the size of the object, *R*

But… $$\frac{F_{VdW,macro}}{F_{gravity}} \cong A\frac{R}{12r^2}\frac{1}{\frac{4}{3}\pi R^3\rho g} \cong \frac{A}{16\pi\rho r^2 g}\frac{1}{R^2}$$

VdW forces between "large" (multimolecular and above) objects:

- **Grow** with the size, R, but **slower than volume forces** (gravity, drag, lift…)
- Become **preponderant at the nanometric scale**

→ *Nanosystems tend to aggregate*

→ ***Nanostructures can inspire dry, reversible adhesives***

Contact Forces

Hertz

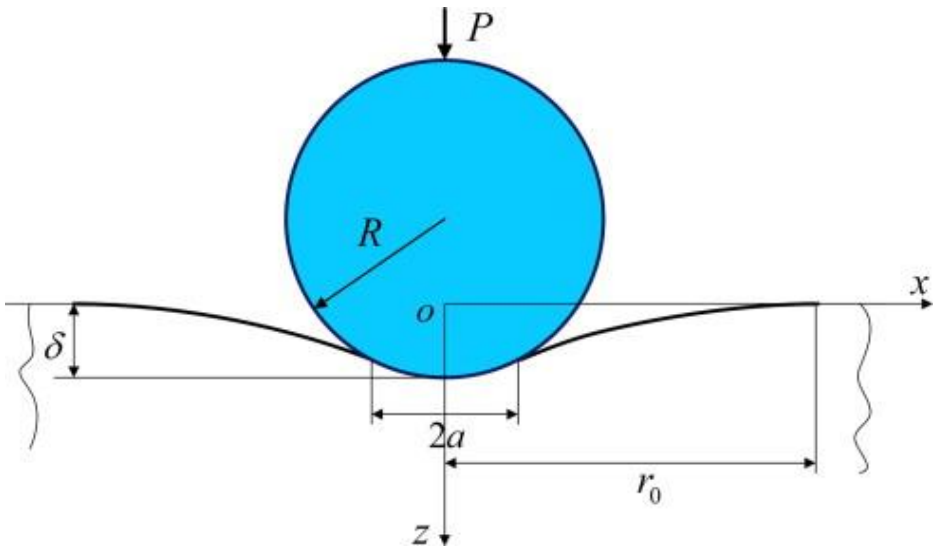

No adhesion

DMT
Deryagin
Muller
Toporov

JKR
Johnson
Kendall
Roberts

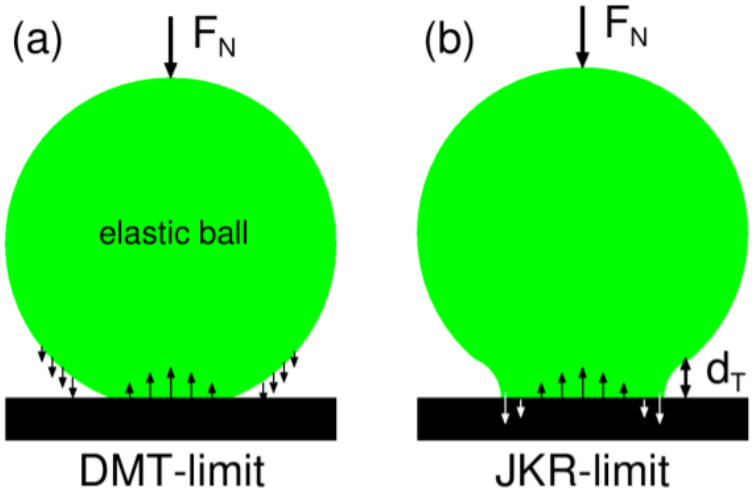

Adhesion

$$F_{ad} = 2\pi W_{ad} R \qquad F_{ad} = \frac{3}{2}\pi W_{ad} R$$

Hertz

The contact between two smooth elastic bodies was investigated by Hertz (1896) who demonstrated that both the size and shape of the zone of contact followed from the elastic deformation of the bodies. For two spheres of radius R_1 and R_2 pressed together under a load P_0 (see figure 1 *a*) the radius a_0 of the circle of contact is given by

$$a_0^3 = \tfrac{3}{4}\pi(k_1+k_2)\frac{R_1R_2}{R_1+R_2}P_0, \tag{1}$$

where k_1 and k_2 are the elastic constants of the material of each sphere; that is

$$k_1 = \frac{1-\nu_1^2}{\pi E_1} \quad \text{and} \quad k_2 = \frac{1-\nu_2^2}{\pi E_2}$$

where ν is the Poisson ratio and E the Young modulus of each material. Resulting from local compression near to the contact region, distant points in the two spheres approach each other by a distance δ given by

$$\delta^3 = \tfrac{9}{16}\pi^2(k_1+k_2)^2\frac{R_1+R_2}{R_1R_2}P_0^2. \tag{2}$$

Hertz used an optical microscope to measure the contact between glass spheres and so verified his theory experimentally.

JKR

The following elementary analysis shows how surface attraction may be interpreted in terms of surface energy.

Consider two elastic spheres in contact under zero external load. Attractive forces between the surfaces produce a finite contact radius, a, a balance eventually being established between stored elastic energy and lost surface energy. The loss in surface energy U_S is given by

$$U_S = -\pi a^2\gamma, \tag{3}$$

where γ is the energy per unit contact area (i.e. the two surfaces). The force F_S associated with this energy change is

$$F_S = -\mathrm{d}U_S/\mathrm{d}x, \tag{4}$$

where x is the movement of the bodies and is approximately the same as δ which is given by the Hertz equations (1) and (2) but cannot be worked out exactly from these because the attractive surface forces disturb the stress distributions in the bodies. Thus we may only write that

$$x \approx a^2(R_1+R_2)/R_1R_2 \tag{5}$$

combining equations (3), (4) and (5) gives

$$F_S \approx \pi R_1R_2\gamma/(R_1+R_2). \tag{6}$$

This force acts in addition to the ordinary load P_0 between surfaces and the simple analysis shows that it may be related to the geometry and energy of the contacting surfaces. Further, the surface force will strongly influence the contact size when

$$P_0 \approx \pi R_1R_2\gamma/(R_1+R_2). \tag{7}$$

Suppose $R_1 = R_2 = 2\,\mathrm{cm}$ and $\gamma = 600\,\mathrm{erg\ cm^{-2}}$ (for mica $\gamma \approx 300\,\mathrm{erg\ cm^{-2}}$ per surface) then P_0 is around 2 g.

Surprisingly, perhaps, the force of adhesion F_S between convex surfaces does not depend upon the elastic moduli of the materials. The modulus influences the contact radius, a, but, however, it can be seen from equations (3) and (5) that both the surface energy and the elastic work vary as a^2, so that the force of adhesion is independent of a and hence of the elastic modulus. The more rigorous analysis which now follows provides the magnitude of the adhesive force but does not change this conclusion.

(dall'articolo originale di JKR!)

Key Adhesion Mechanisms

- **Van der Waals (main mechanism)**
- Capillary forces (secondary mechanism in humid conditions)

1. Fundamental force: Johnson-Kendall-Roberts (JKR) $$F_{ad} = \frac{3}{2}\pi W_{ad} R$$

2. Multiple (n) contacts, constant contact area: $$F'_{ad} = \frac{3}{2}\pi W_{ad}\left(\frac{R}{\sqrt{n}}\right) \quad n = \sqrt{n}F_{ad}$$

3. More realistic mechanism: peeling $$F_{peel} \approx \frac{2W_{ad}b\theta}{\pi(1-cos\theta)sin\theta}$$

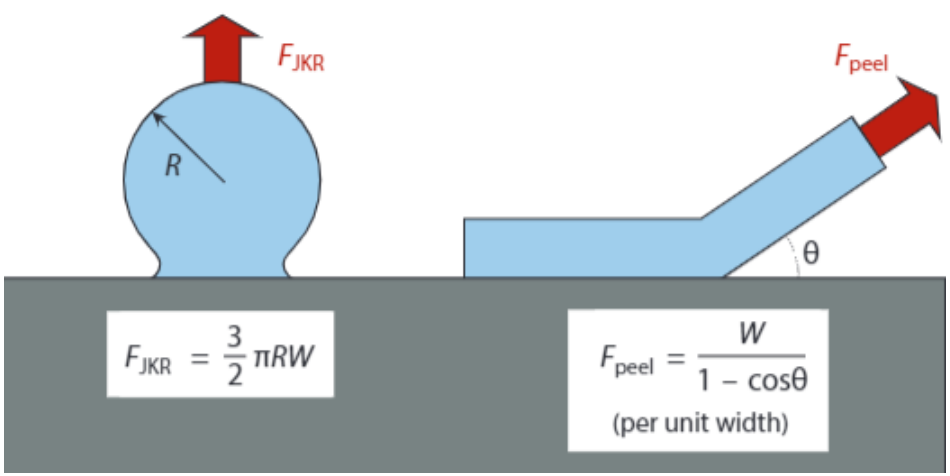

$$W_{ad} \approx 50\ \frac{mJ}{m^{-2}}$$

Effect of Multiple Contacts in Peeling

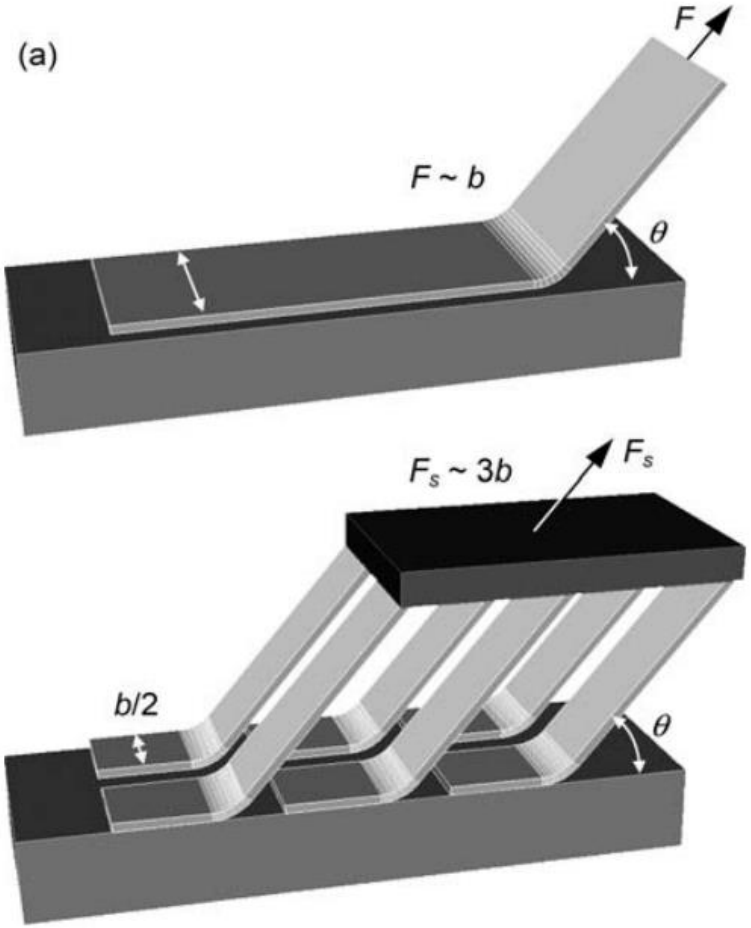

Varenberg, Soft Matter 6, 3269 (2010)

Adhesive Force per Spatula

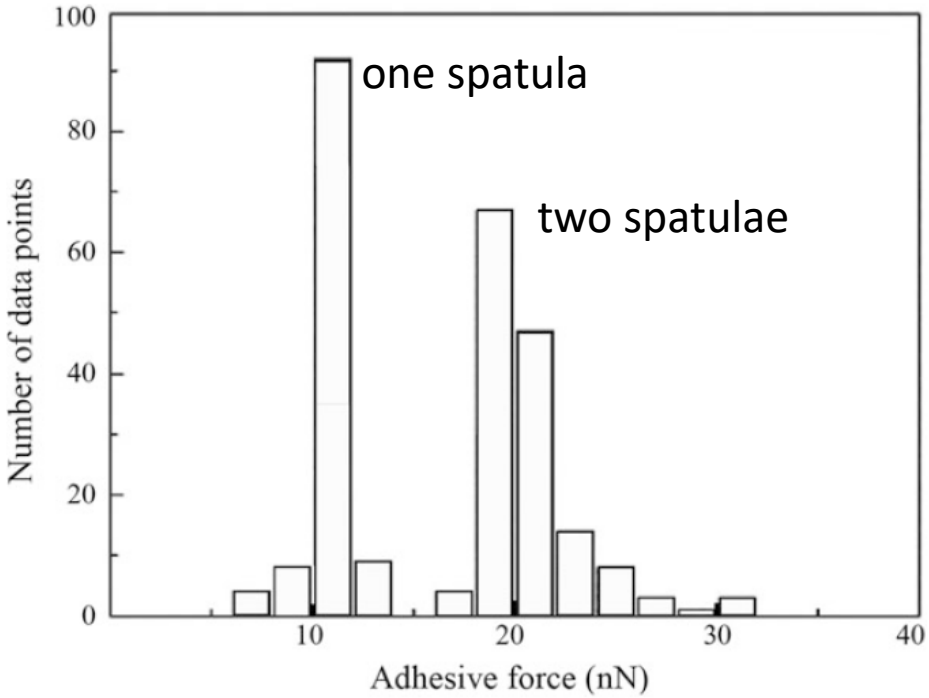

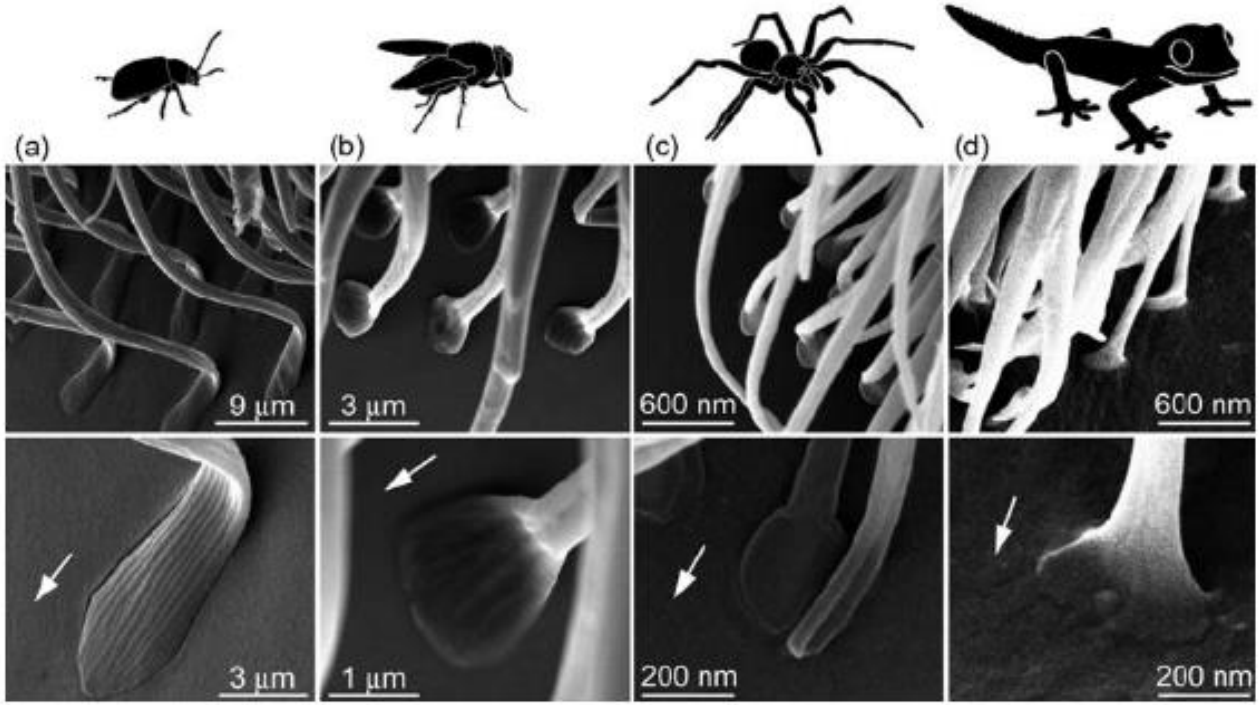

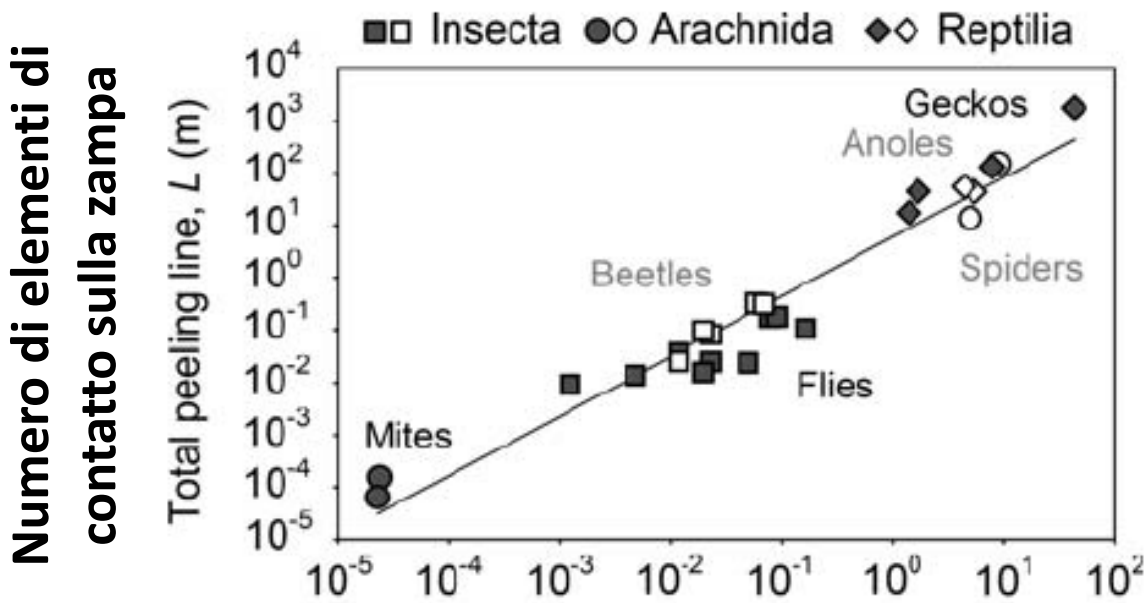

Numero di elementi di contatto sulla zampa

Massa corporea (grammi)

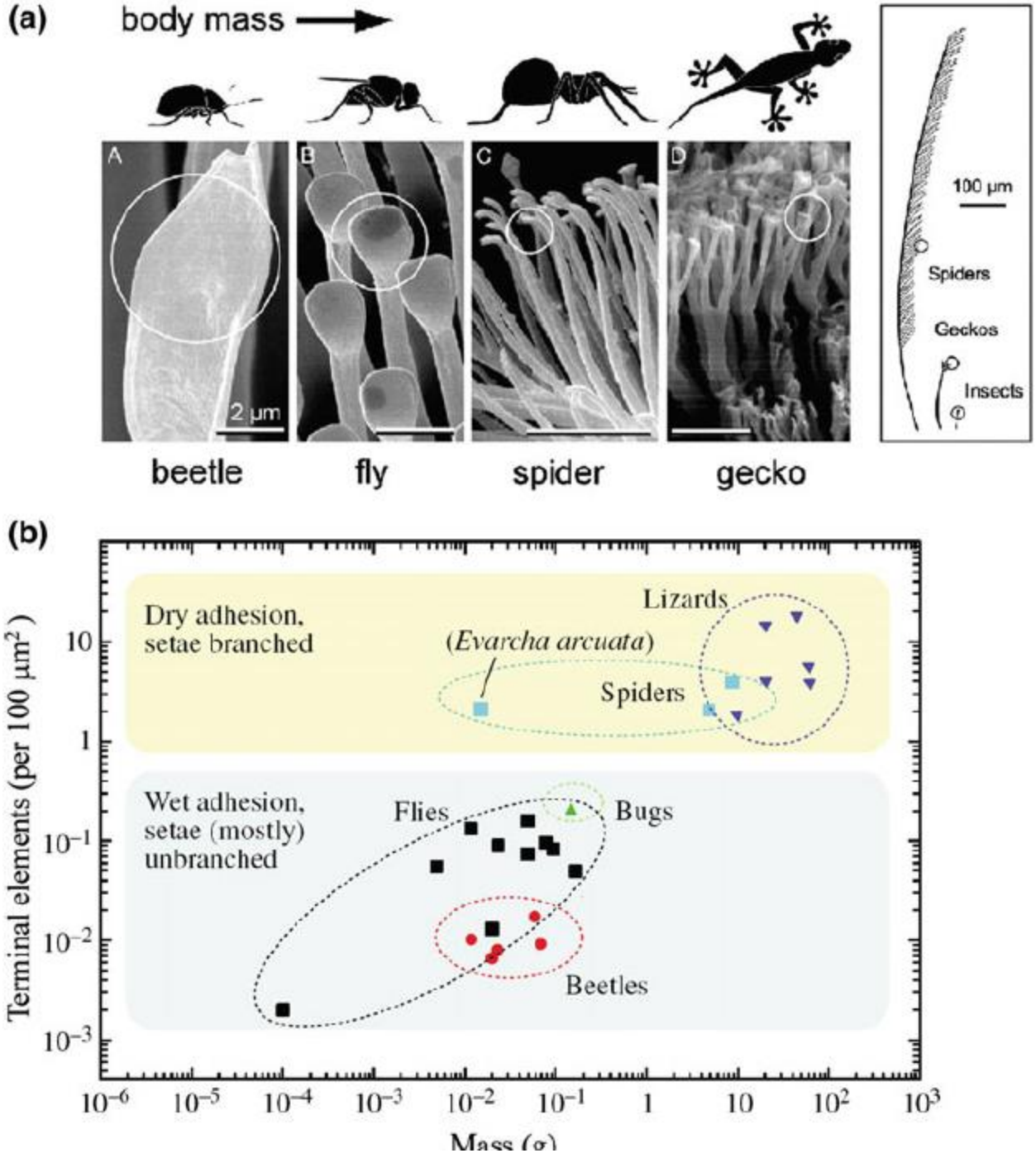
(a)
body mass
A
B
C
D
2 µm
100 µm
Spiders
Geckos
Insects
beetle
fly
spider
gecko
(b)
Dry adhesion,
setae branched
Lizards
(Evarcha arcuata)
Spiders
Wet adhesion,
setae (mostly)
unbranched
Flies
Bugs
Beetles
Terminal elements (per 100 µm²)
10
1
10⁻¹
10⁻²
10⁻³
10⁻⁶
10⁻⁵
10⁻⁴
10⁻³
10⁻²
10⁻¹
1
10
10²
10³
Mass (g)

Effect of Humidity

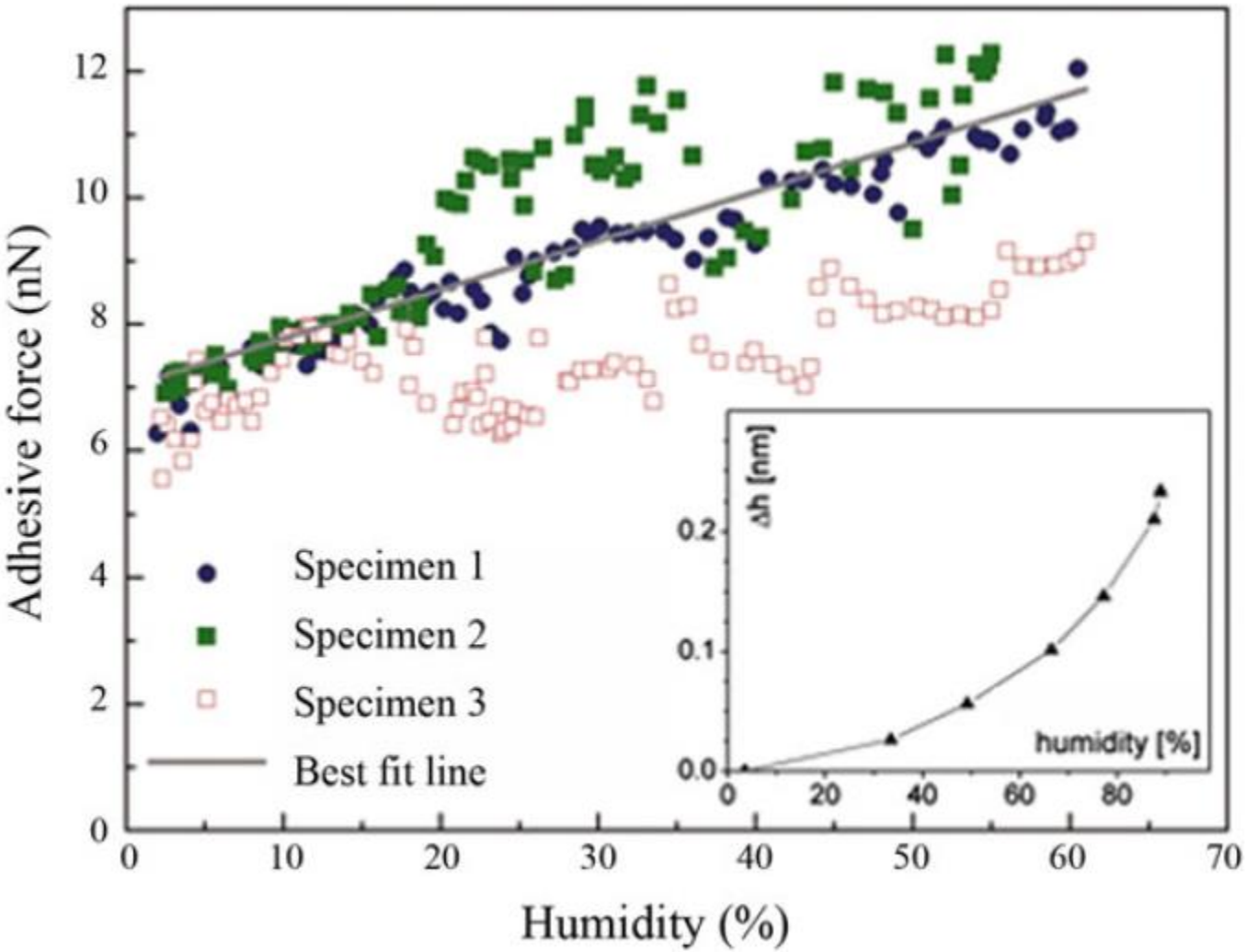

Detachment Mechanism

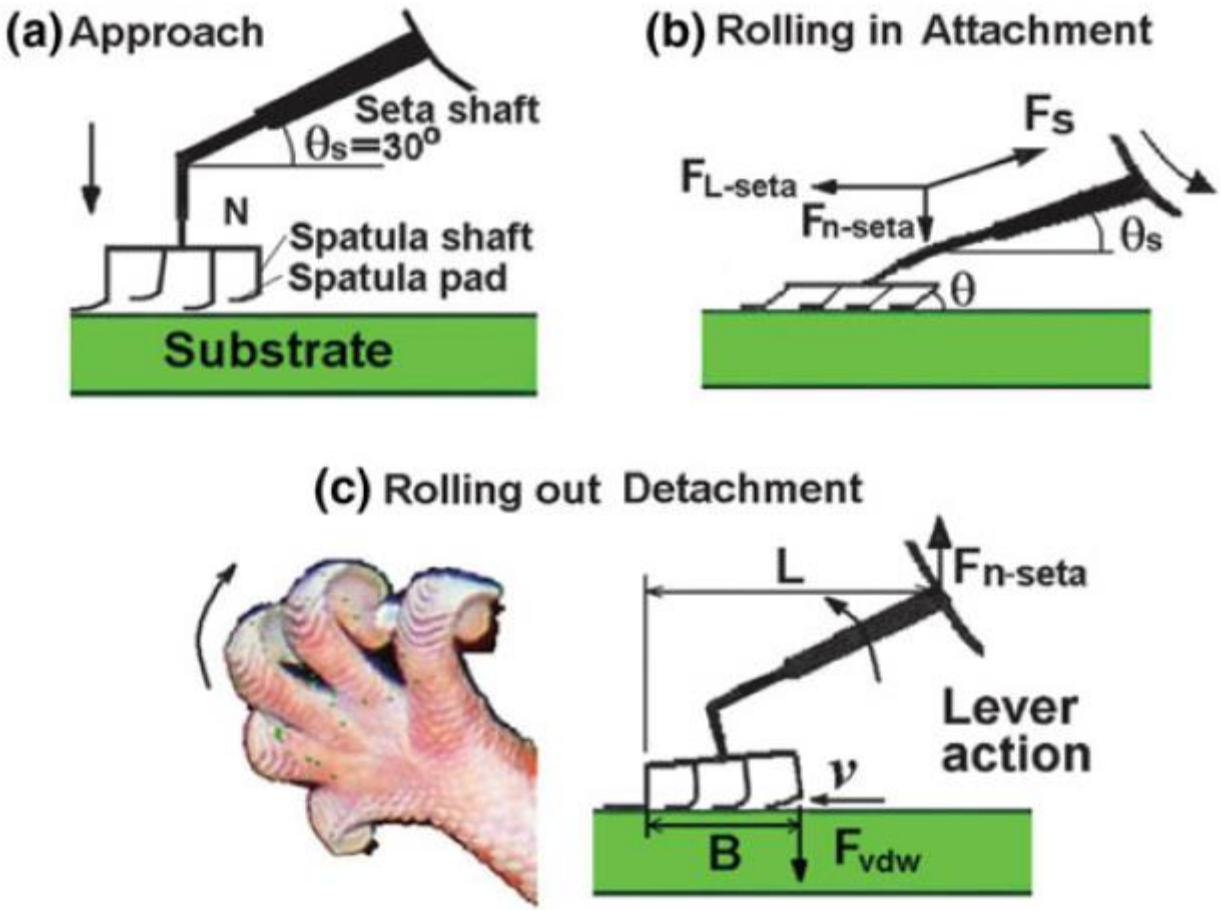

Detachment Mechanism

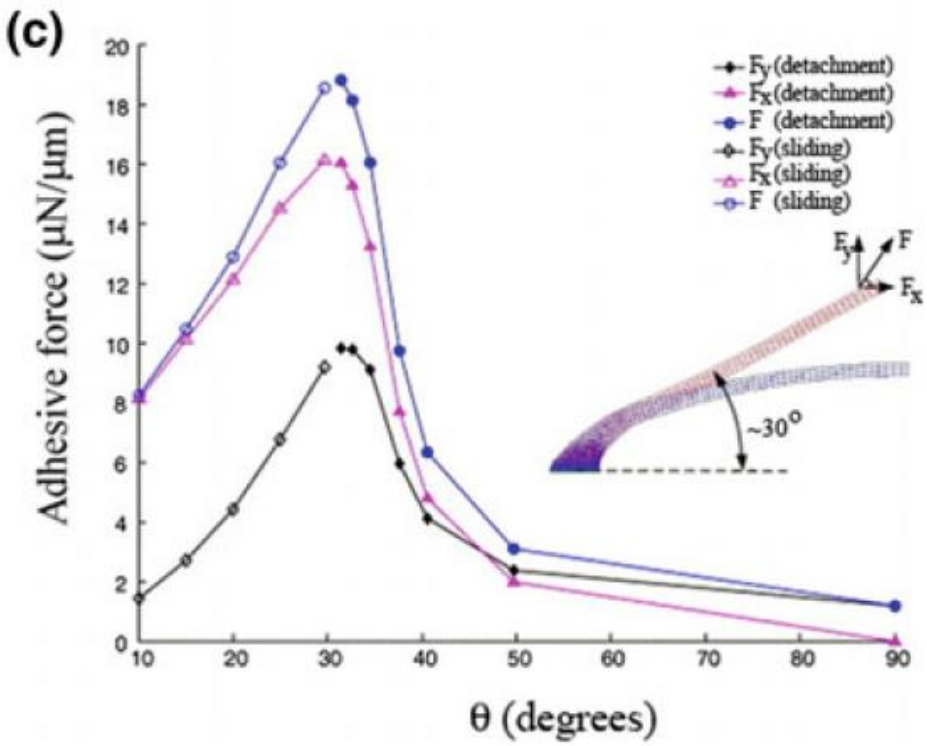

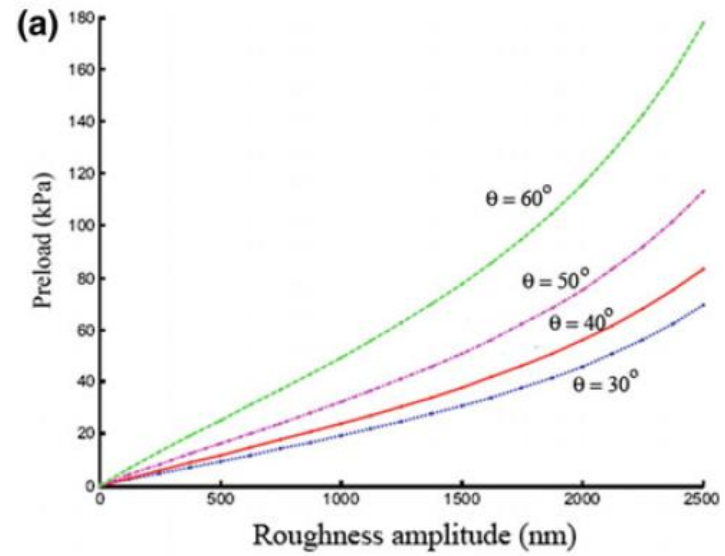

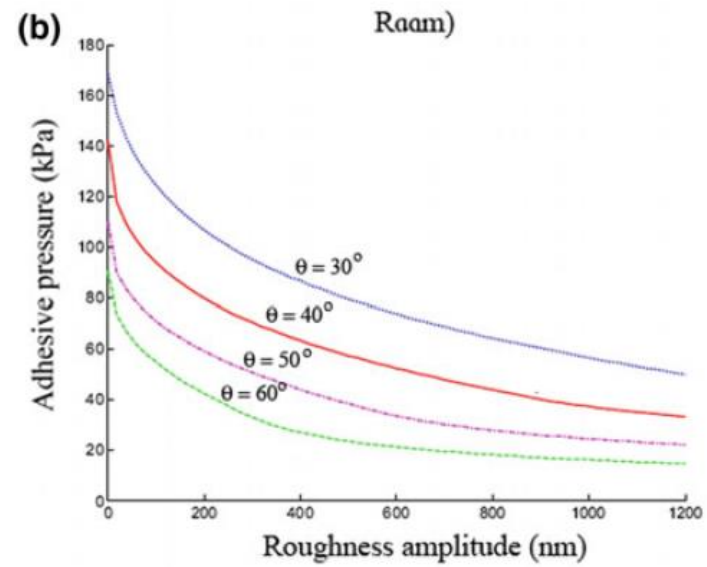

Self-cleaning

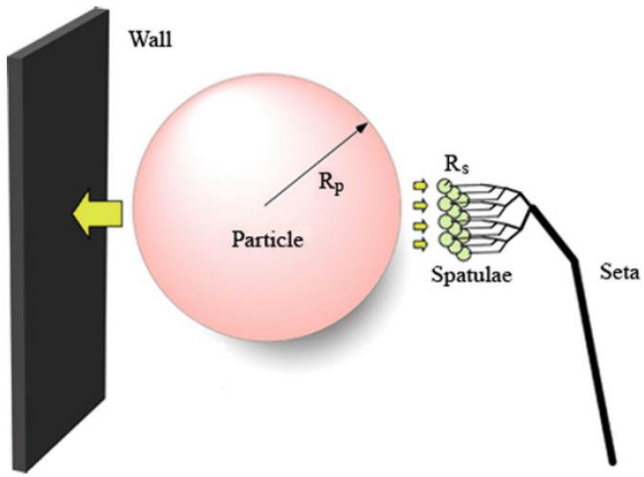

$$W_{pw} = \frac{-H_{pw}R_p}{6D_{pw}} > W_{ps} = \frac{-H_{ps}R_pR_s}{6D_{ps}(R_p + R_s)}$$

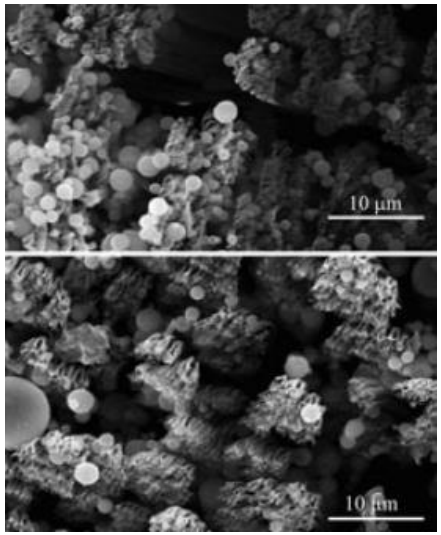

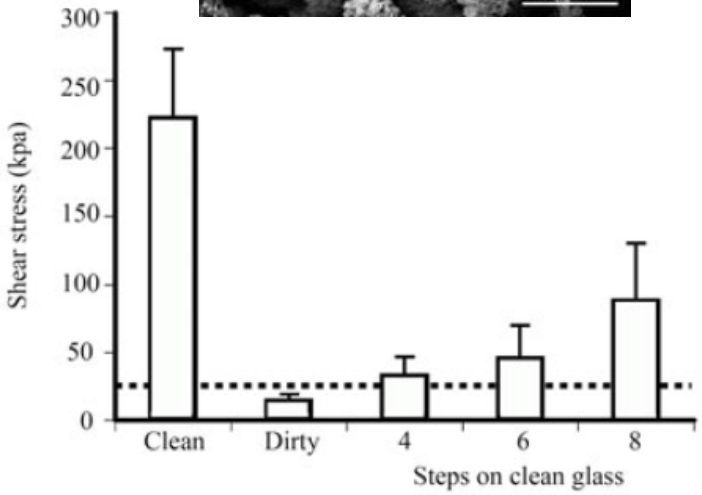

Role of hierarchy

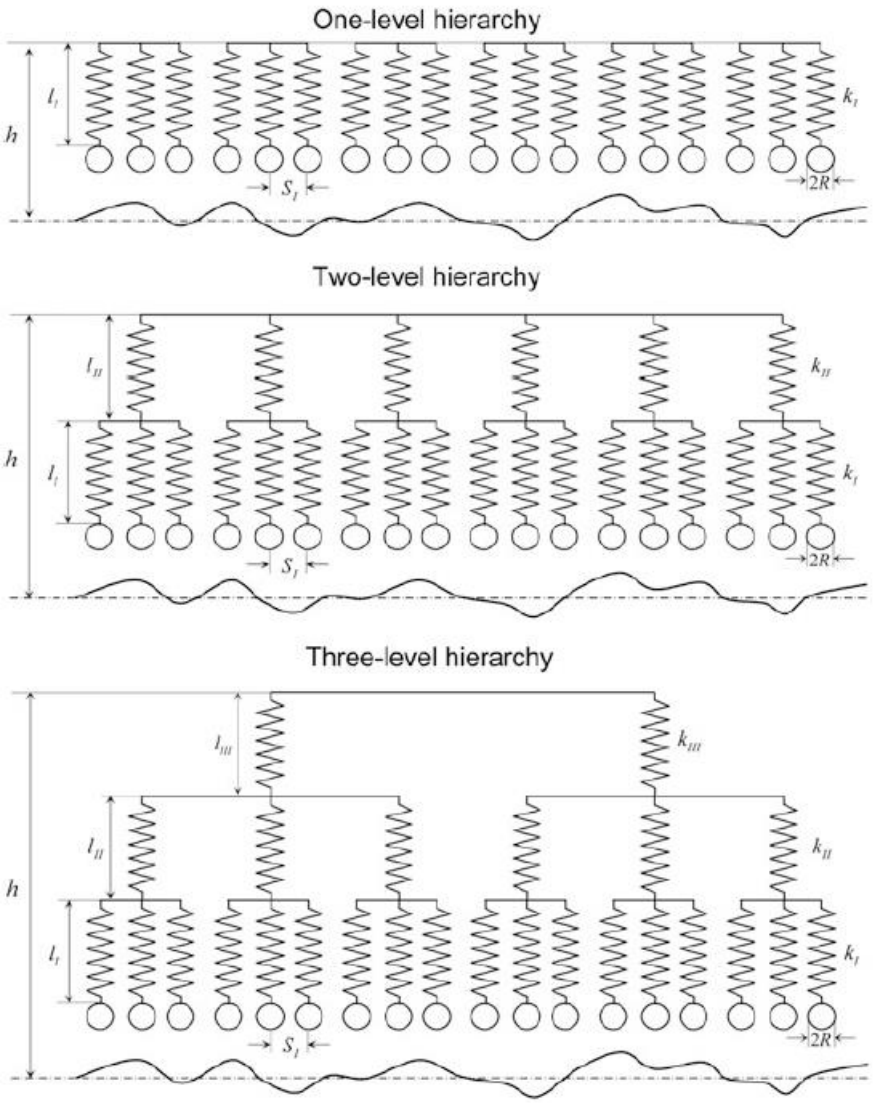

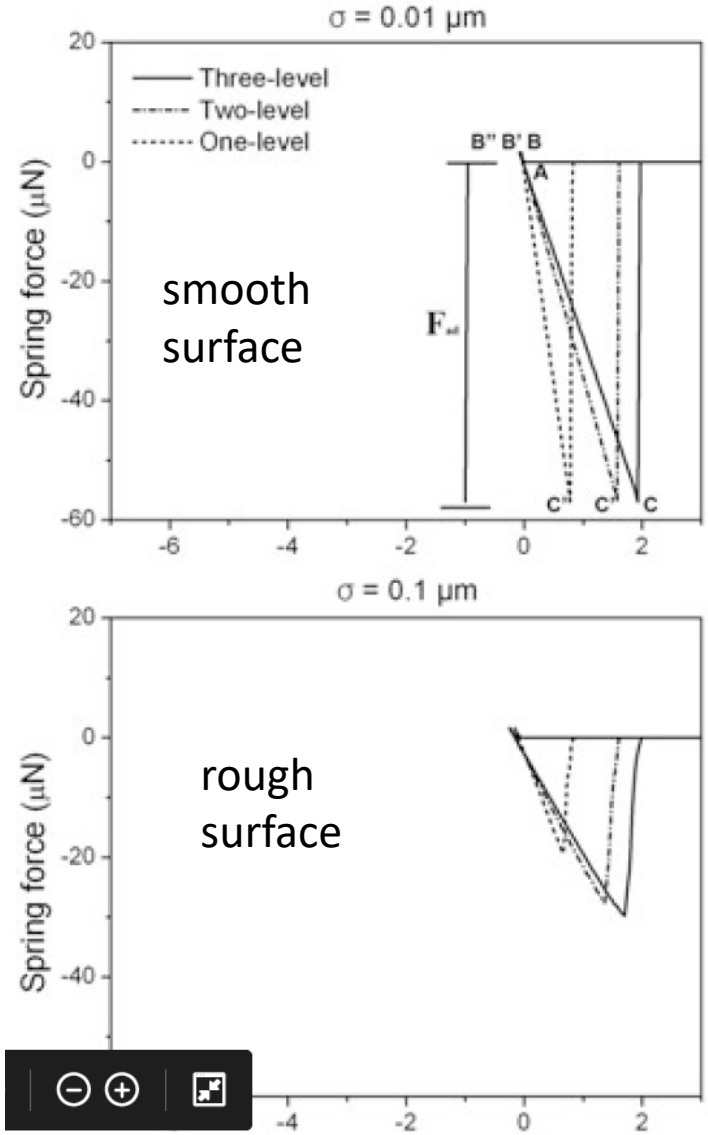

Fabrication of Gecko-like Structures

One-level features

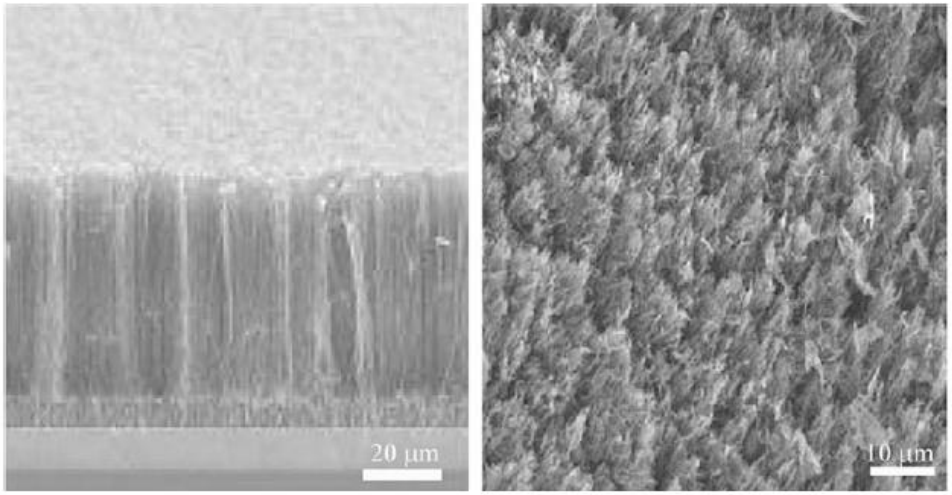

Fig. 19.34 Multi-walled carbon nanotube structures: (left) grown on silicon by chemical vapor deposition, (right) transferred into a PMMA matrix, and then exposed on the surface after solvent etching (Yurdumakan et al. 2005)

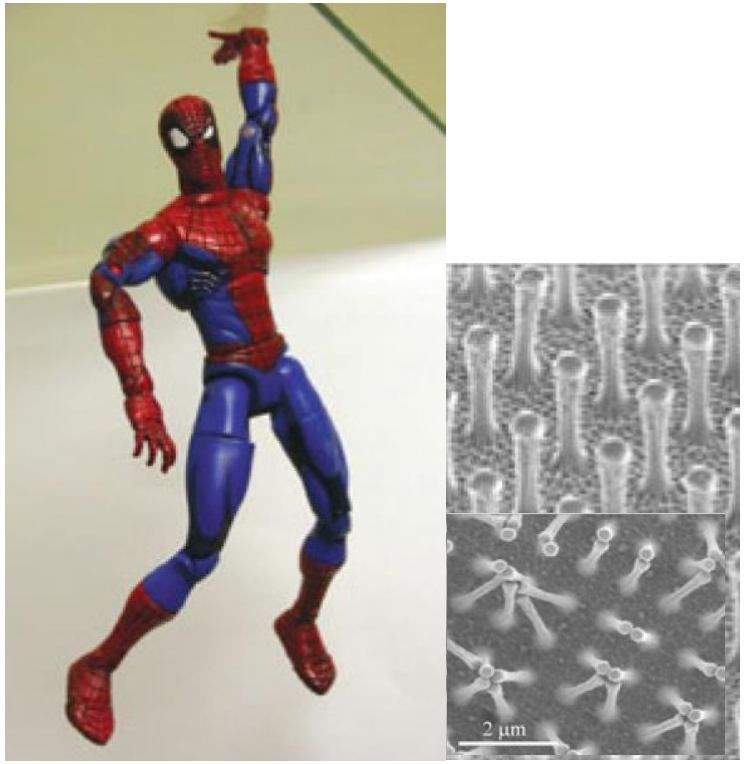

Polyimide pillars (before and after use)

Fabrication of Gecko-like Structures

One-level features

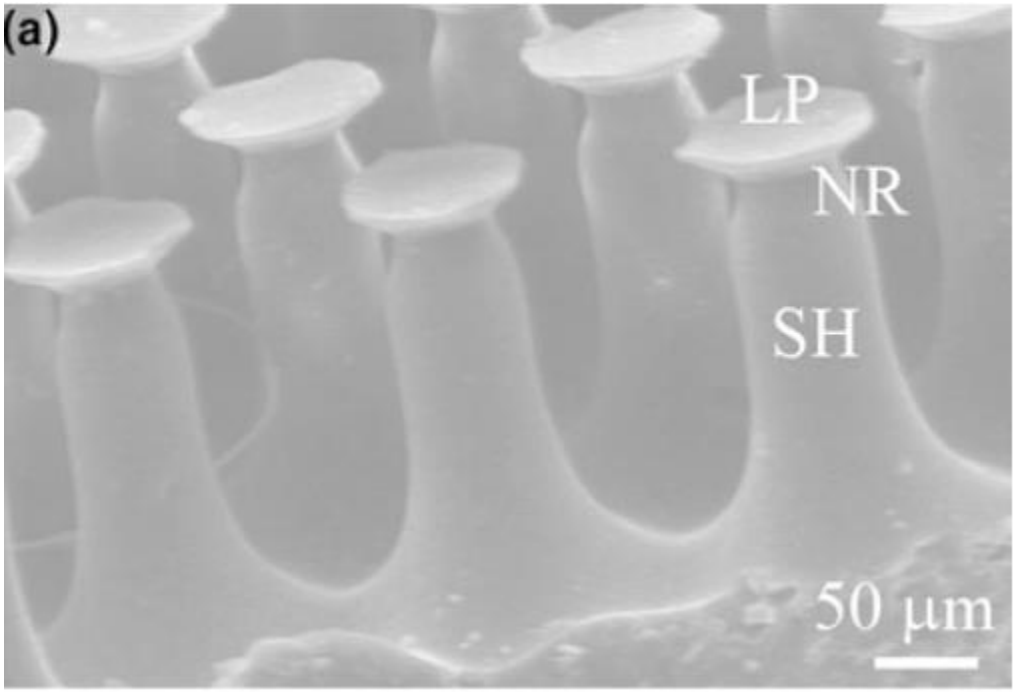

Fabrication of Gecko-like Structures

One-level features

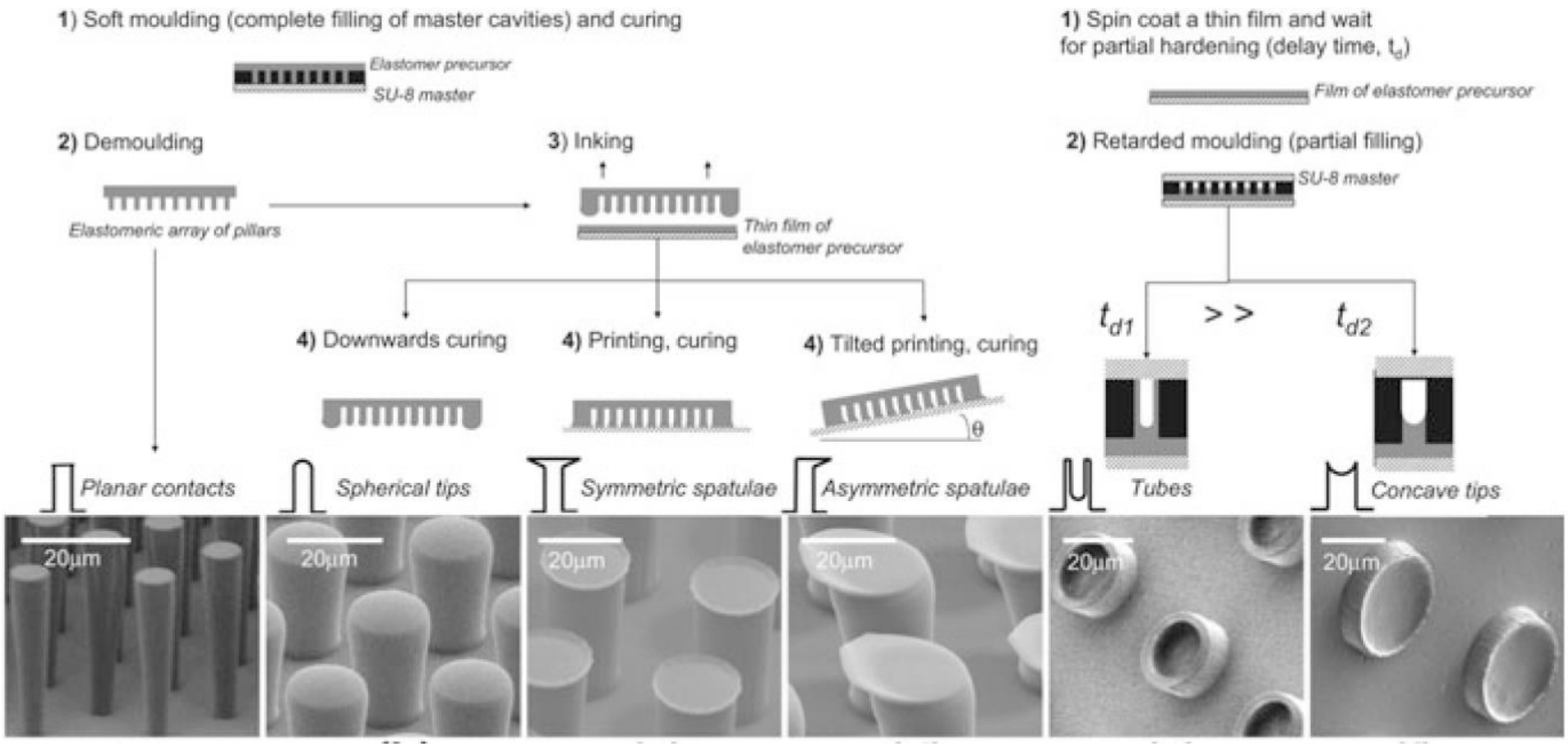

Fabrication of Gecko-like Structures

One-level features

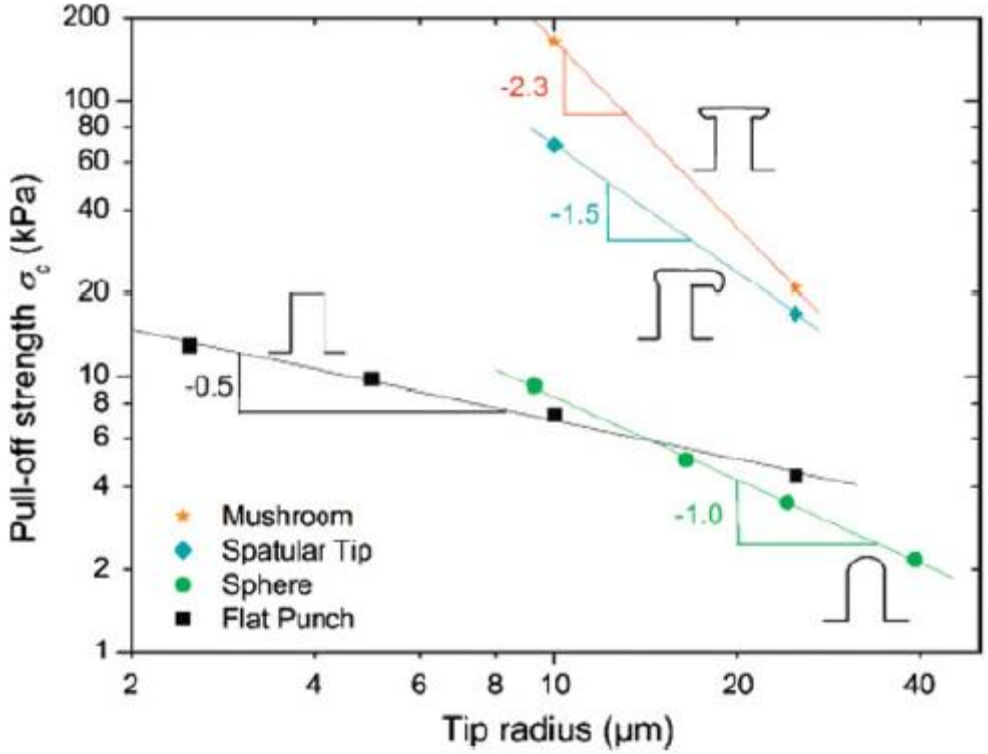

Fabrication of Gecko-like Structures

Multi-level features

Nanotechnology **16** (2005) 1159–1166 doi:10

A batch fabricated biomimetic dry adhesive

Michael T Northen[1,3] and Kimberly L Turner[2]

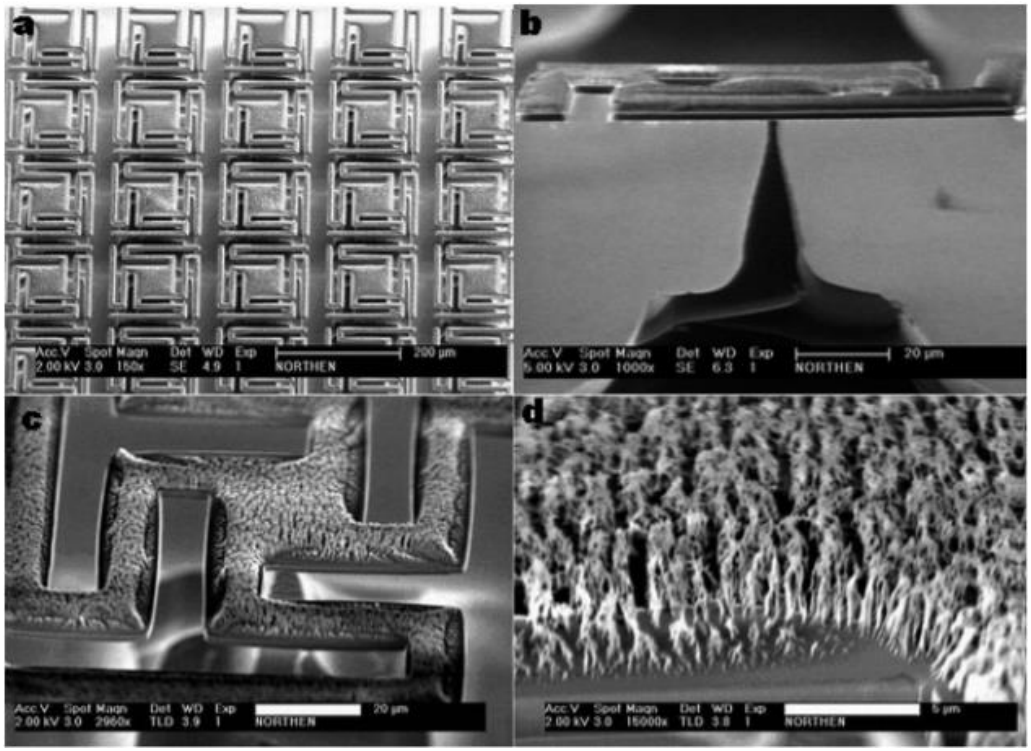

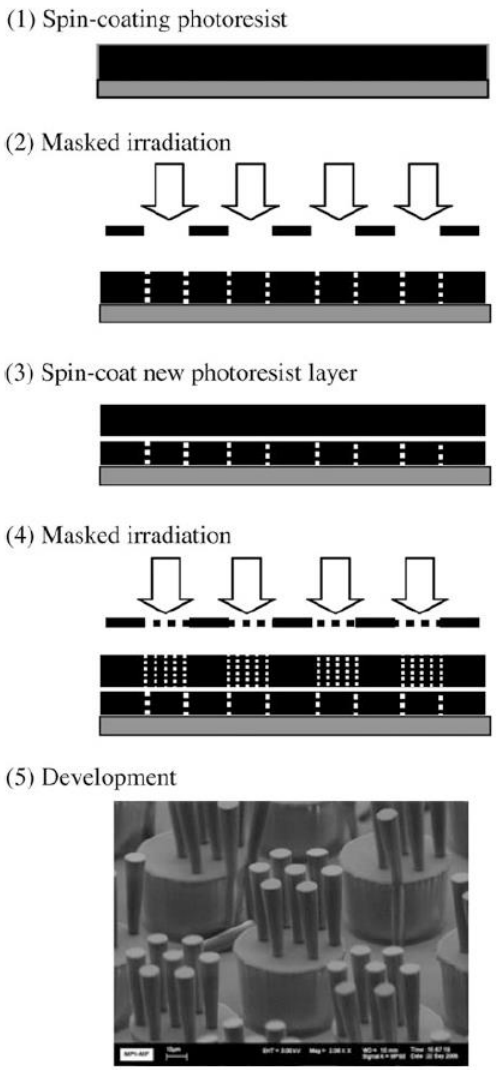

Fabrication of Gecko-like Structures

ADVANCED MATERIALS

DOI: 10.1002/adma.200801340

A Gecko-Inspired Reversible Adhesive**

By *Michael T. Northen, Christian Greiner,* Eduard Arzt,* and *Kimberly L. Turner*

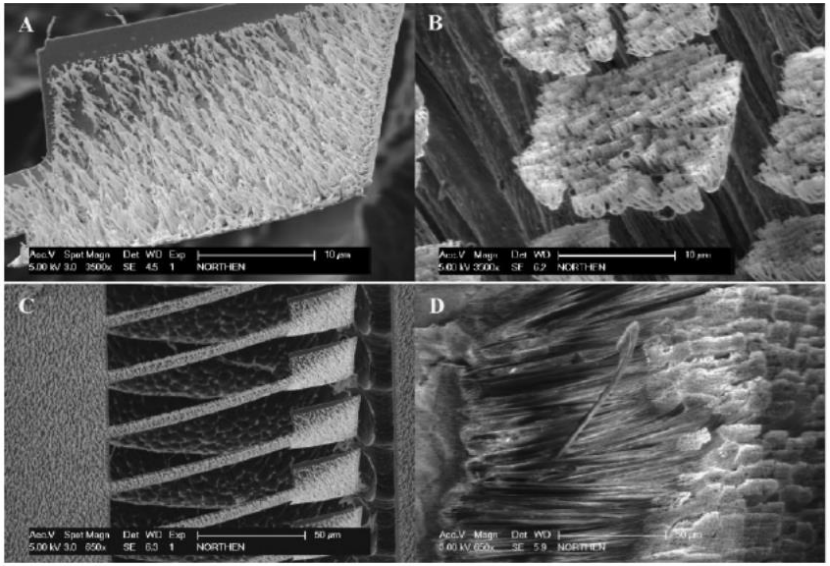

Figure 1. Electron micrographs of synthetic structures (left) and the analogous gecko structures (right), samples from a Tokay Gecko (*Gekko Gecko*). A) Paddle surface coated with evenly spaced uncondensed aligned vertical polymer nanorods (left) and B) the branched terminus of a seta into spatulae (right), same magnification and scale bar 10 μm. C) Freestanding nickel cantilevers and paddles coated with nanorods (left) and an array of setae (D) (right), same magnification and scale bar 50 μm.

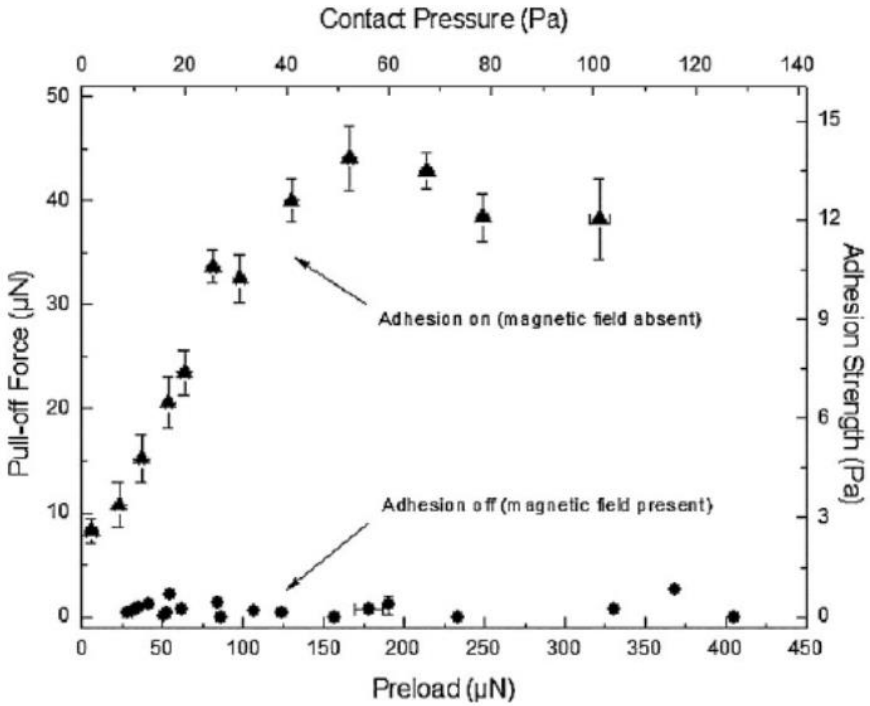

Quanta superficie corporea deve essere coperta da elementi adesivi per sostenere il peso del corpo?

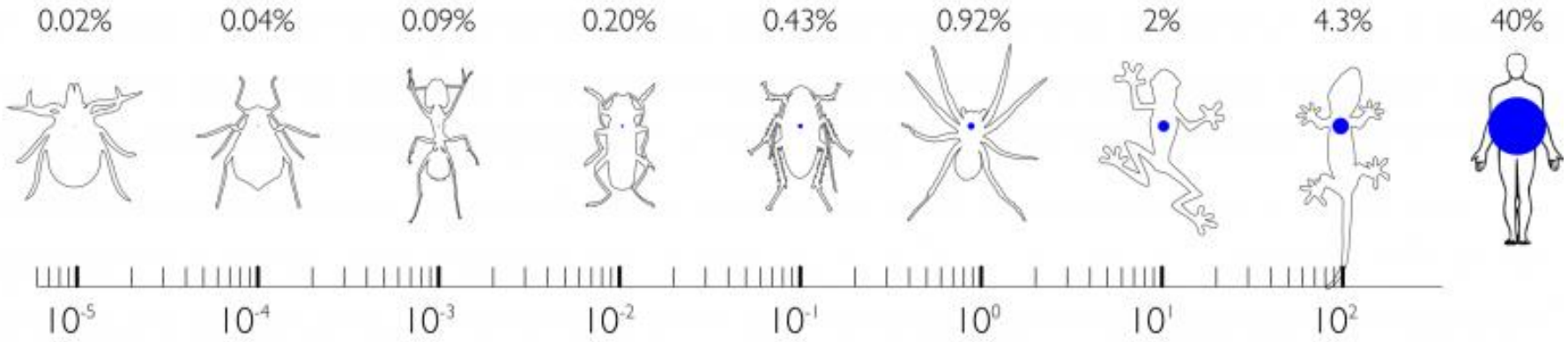

Massa corporea (grammi)


I Love myself
Stay happy
Stay positive
Keep calm
Be happy!!
KISS
Mother
With all the inventors of shuttle quest company

Superliquiphobicity

(ϑ > 150°)

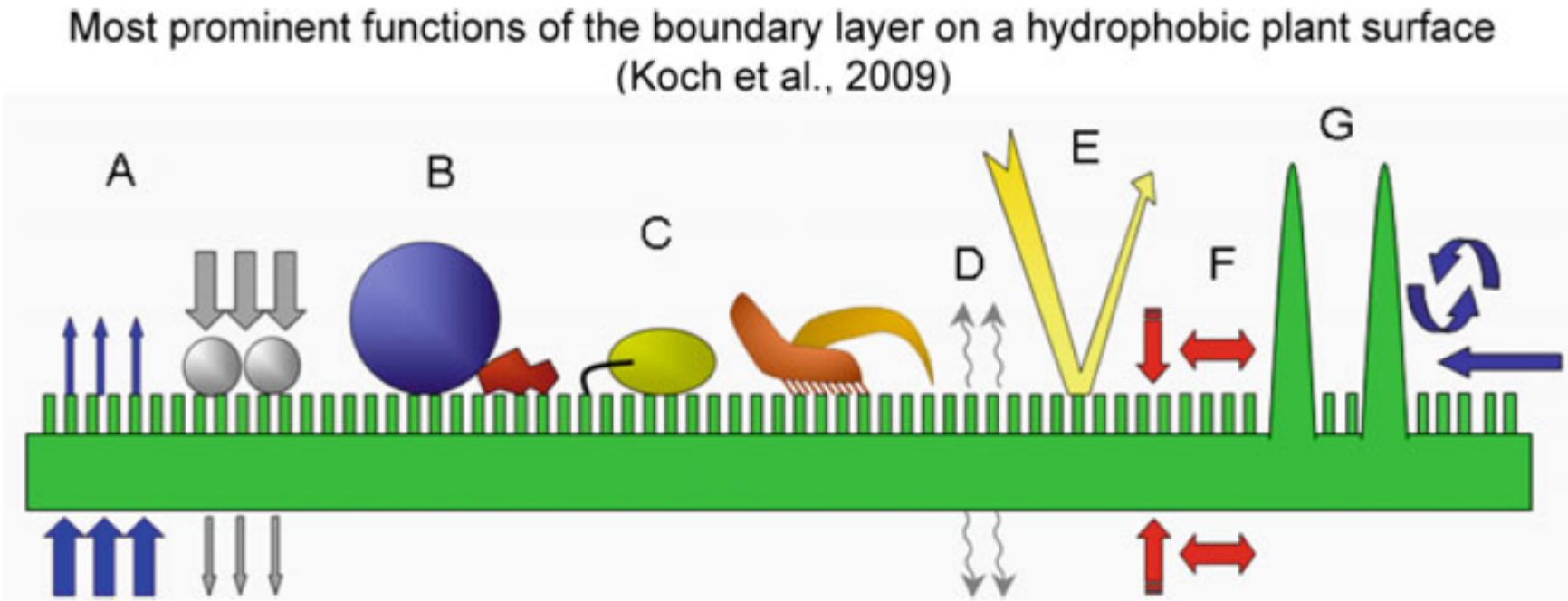

Fig. 4.1 Schematic of the most prominent functions of the boundary layer on a hydrophobic microstructured plant surface. (A) Transport barrier limitation of uncontrolled water loss/leaching from interior and foliar uptake, (B) surface wettability, (C) anti-adhesive, self-cleaning properties: reduction of contamination, pathogen attack and reduction of attachment/locomotion of insects, (D) signaling: cues for host–pathogens/insect recognition and epidermal cell development, (E) optical properties: protection against harmful radiation, (F) mechanical properties: resistance against mechanical stress and maintenance of physiological integrity, and (G) reduction of surface temperature by increasing turbulent air flow over the boundary air later (adapted from Koch et al. 2009a)


20 micron

Fundamentals of Wetting

γ_{SL} : solid-liquid surface tension

γ_{SV} : solid-liquid surface tension

γ_{LV} : solid-liquid surface tension

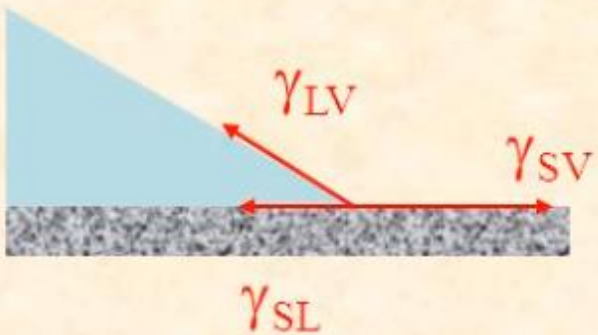

equilibrium contact angle :
Young Dupré relation

$$\gamma_{SV} - \gamma_{SL} = \gamma_{LV} \cos\theta$$

partially wetting liquid : $\theta < 90°$

non wetting liquid : $\theta > 90°$

perfect wetting liquid : $\theta = 0°$

Wetting of a Rough Surface

Young's law on rough surface:

$$r\gamma_{SV} - r\gamma_{SL} = \gamma_{LV}\cos\theta$$

$$\boxed{\cos\theta = r\,\cos\theta_o}$$

θ_o : contact angle on flat chemically same surface

Wenzel law

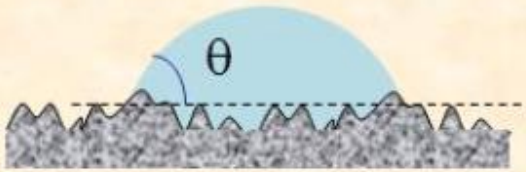

$$r = \frac{\text{real area}}{\text{projected area}} > 1$$

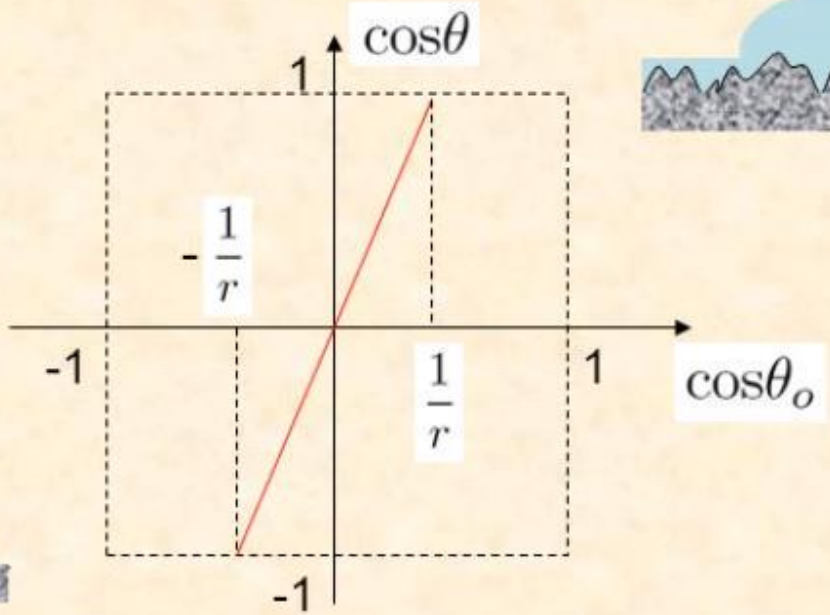

Wetting States

$$r = 1 + 2\pi nah > 1$$
$$\phi = n\pi a^2 < 1$$

Wenzel state

Cassie Baxter state

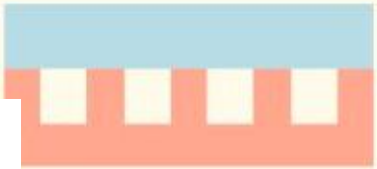

$$\phi\gamma_{SL} + (1-\phi)(\gamma_{LV} + \gamma_{SV}) + (r-1)\gamma_{SV}$$

Trapped air is favorable if

$$(1-\phi)\gamma_{LV} < (r-\phi)(\gamma_{SL} - \gamma_{SV})$$

$$\cos\theta_o < \frac{\phi - 1}{r - \phi}$$

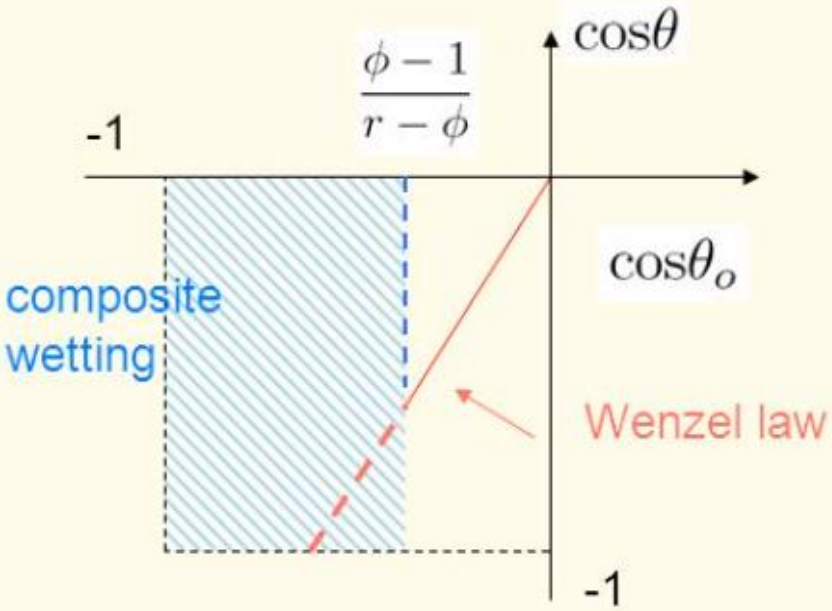

Liquid must be non-wetting

Transition between wetting states

décompresseur TIFF (non compressé)
sont requis pour visionner cette image.

décompresseur TIFF (non compressé)
sont requis pour visionner cette image.

$$\phi\gamma_{SL} + (1-\phi)(\gamma_{LV} + \gamma_{SV}) + (r-1)\gamma_{SV}$$

Young's law for Cassie wetting:

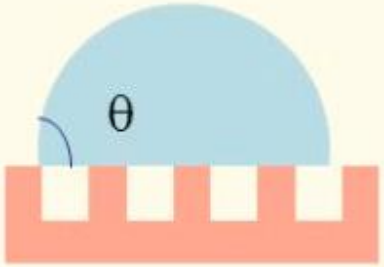

$$r\gamma_{SV} - \gamma_{SL,composite} = \gamma_{LV}\cos\theta$$

$$\boxed{\cos\theta = \phi\cos\theta_o + \phi - 1}$$

Cassie-Baxter's law

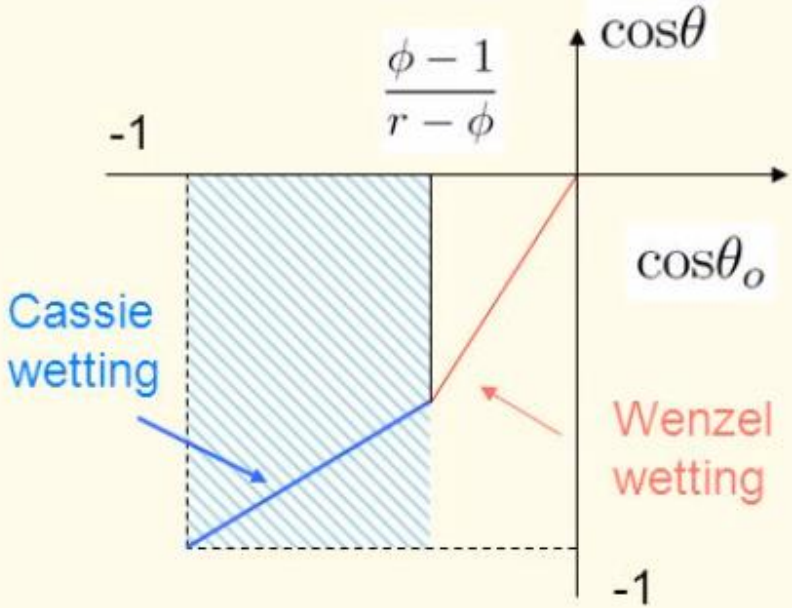

Metastability of Wetting States

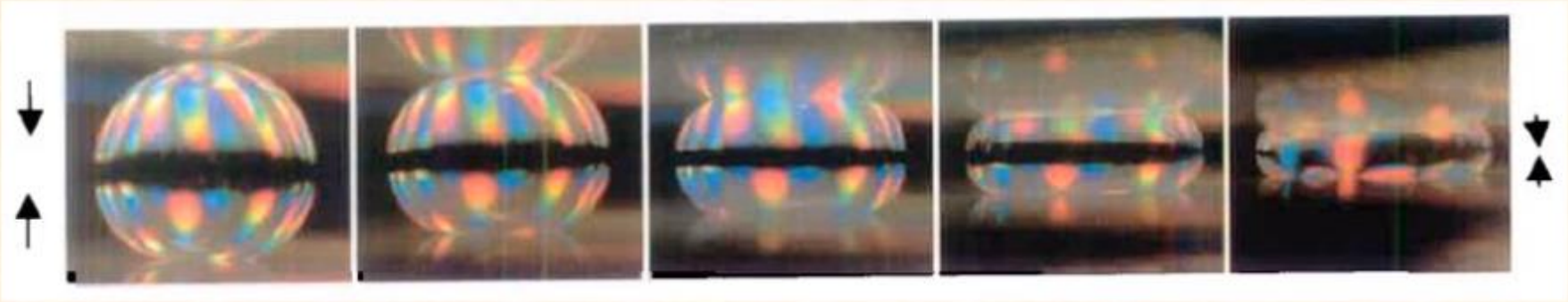

Compression of a water drop between two identical microtextured hydrophobic surfaces. The contact angle is measured as a function of the imposed pressure.

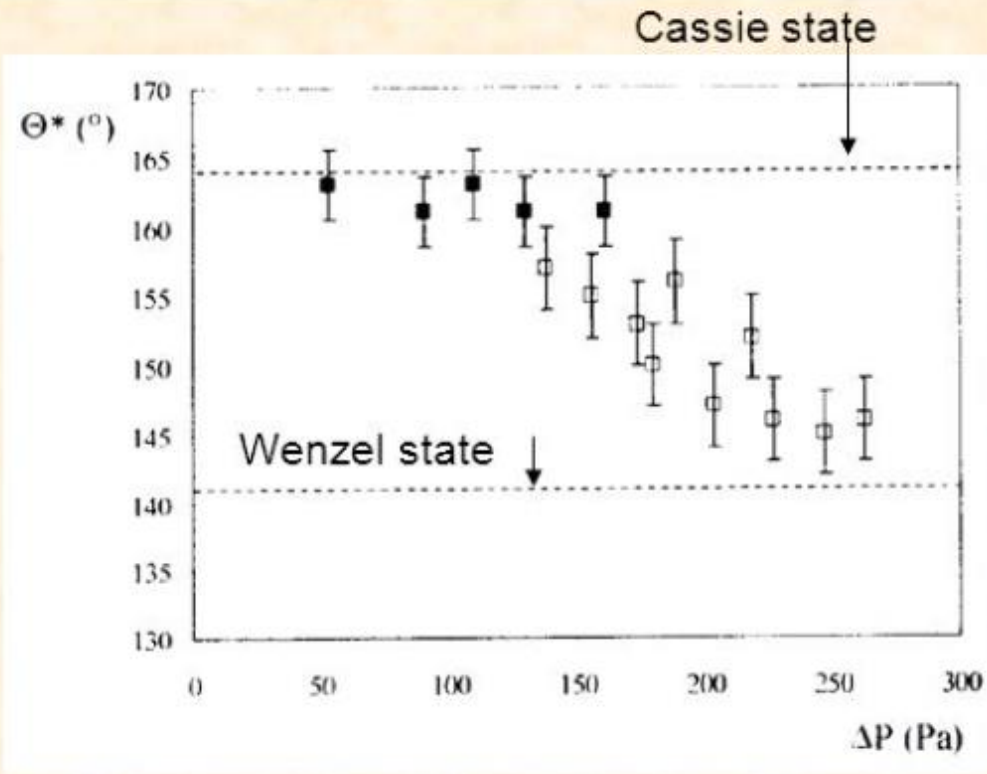

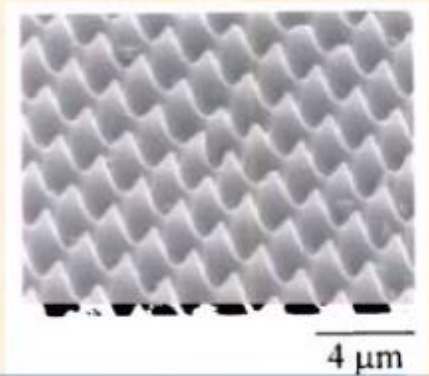

Metastability of wetting states

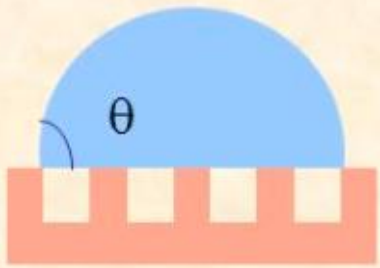

prepared in Cassie state

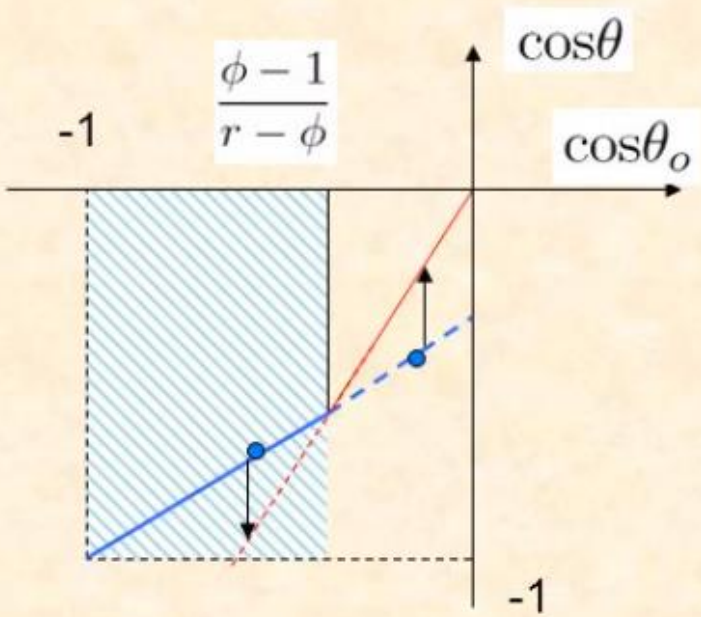

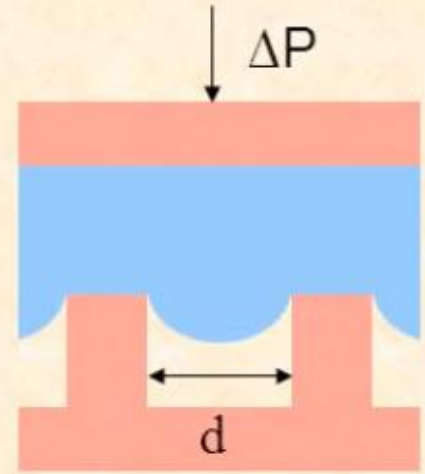

Transition to Wenzel state at

$$\Delta P \leq P_{cap} \sim -\frac{\gamma_{LV}\cos\theta}{d}$$

Robust Cassie state requires small scale and deep holes

Metastability and irreversibility

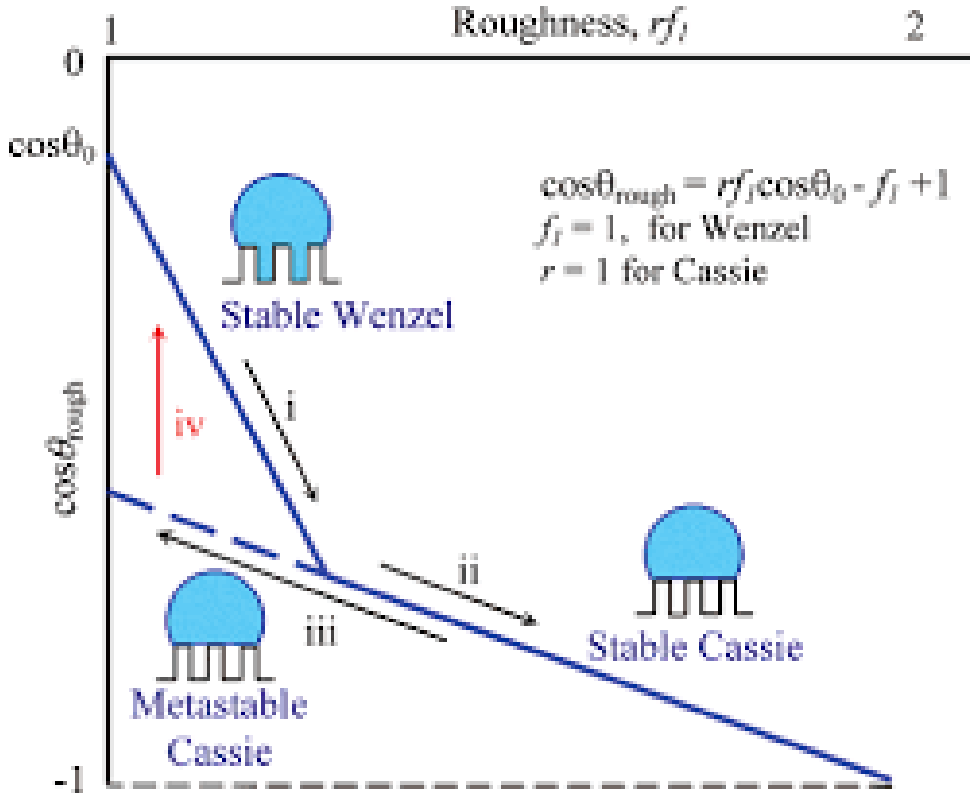

Superficie liscia

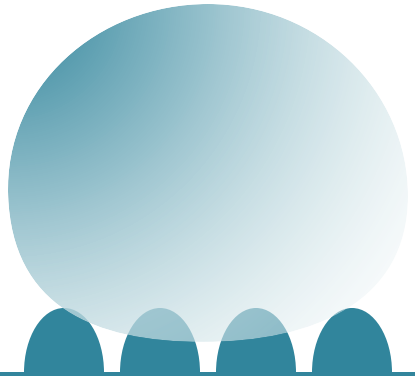

Rugosità micrometrica

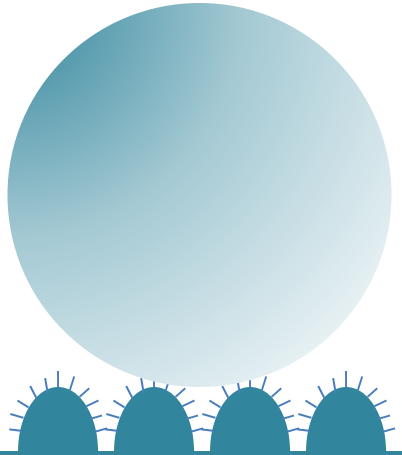

Rugosità nanometrica e gerarchica

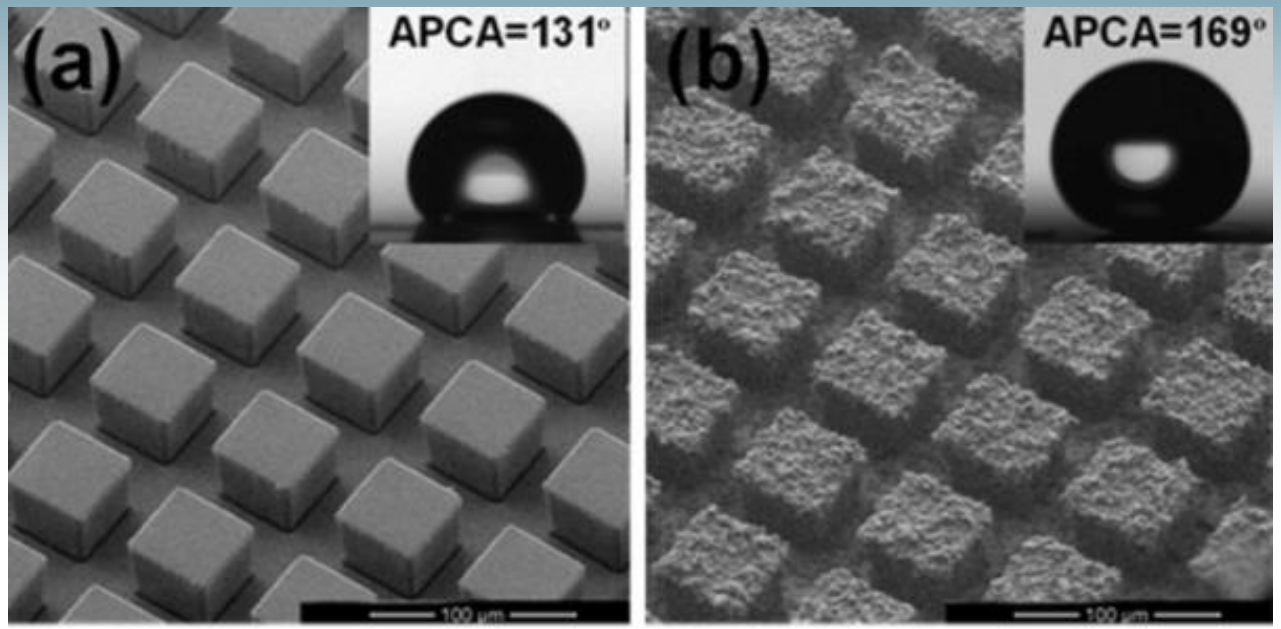

Petal Effect

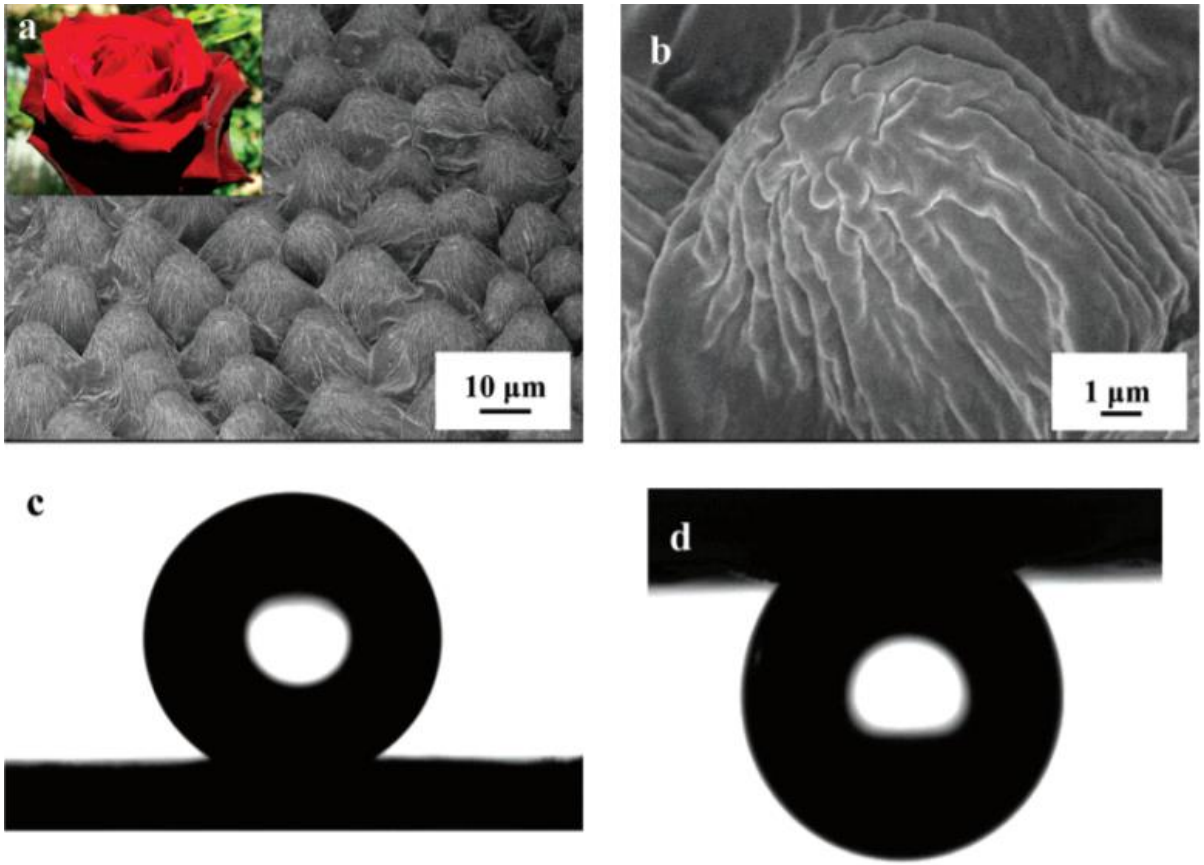

Petal Effect

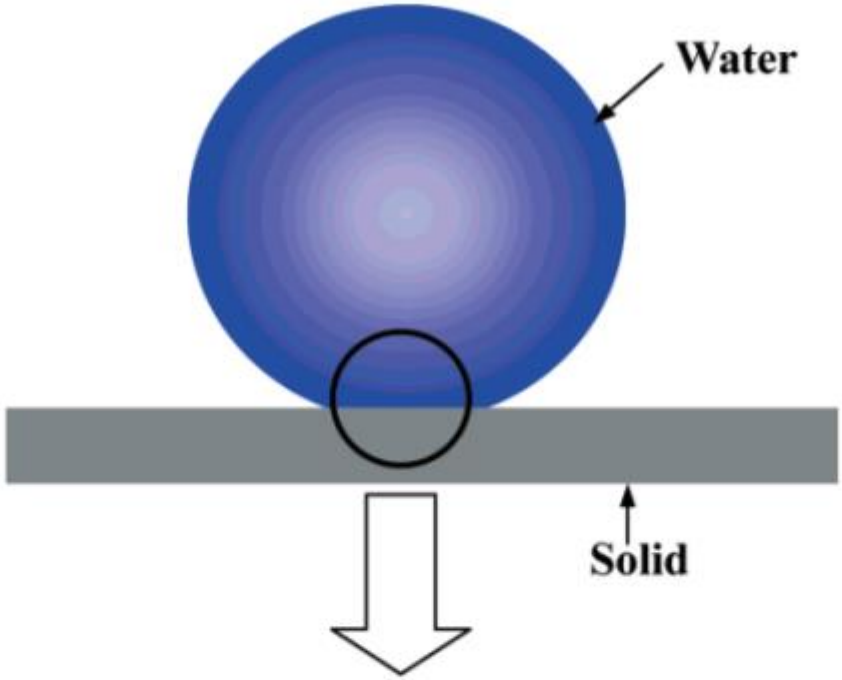

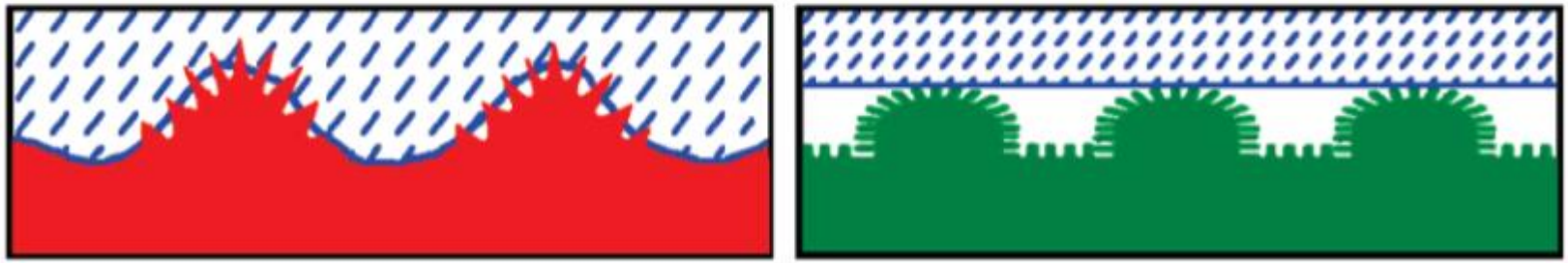

Petal (Cassie impregnating wetting state)

Lotus (Cassie's state)

Petal Effect

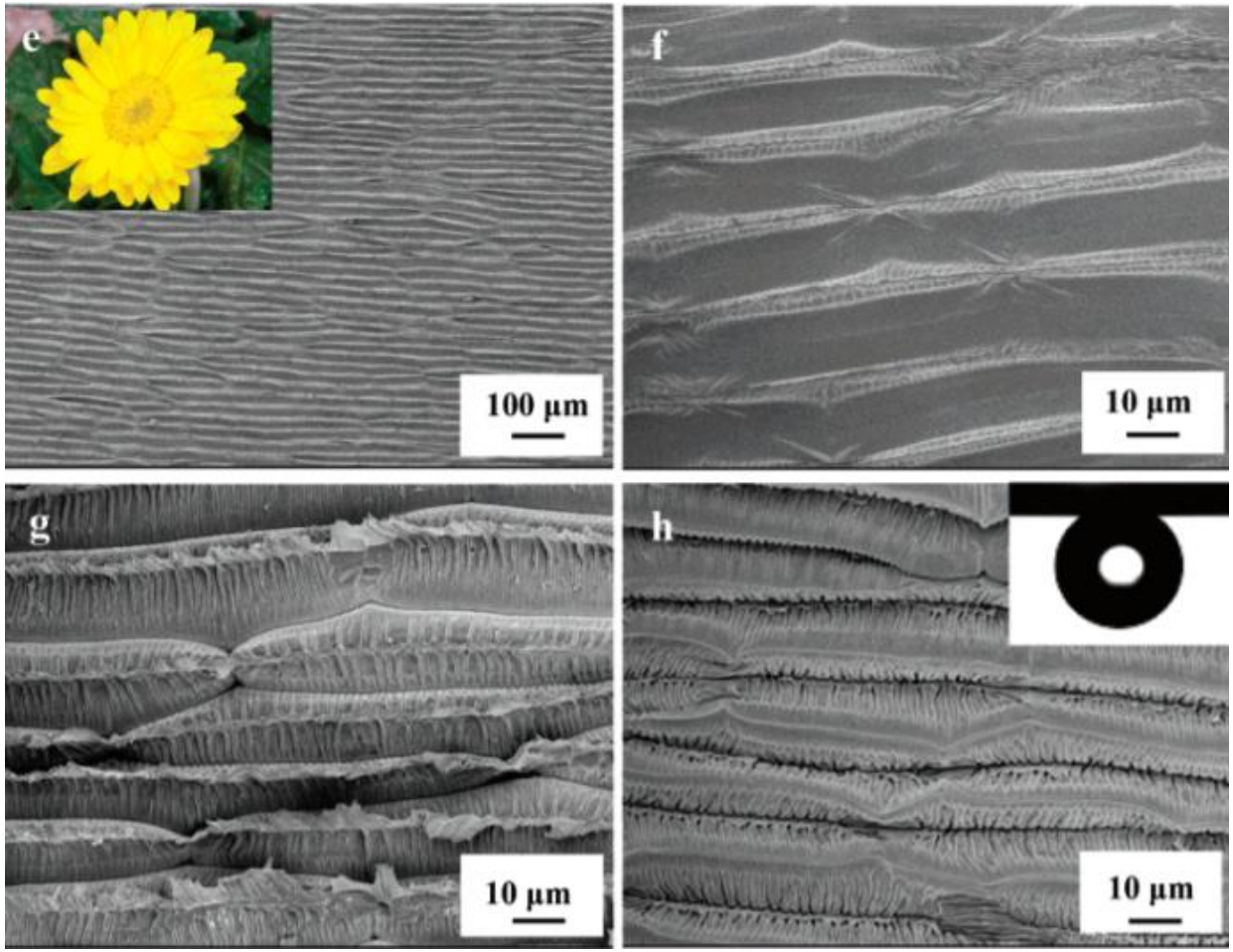

Petal Effect

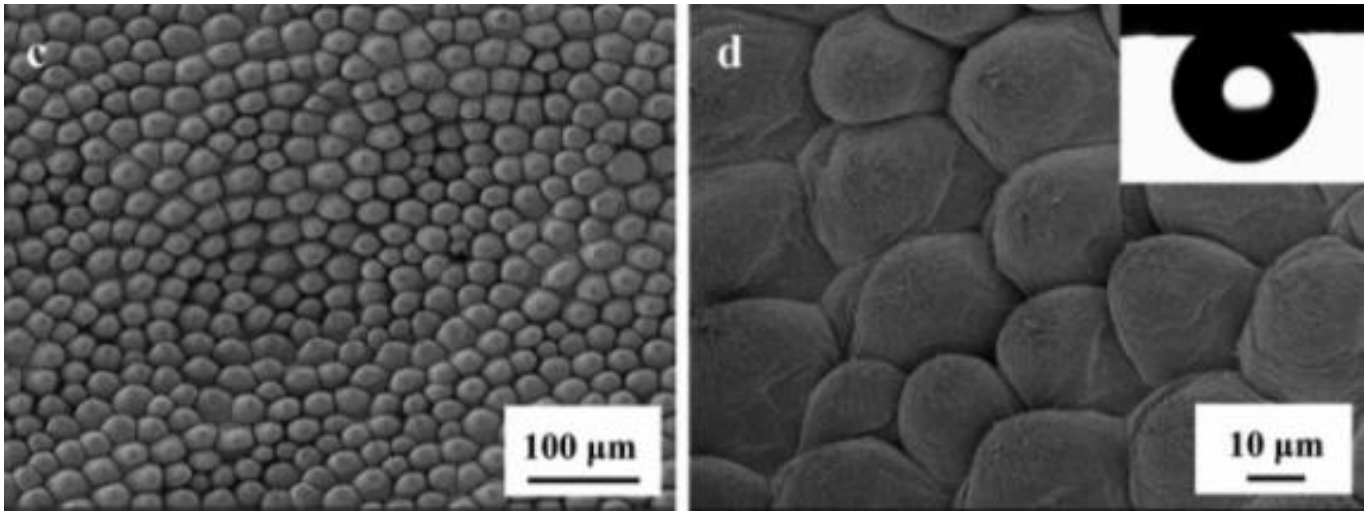

PS Replica

Modes of Superhydrophobicity

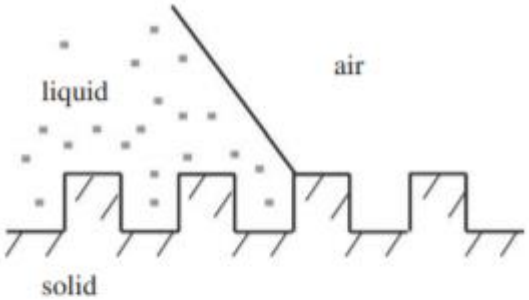

Wenzel

$$\cos\theta = R_f \cos\theta_0$$

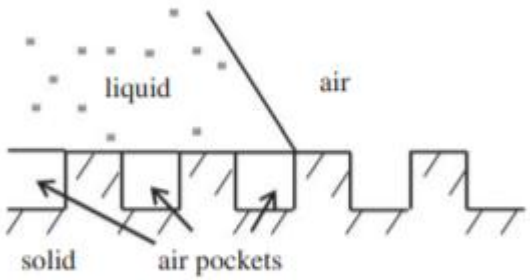

Cassie-Baxter

$$\cos\theta = R_f f_{SL} \cos\theta_0 - 1 + f_{SL}$$

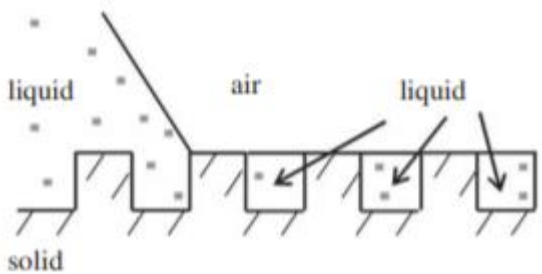

Impregnating Cassie

$$\cos\theta = 1 + f_{SL}(\cos\theta_0 - 1)$$

Hysteresis

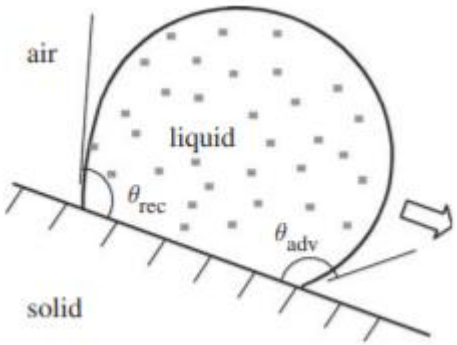

$$\cos\theta_{\mathrm{adv}} - \cos\theta_{\mathrm{rec}} = R_{\mathrm{f}}(1 - f_{\mathrm{LA}})(\cos\theta_{\mathrm{adv0}} - \cos\theta_{\mathrm{rec0}}) + H_{\mathrm{r}}$$

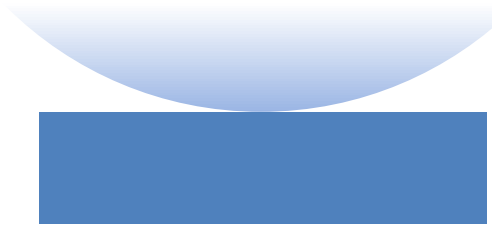

Homogeneous surface*

$f_{LA} \rightarrow 0$ Hysteresis increases with R_f

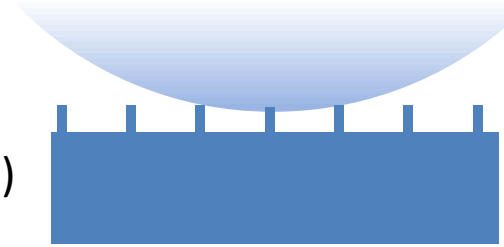

Composite surface*

$f_{LA} \rightarrow 1$ large CA and low Hysteresis (good for self-cleaning)

under the droplet!

Modes of Superhydrophobicity

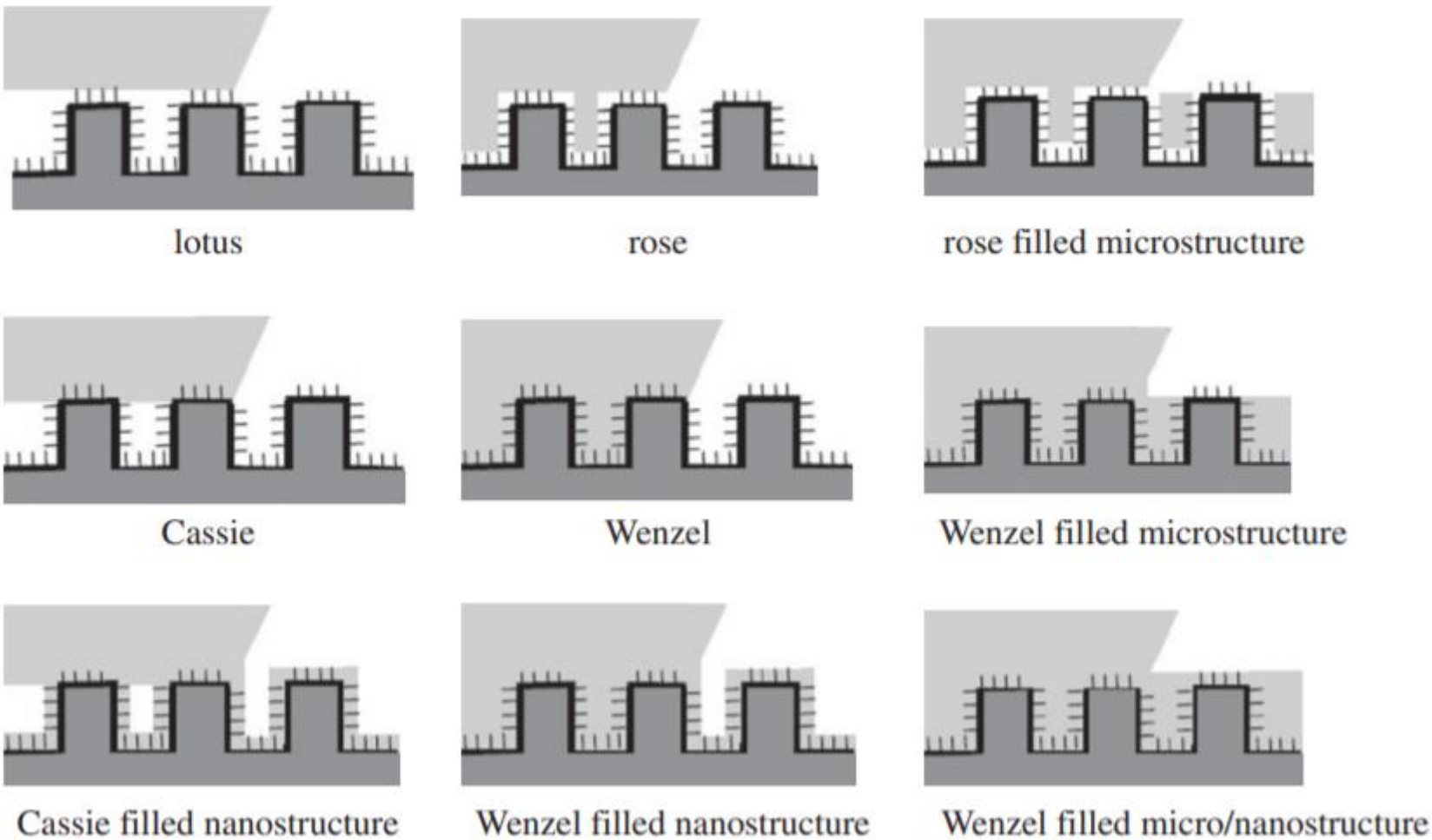

Modes of Superhydrophobicity

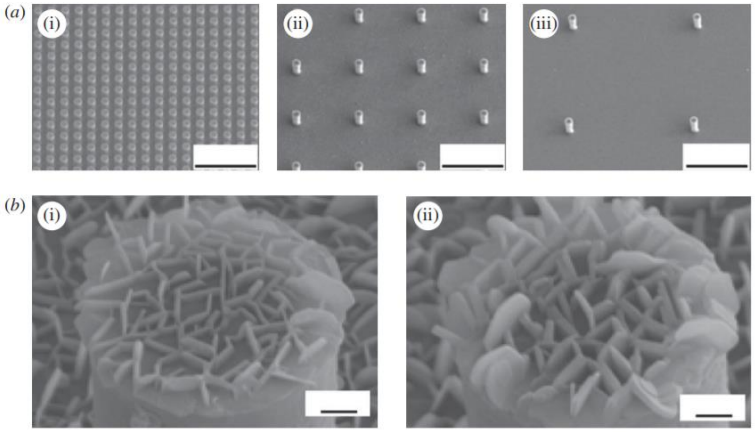

Scale bars, (a) 100 μm and (b) 2 μm.

Superhydrophobic with high adhesion surface

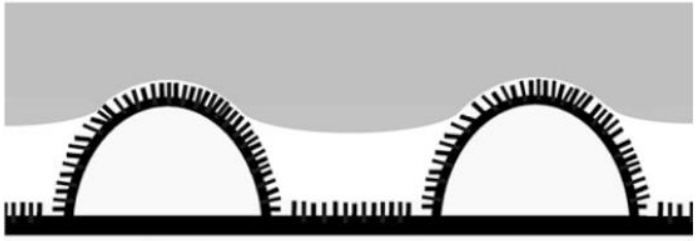

Superhydrophobic with low adhesion surface

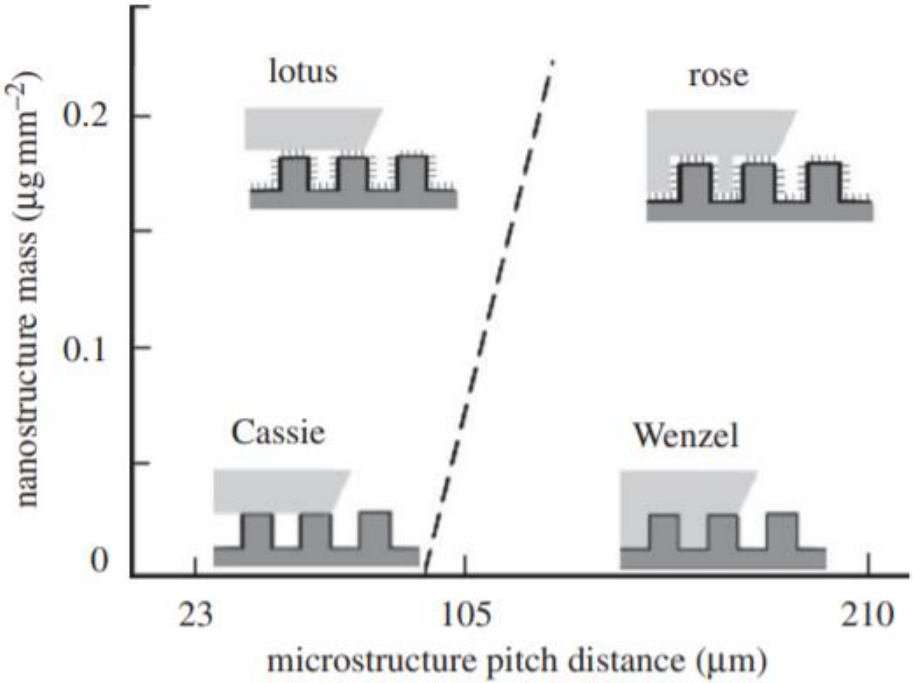

Modes of Superhydrophobicity

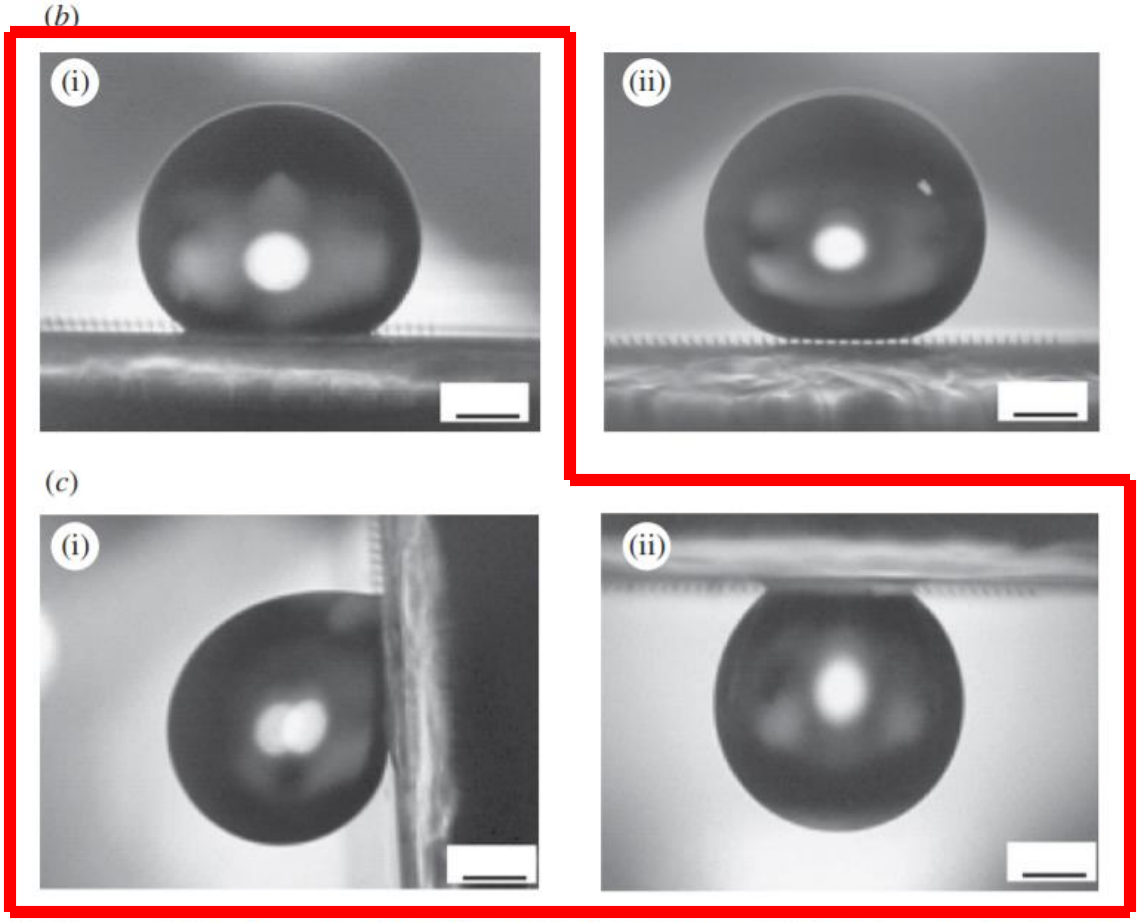

Figure 7. Shapes of droplets on various hierarchical structures. (*a*) Droplet on a horizontal surface of hierarchical structure with 23 μm pitch and 0.1 μg mm^{-2} *n*-hexatriacontane, showing air pocket formation. (*b*) Droplet on a horizontal surface of hierarchical structure with 105 μm pitch and (i) 0.1 μg mm^{-2} and (ii) 0.2 μg mm^{-2} *n*-hexatriacontane, showing (i) no air pocket and (ii) air pocket formation, respectively. (*c*) Droplet on inclined surfaces of hierarchical structure with 105 μm pitch and 0.1 μg mm^{-2} *n*-hexatriacontane, showing that droplet is still suspended when (i) vertical and (ii) upside down. Adapted from Bhushan & Her (2010). Scale bars, all 500 μm.

Modes of Superhydrophobicity

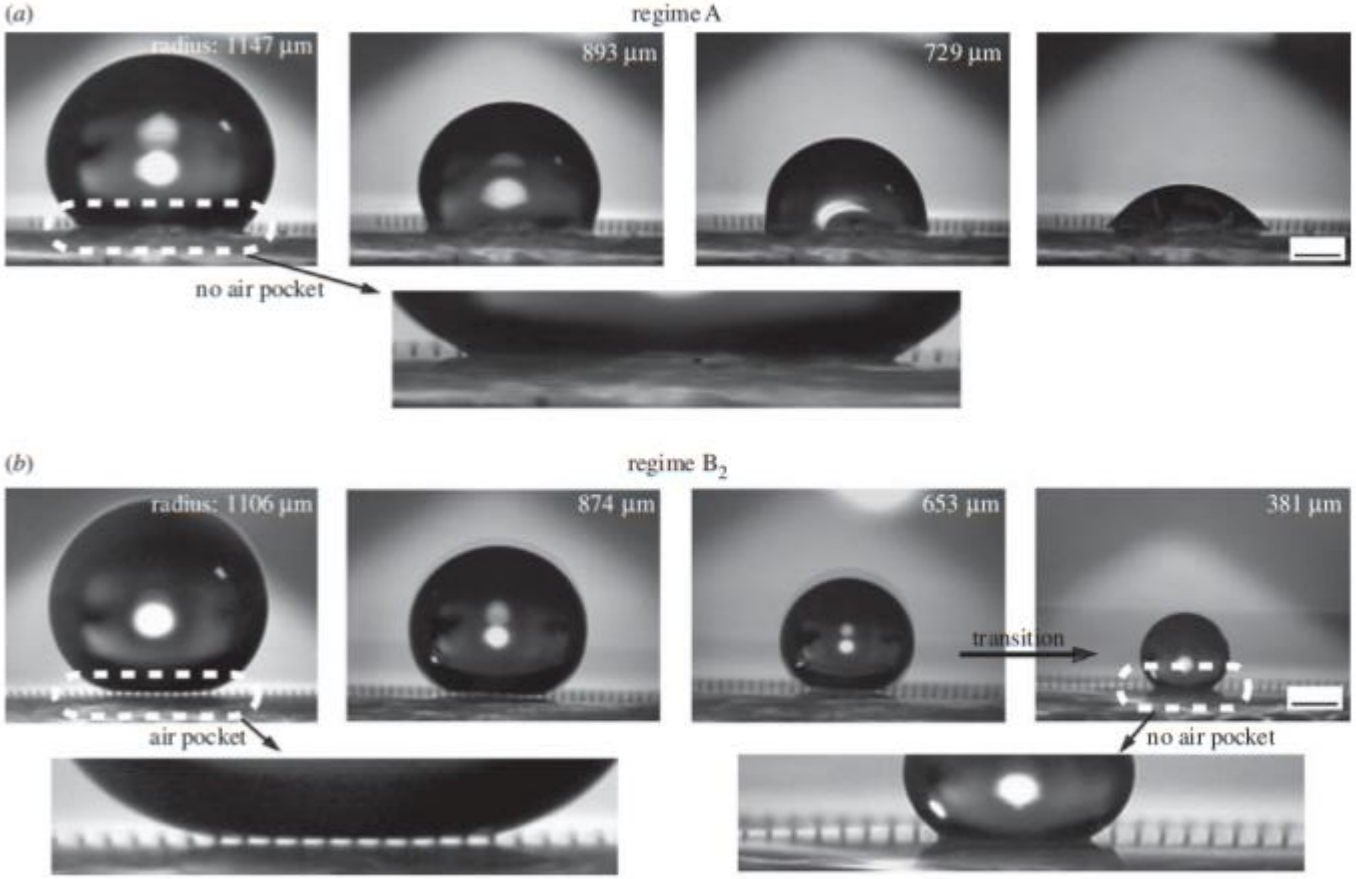

Figure 8. Optical micrographs of droplet evaporation on hierarchical structured surfaces with 105 µm pitch value and (*a*) 0.1 µg mm^{-2} or (*b*) 0.2 µg mm^{-2} *n*-hexatriacontane. (*a*) The 0.1 µg mm^{-2} *n*-hexatriacontane coated sample has no air pocket formed between the pillars in the entire contact area until evaporation was complete. (*b*) The 0.2 µg mm^{-2} *n*-hexatriacontane coated sample has an air pocket, and then transition from the lotus regime to the 'rose petal' regime occurs. Adapted from Bhushan & Her (2010). Scale bars, both 500 µm.

Design of general liquiphobic surfaces

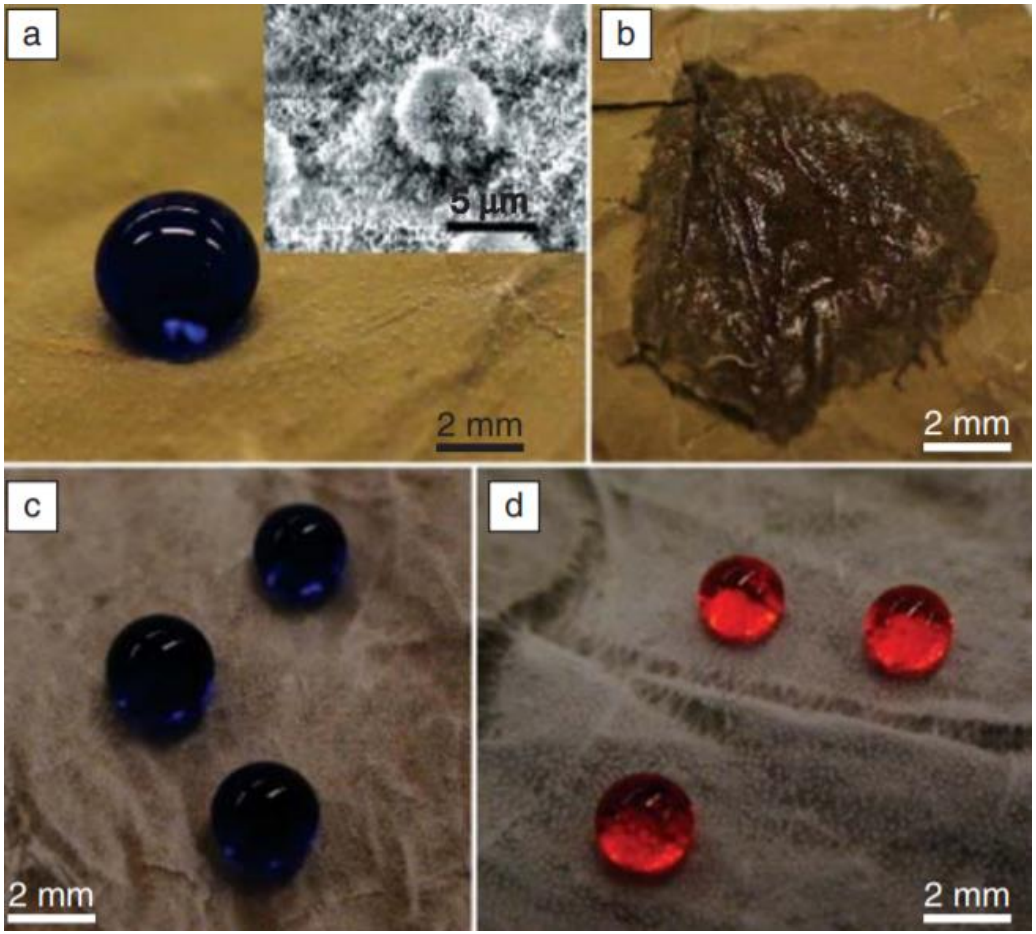

- **The matter of superhydrophobic surfaces is solved**
- **A fundamental problem in designing superoleophobic surfaces remains:**

$$\cos\theta_c = \frac{(\phi_s - 1)}{(r - \phi_s)}$$

Critical angle for transition Wenzel-Cassie

$\Rightarrow$ $\theta_c > 90°$

$\Rightarrow$ $\theta_0 > \theta_c > 90°$

BUT there are no materials with surface energy low enough to guarantee $\theta_0 > 90°$ with alkanes and other oily liquids

How to overcome this limitation?

HINT: Note that the wax on the lotus leaf is only weakly hydrophobic $\theta_0 = 74°$, so there must be a strong structural reason for superhydrophobicity!

Key Engineering Parameters

- Surface Energy
- Roughness
- Geometry

Role of re-entrant geometry

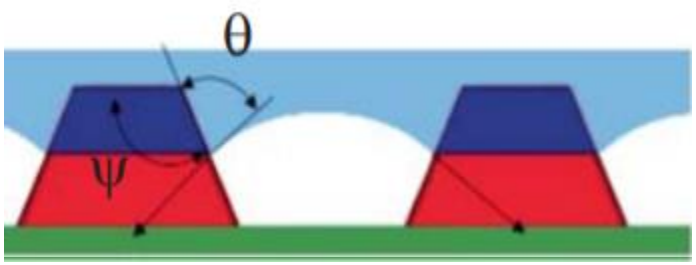

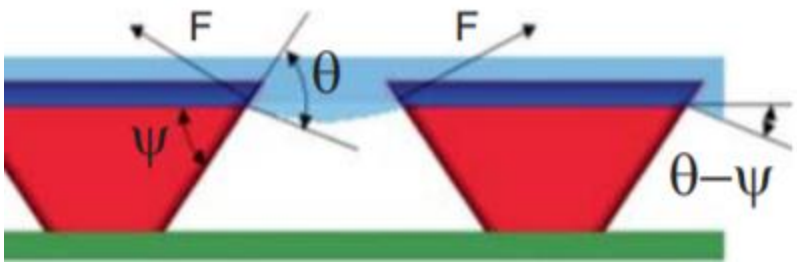

$\theta_0 > \theta_c > 90°$

Key Engineering Parameters

Variable angle structures: composite surface with any contact angle

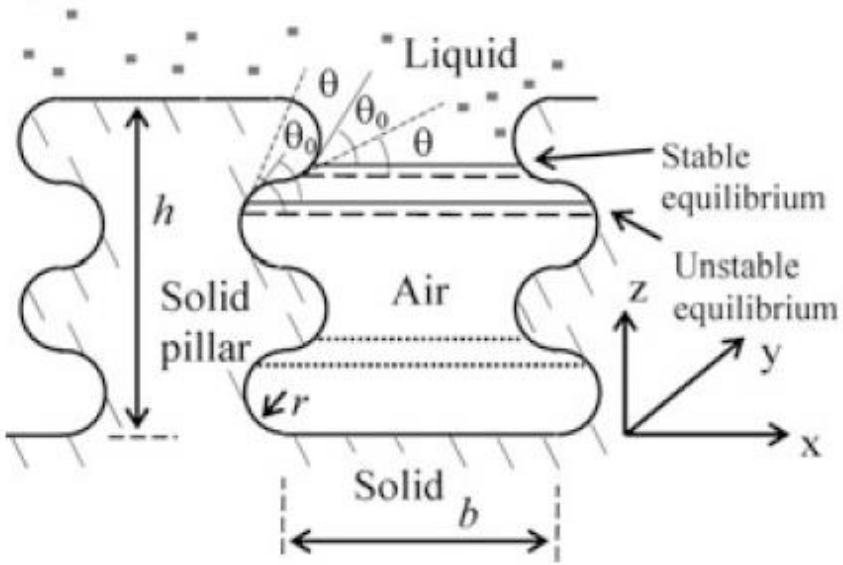

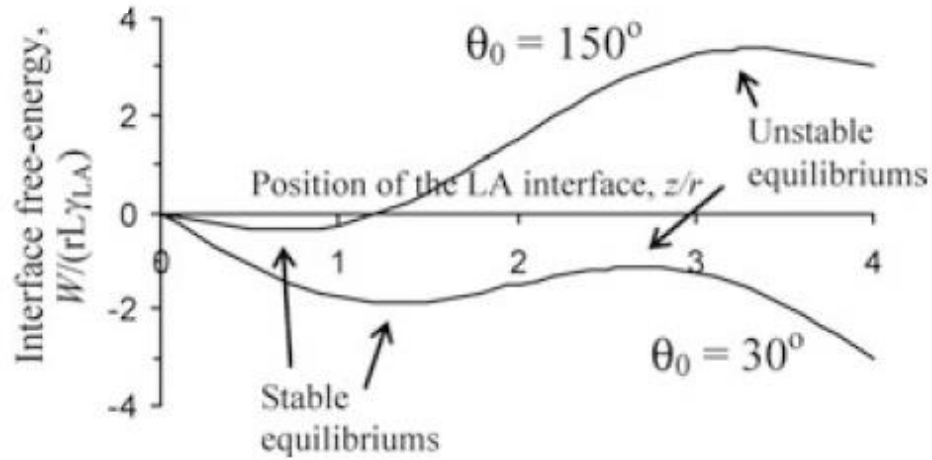

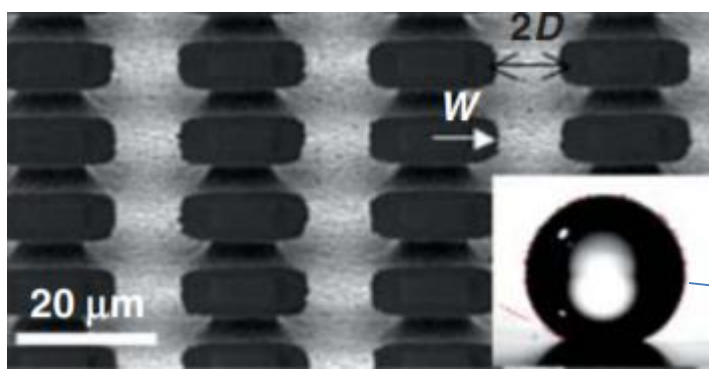

octane!!!

Key Engineering Parameters

Variable angle structures: composite surface with any contact angle

Use of a mixture of PMMA and fluoroPOSS to systematically change the contact angle

Plot *adv* and *rec* angles for smooth vs rough (reentrant) surfaces

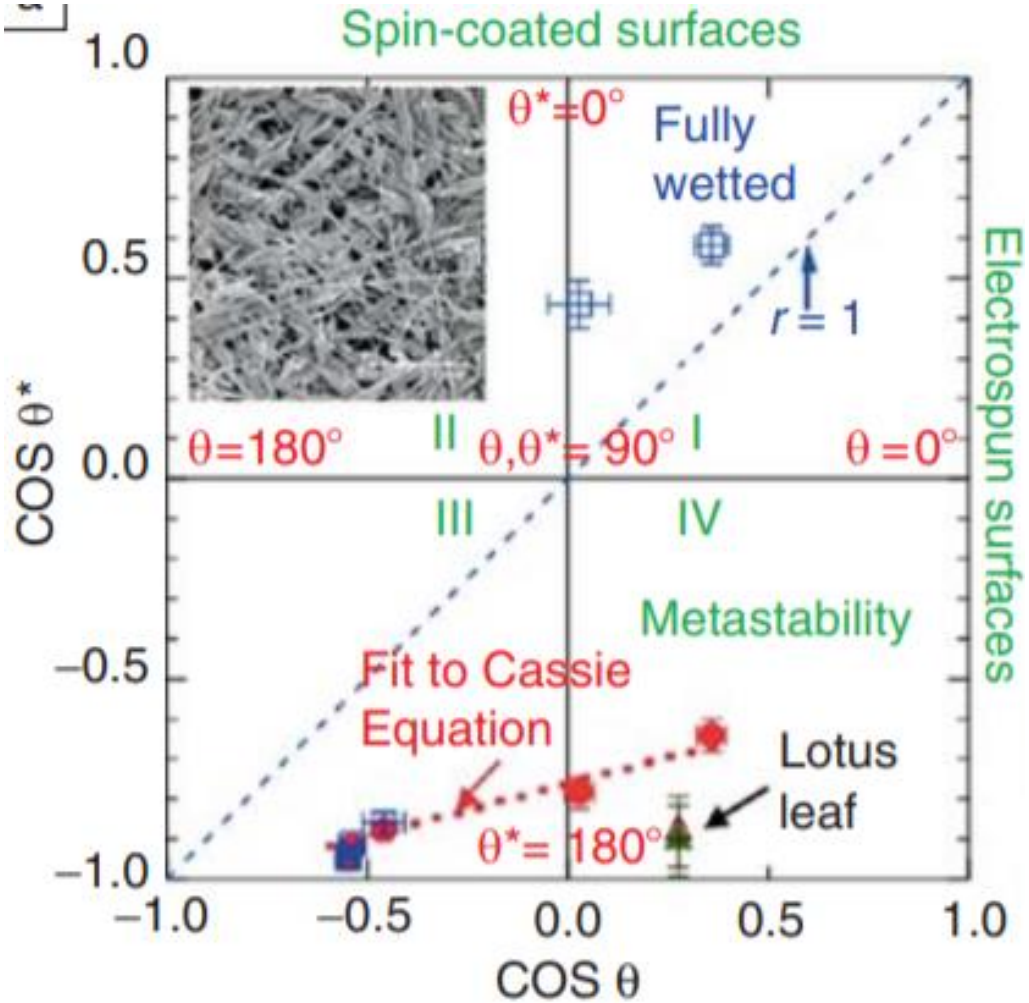

Robustness

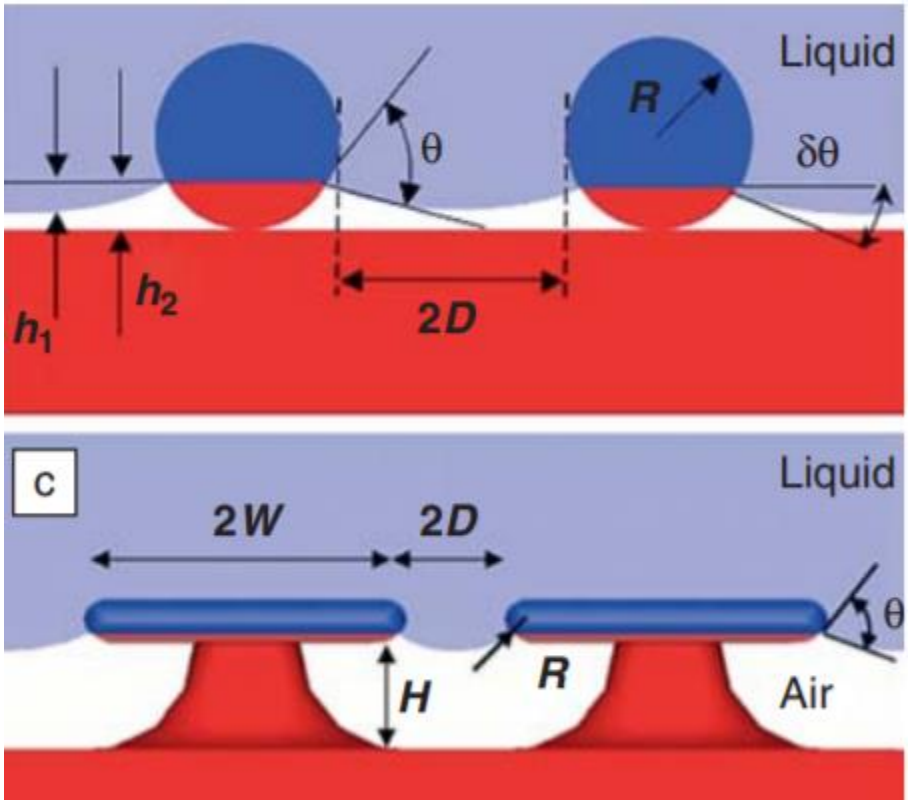

Hodoos

Engineering Surfaces for Liquiphobicity

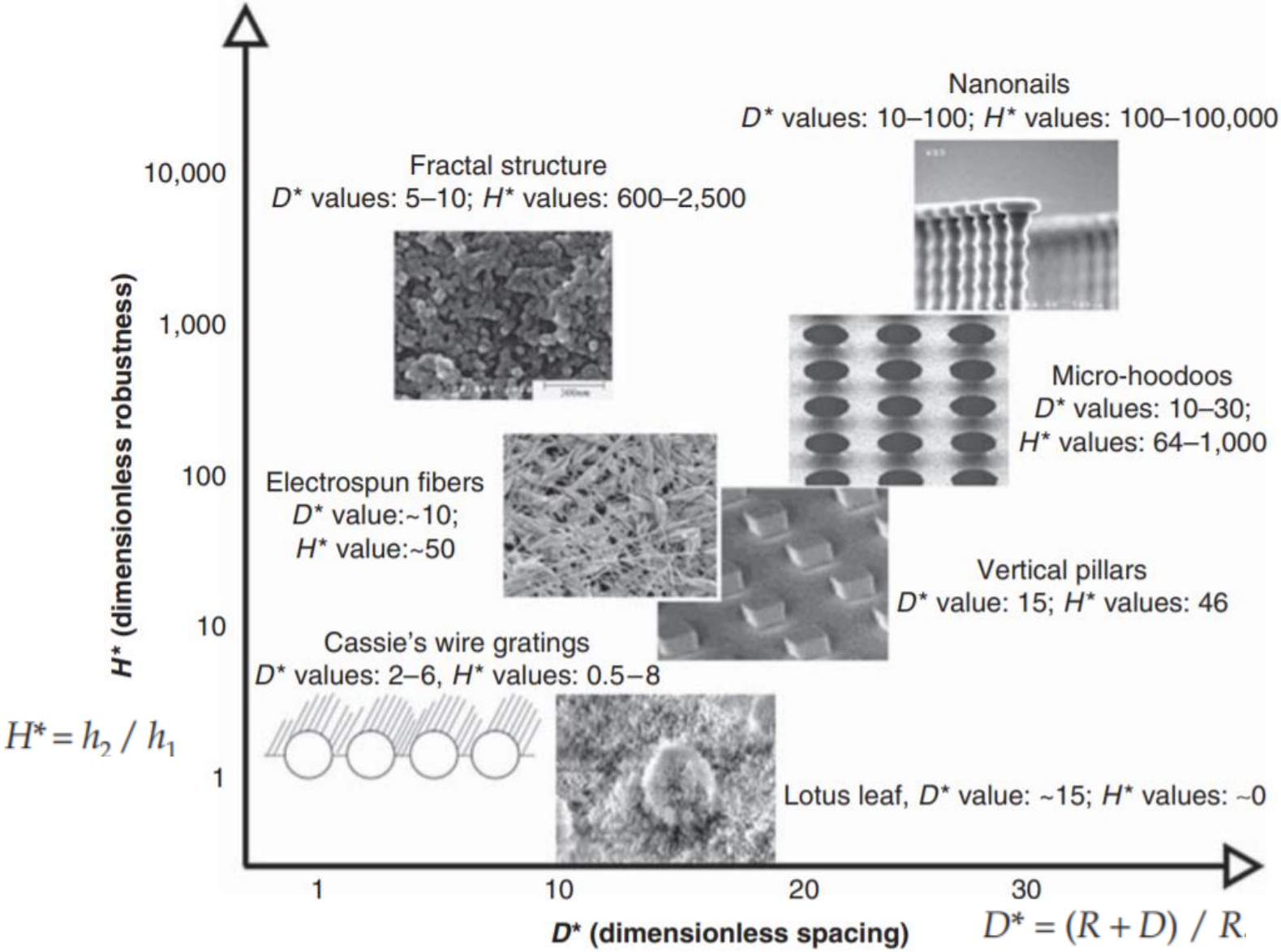

Engineering Surfaces for Liquiphobicity

Table I: Values of the Apparent Contact Angles (θ^*) with Water and Octane and Corresponding Values of the Robustness Parameter H^* for Various Natural and Artificial Surfaces Discussed in the Literature.

	Water			Octane		
	θ^* (deg)	H^*	$\theta - \psi^a$ (deg)	θ^* (deg)	H^*	$\theta - \psi^a$ (deg)
Vertical pillars[23]	~160	~70	30	0	~50	–30
Fractal structure[8 b]	~165	740–3,800	75	0	600–2,500	0
Cassie's wire gratings[19]	~150	3.4–34	105	NA[d]	0.5–8	45
Electrospun fiber surface[6]	~165	~210	120	~140	~50	60
Lotus leaf[c]	~155	~180	~15	0	~0	NA[d]
Micro-hoodoos[6]	~165	95–1,500	120	140–165	64–1,000	60
Nanonails[10]	~150	150–150,000	120	130–150	100–100,000	60

[a]Any liquid for which $\theta - \psi < 0°$ will immediately yield a fully wetted interface.
[b]The reentrant angle ψ is hard to measure on randomly shaped textures. On these fractal-like structures, ψ is expected to be ~45° as octane penetrates into the surface texture.
[c]The geometry of the lotus leaf has been estimated through the inspection of various published scanning electron microscopy (SEM) images and is possibly prone to error.
[d]Not available.

Engineering surfaces for selective liquiphobicity

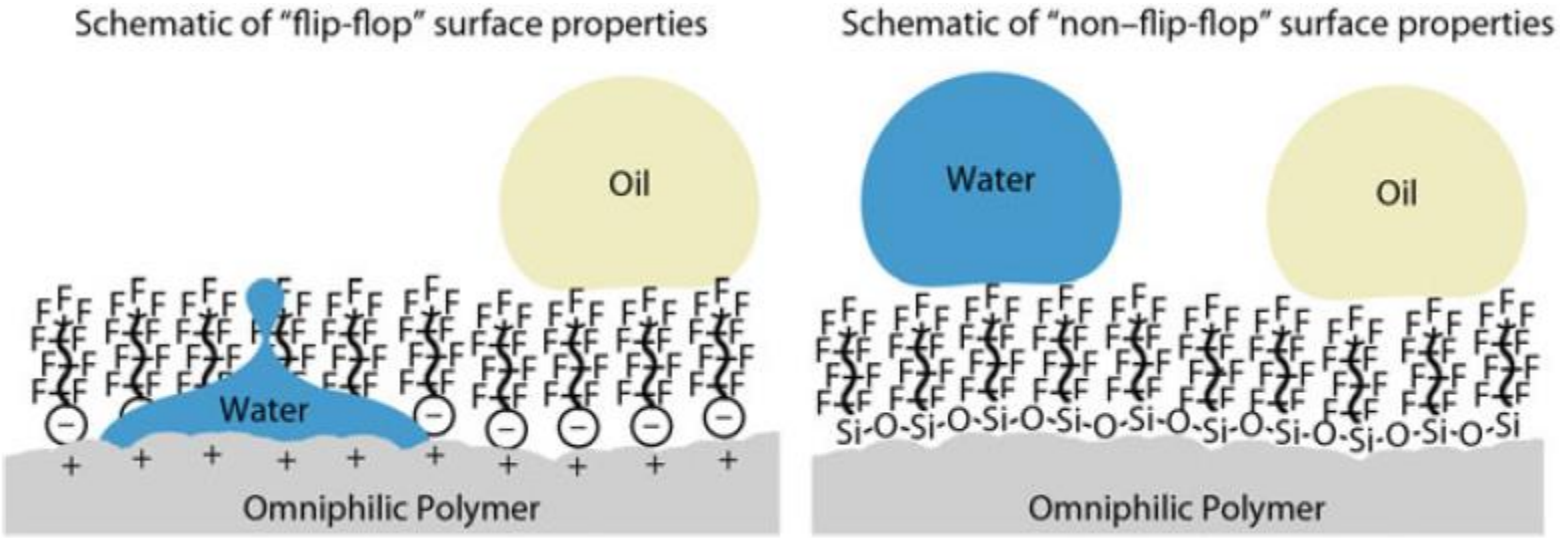

Self-cleaning

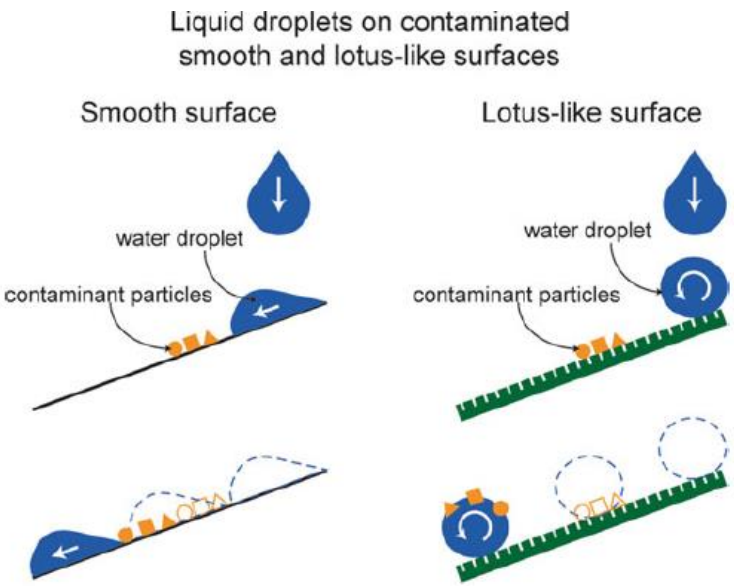

(a)

Water droplet cleaning Lotus leaf

Mercury droplet cleaning Taro leaf

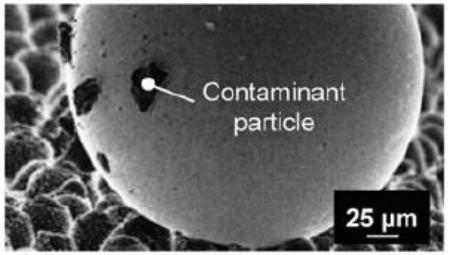

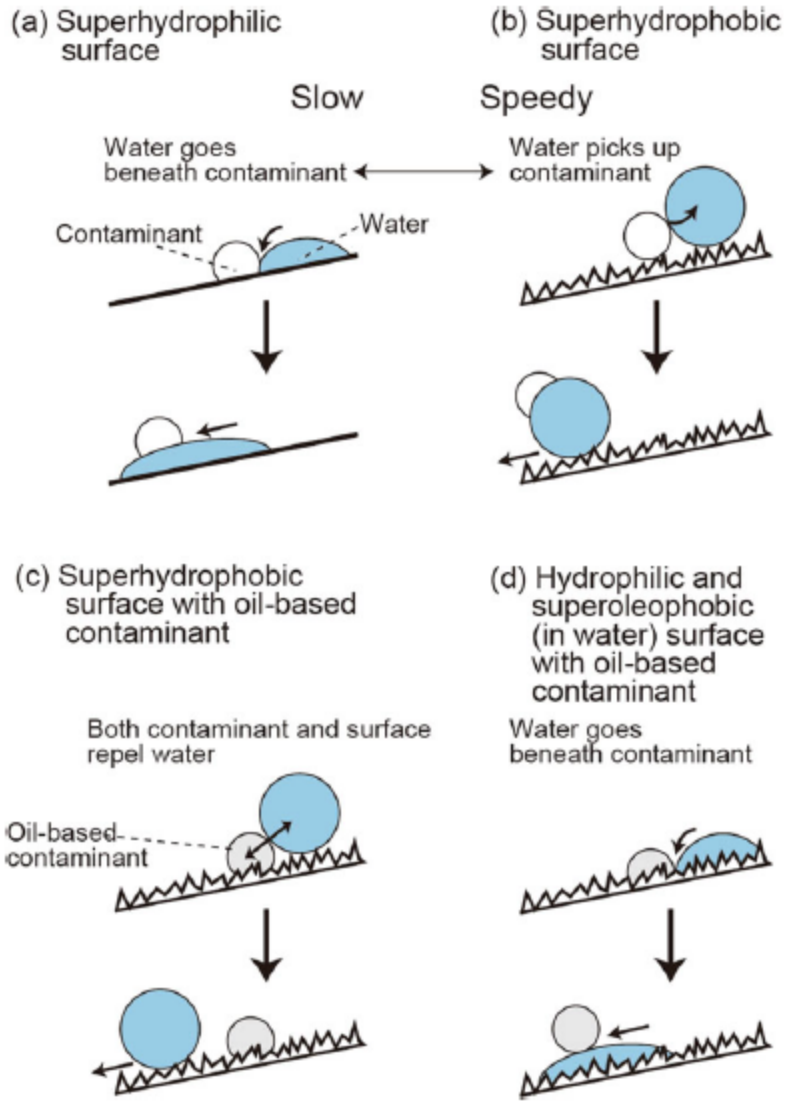

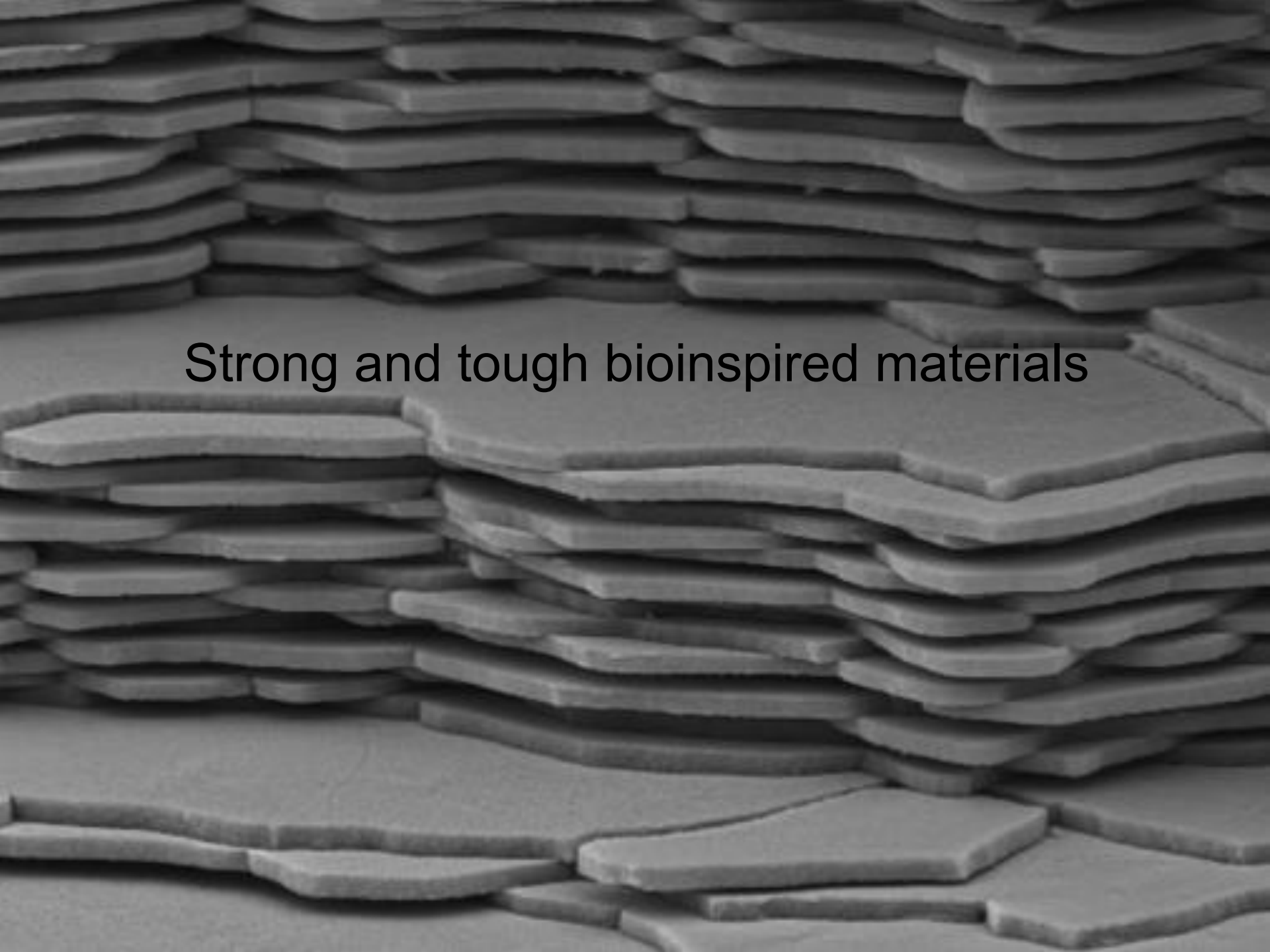

Strong and tough bioinspired materials

Structural Materials

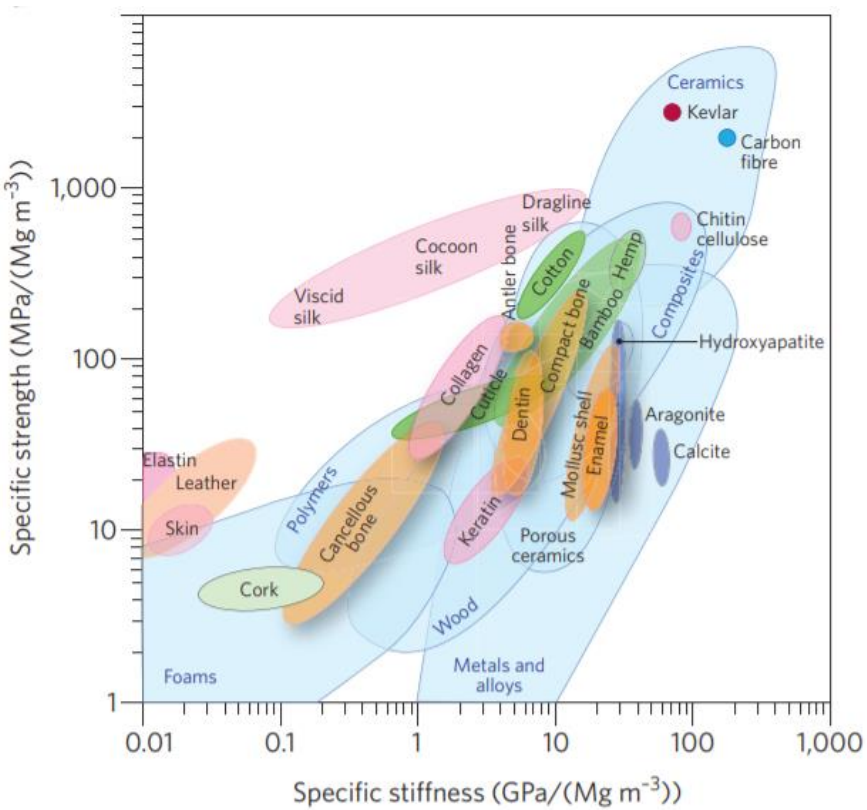

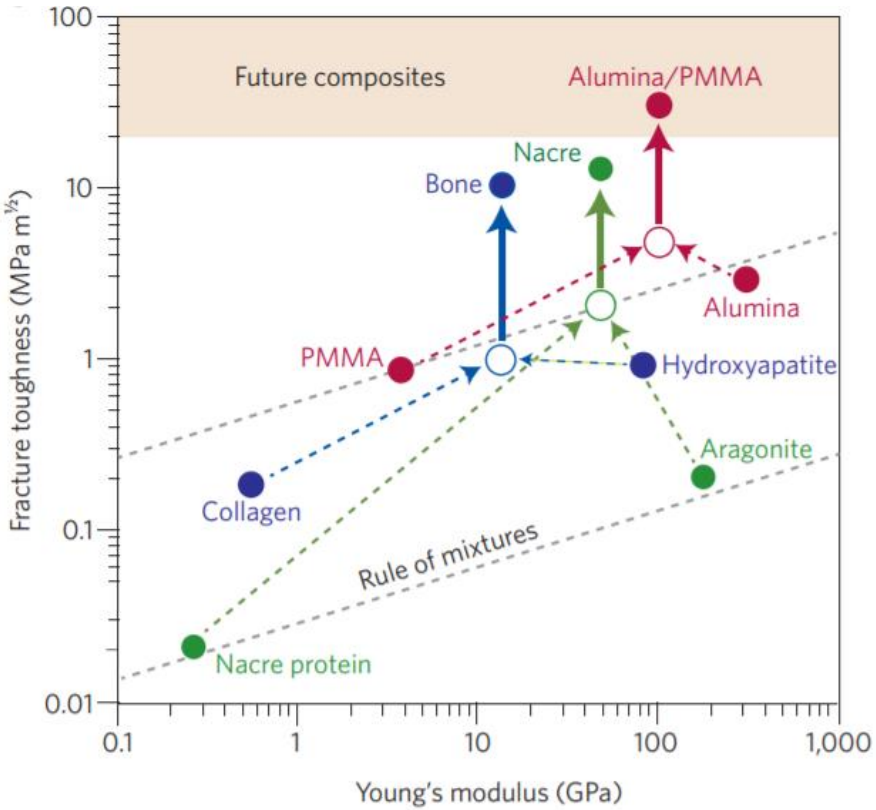

DOI: 10.1038/NMAT4089

Biopolymers

Microstructure and mechanical properties

Unfurling and straightening $\frac{d\sigma}{d\varepsilon} \propto \varepsilon^n \quad (n > 1)$

Chain bone stretching $\frac{d\sigma}{d\varepsilon} \propto E$

$$\sigma = k_1 \varepsilon^{n+1} + H(\varepsilon_c) E(\varepsilon - \varepsilon_c)$$

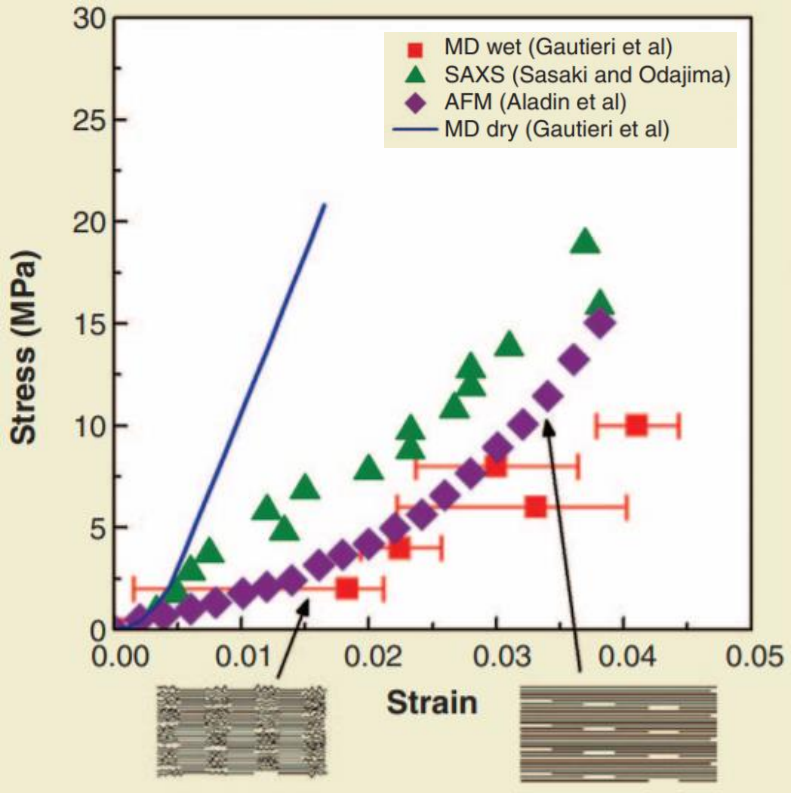

doi: 10.1126/science.1220854

Biopolymers

Spider silk

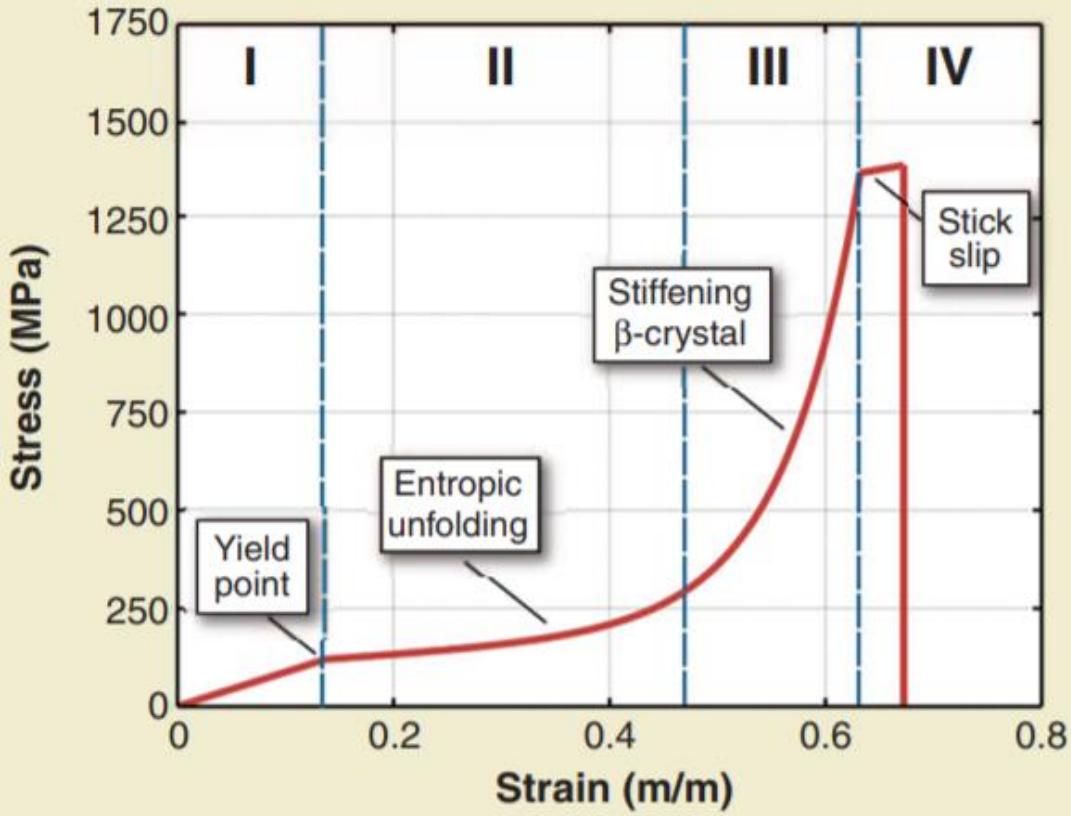

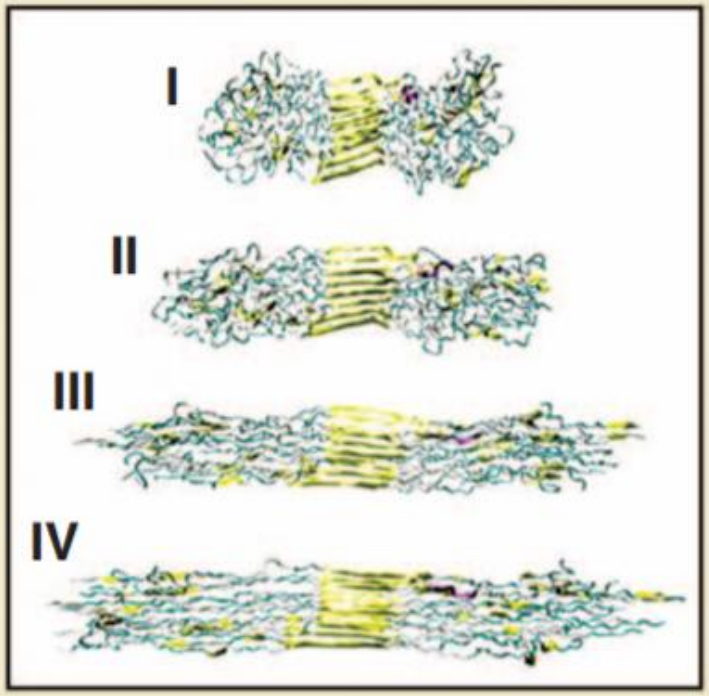

Fibroin stretching mechanism

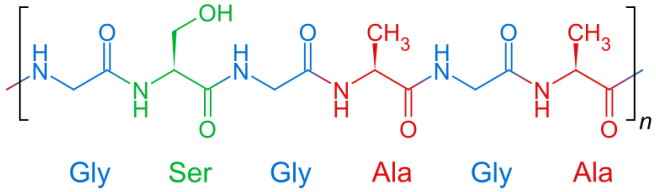

doi: 10.1126/science.1220854

Bone

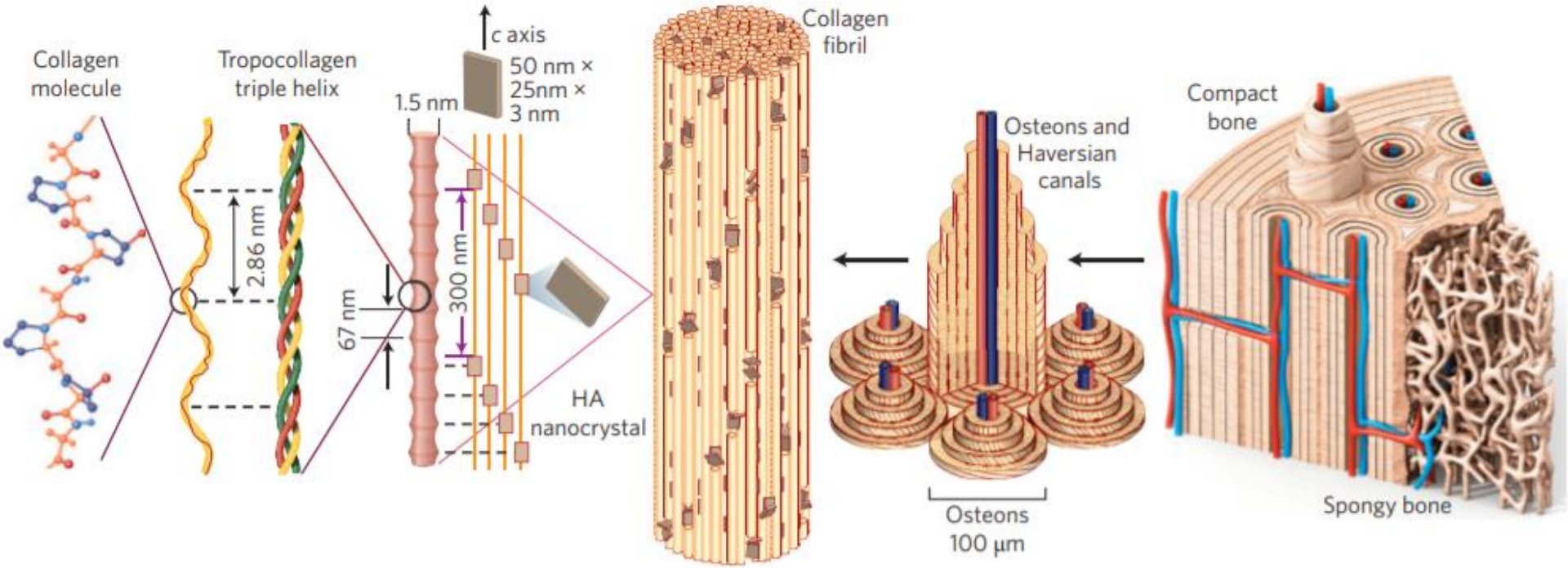

DOI: 10.1038/NMAT4089

Similarity between bone and bamboo

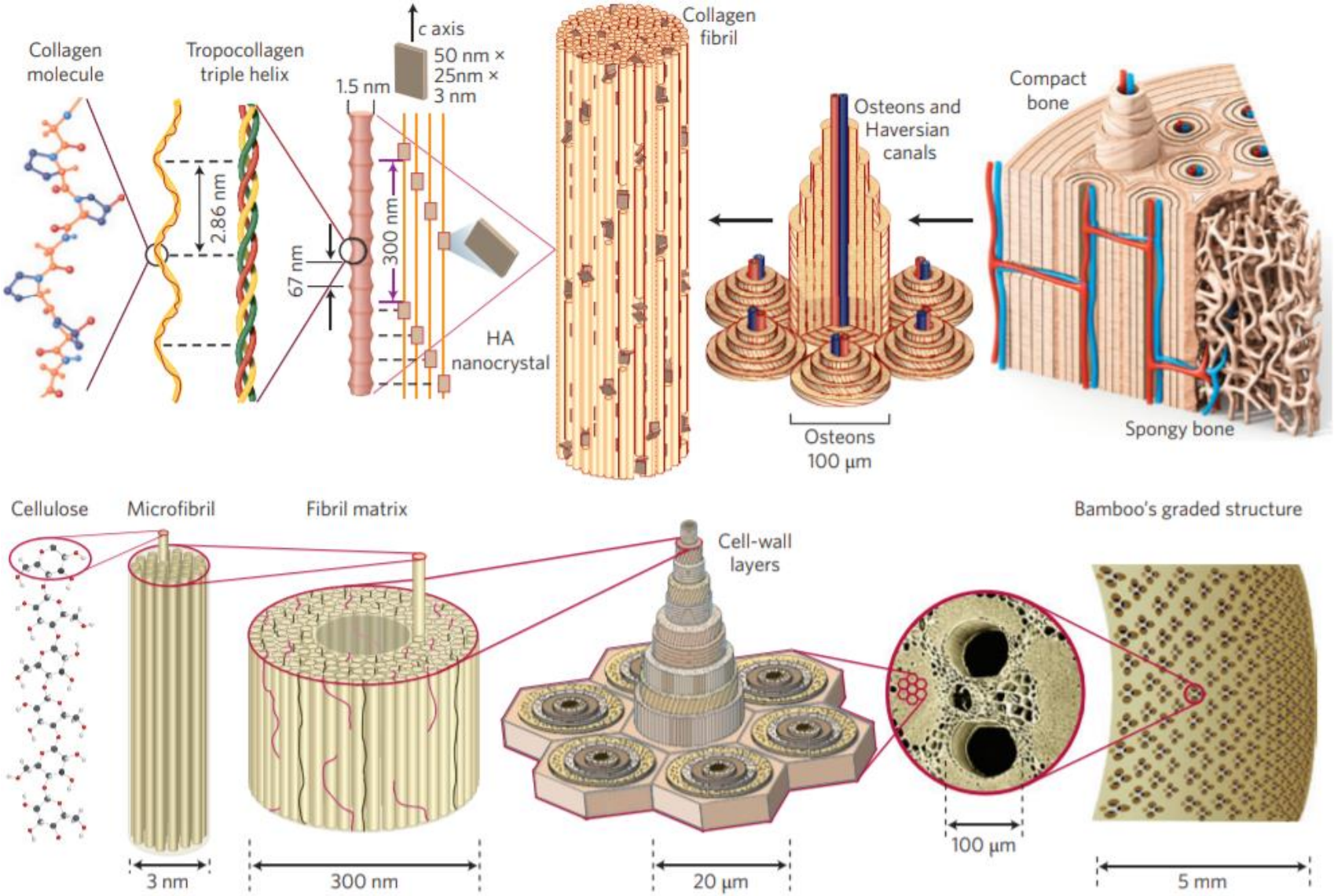

DOI: 10.1038/NMAT4089

Bone

Toughening mechanisms

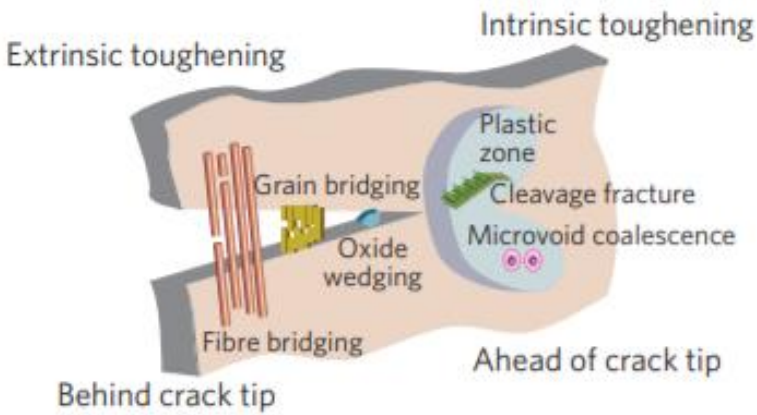

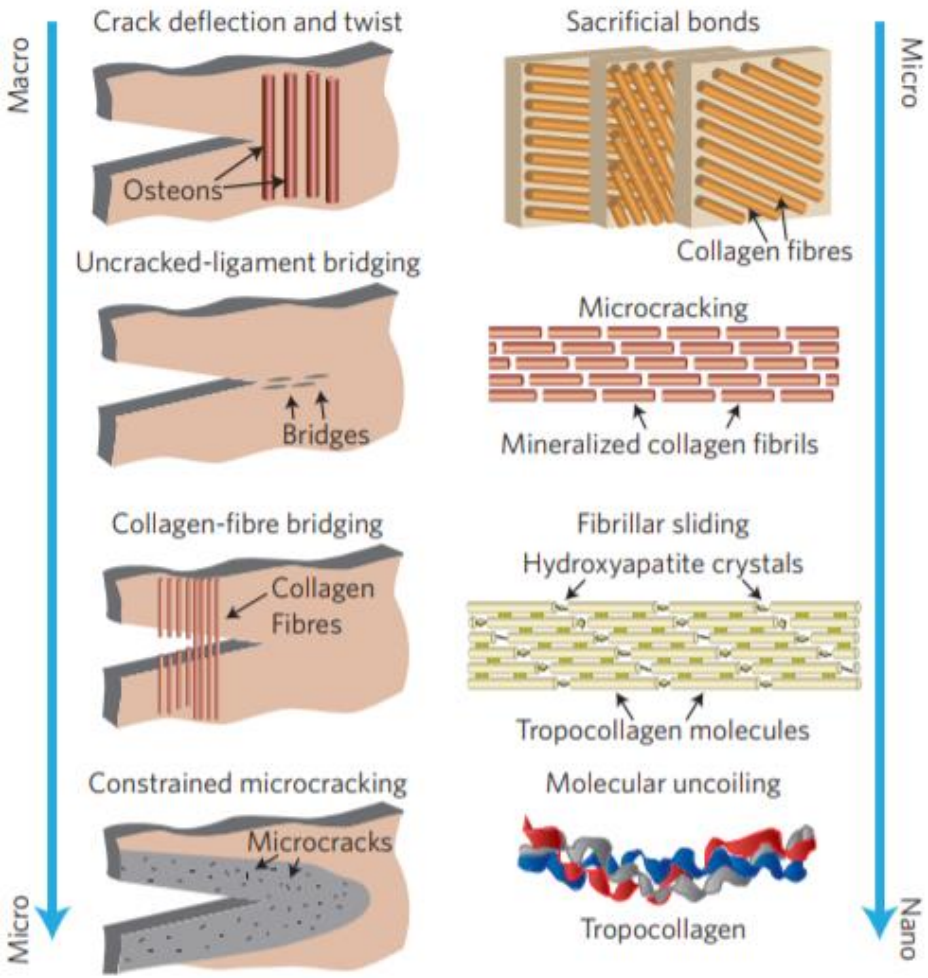

DOI: 10.1038/NMAT4089

Nacre

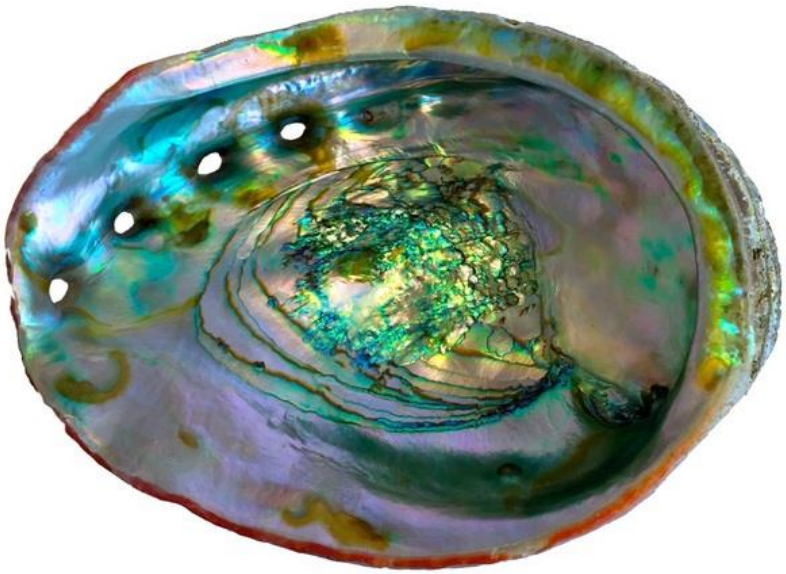

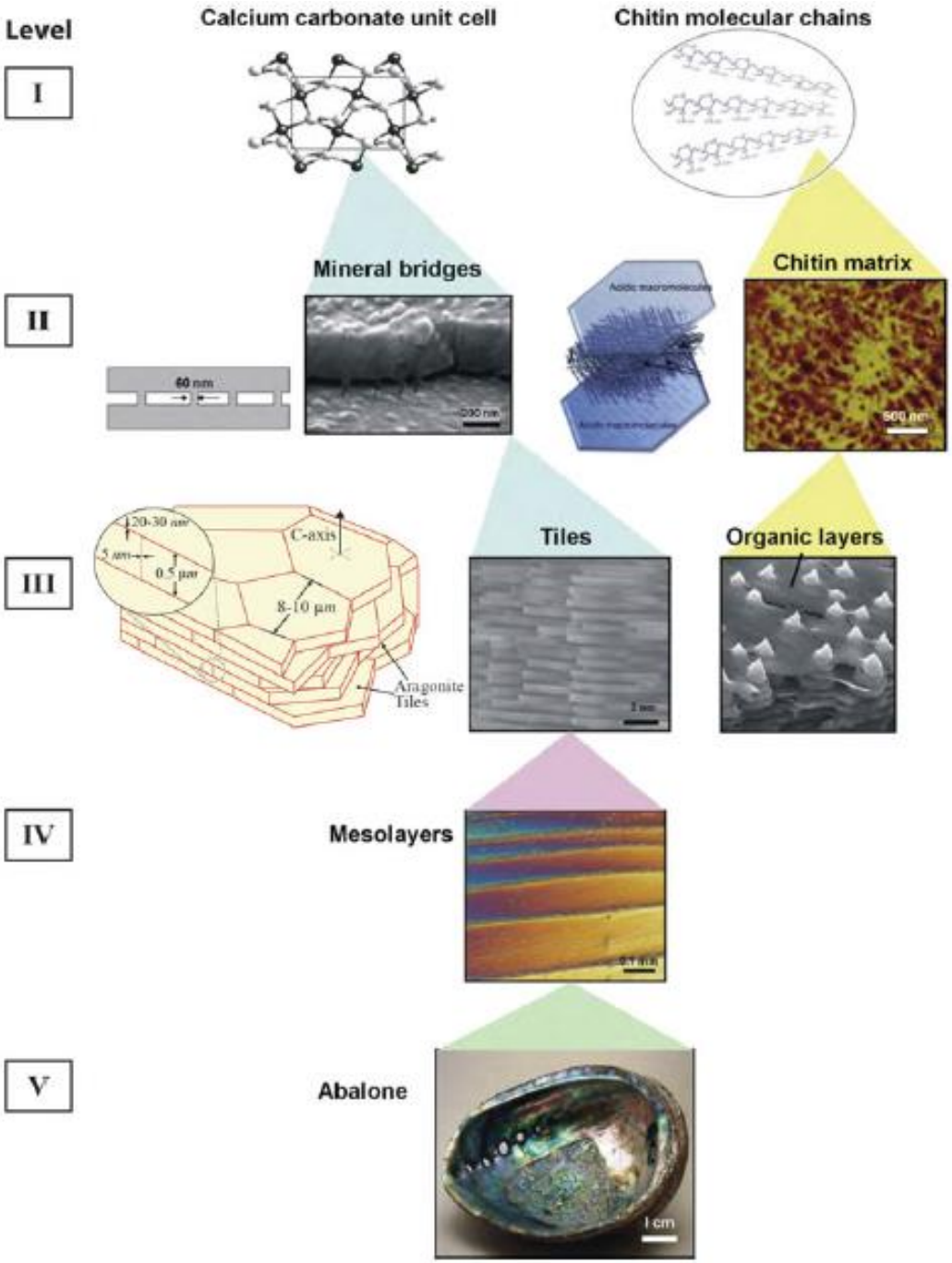
Level
I
II
III
IV
V
Calcium carbonate unit cell
Chitin molecular chains
Mineral bridges
Chitin matrix
60 nm
Tiles
Organic layers
20-30 nm
5 nm
0.5 µm
C-axis
8-10 µm
Aragonite Tiles
Mesolayers
Abalone
1 cm

Nacre

Hierarchical architecture and selected toughening mechanisms

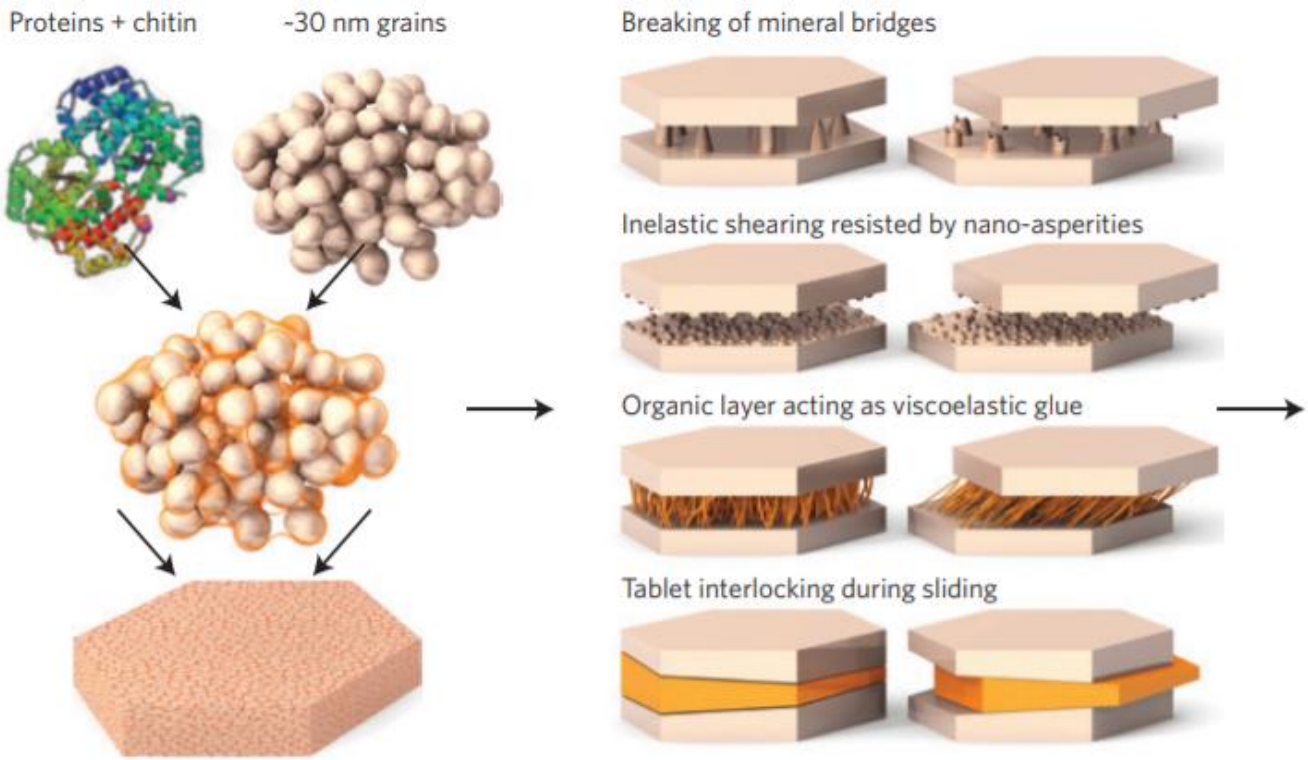

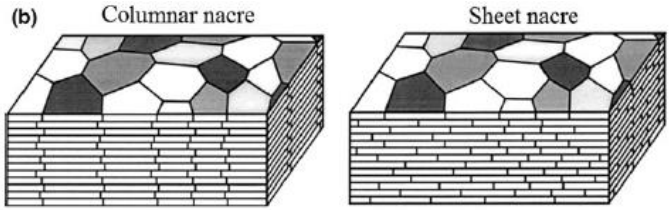

DOI: 10.1038/NMAT4089

Nacre

Toughening mechanisms

Crack deflection at soft interlayers
Crack bridging
Breaking of mineral bridges
Viscoelastic behavior of organic component
Tablet interlock
Plastic deformation ahead of the crack
Crack blunting
Nanograin rotation

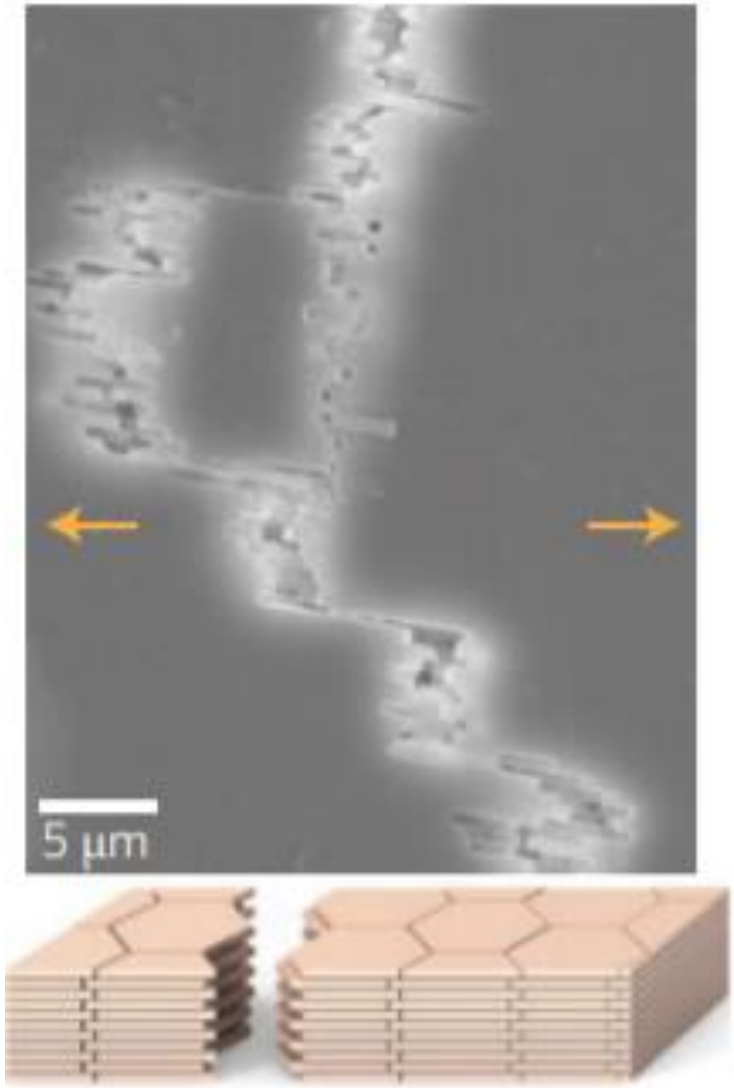

DOI: 10.1038/NMAT4089

Nacre

Toughening mechanisms: nano grain rotation

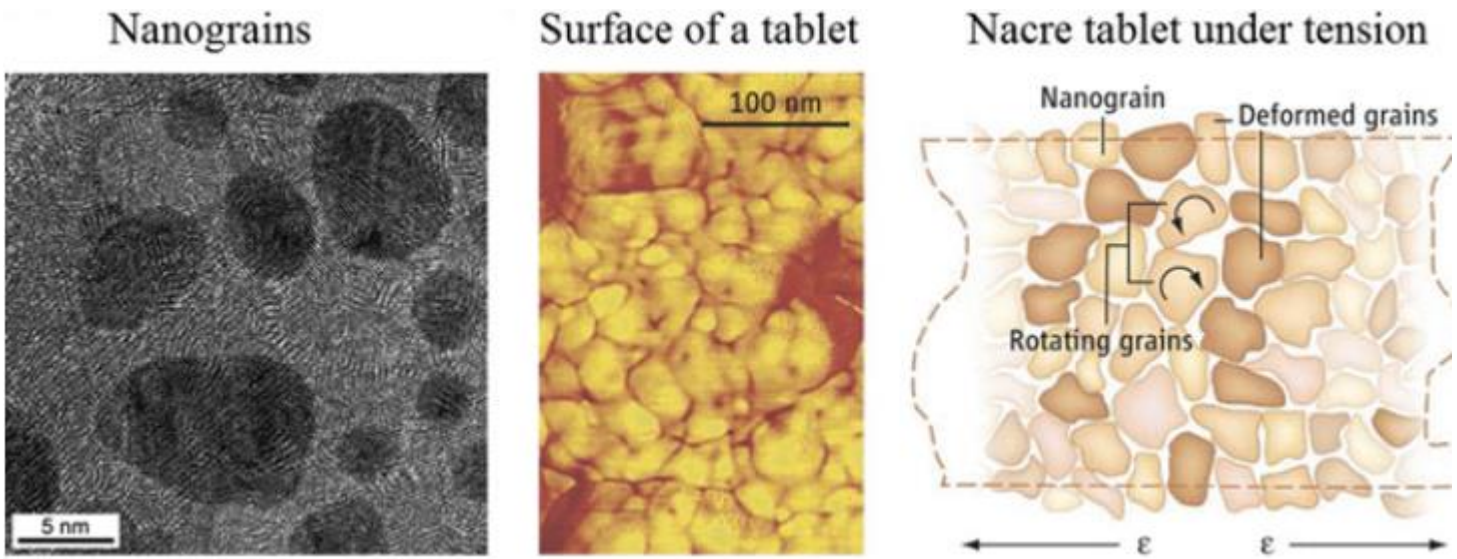

DOI: 10.1038/NMAT4089

Nacre: mechanical properties

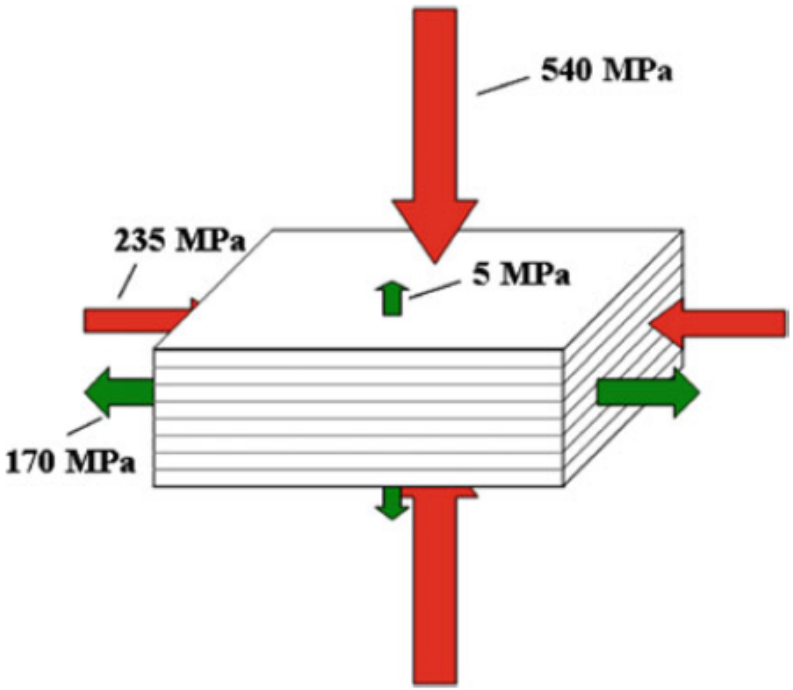

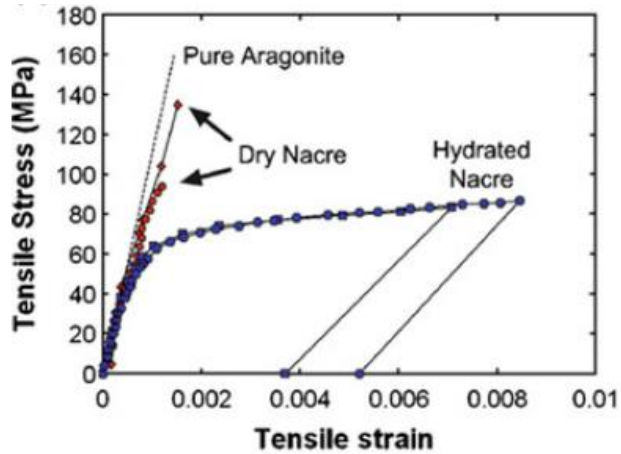

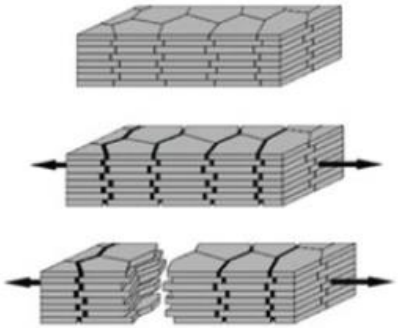

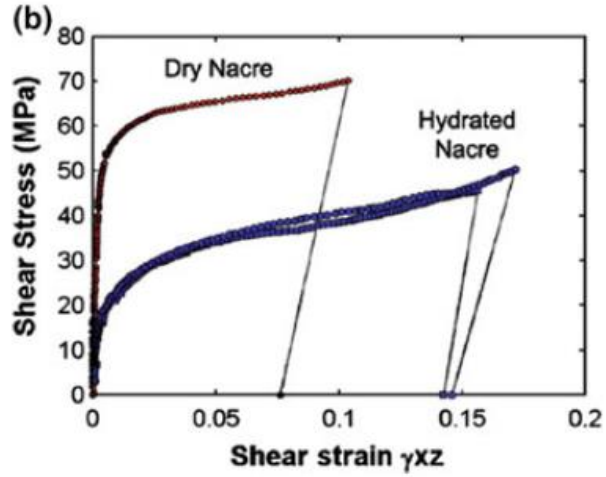

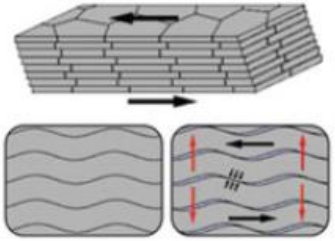

Nacre: mechanical properties

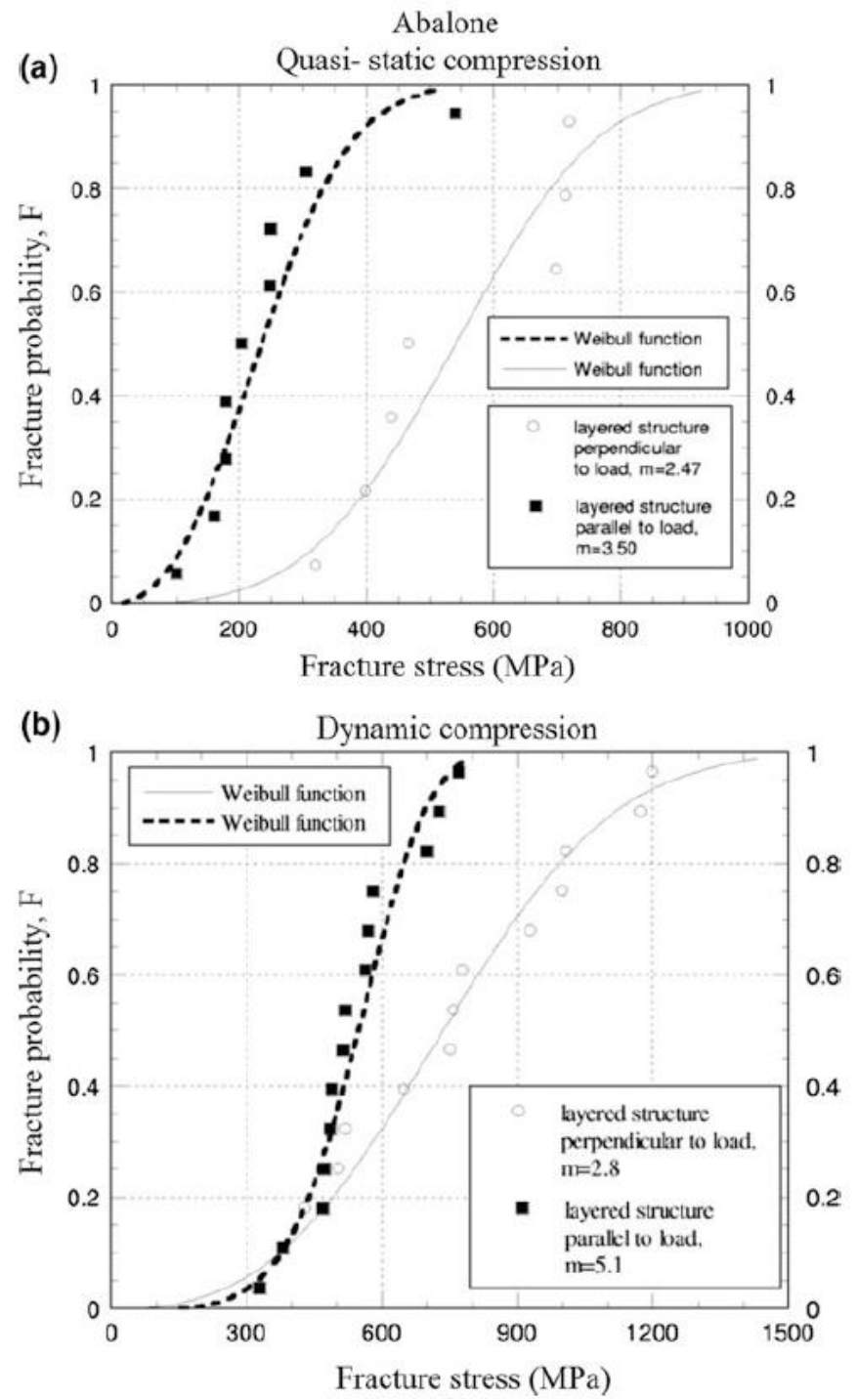

Nacre-like hybrids

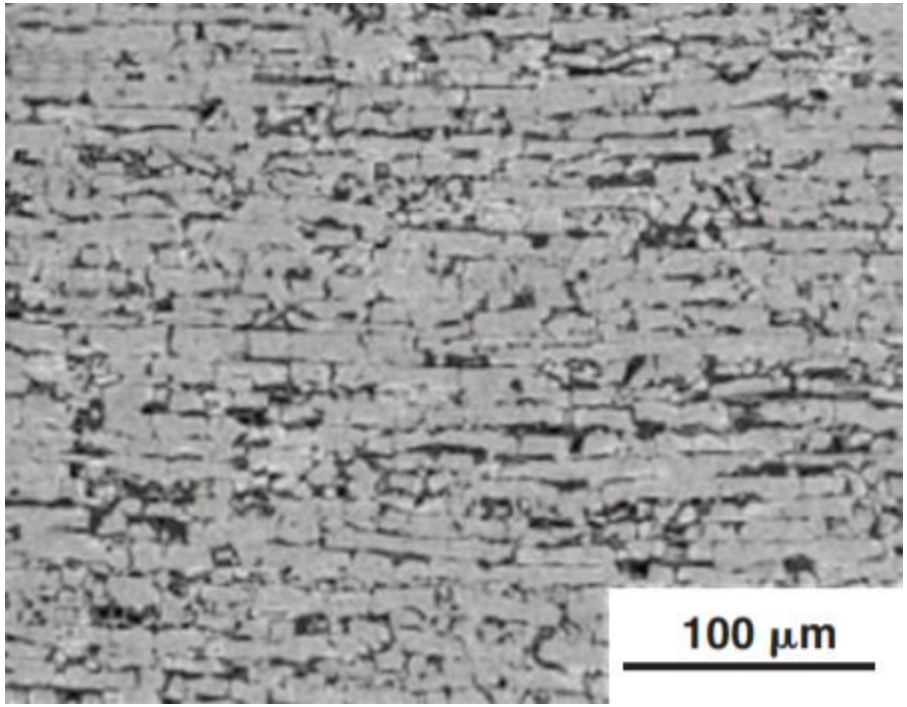

Mechanical properties

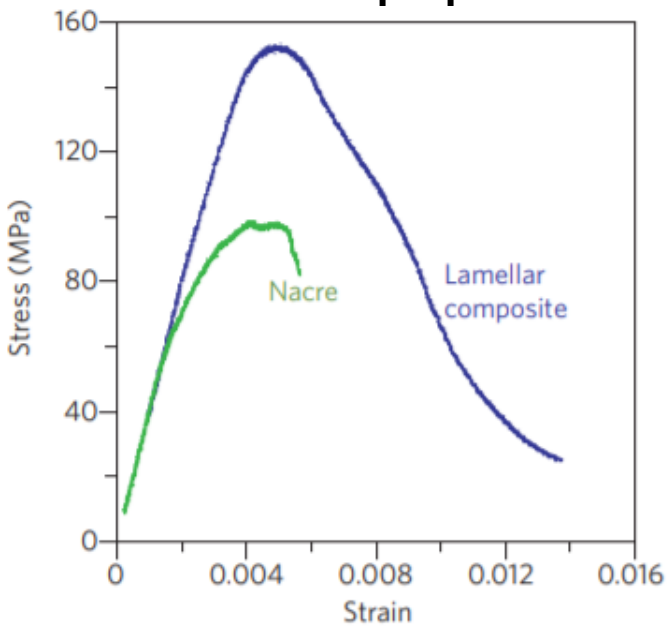

Toughness

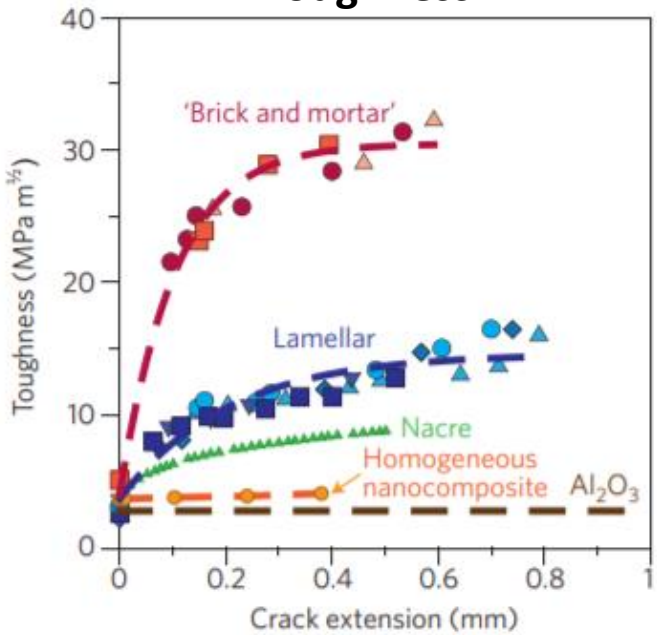

DOI: 10.1038/NMAT4089

Nacre-inspired structures

Alumina / Cyanate Ester Composite (freeze casting + CE infusion

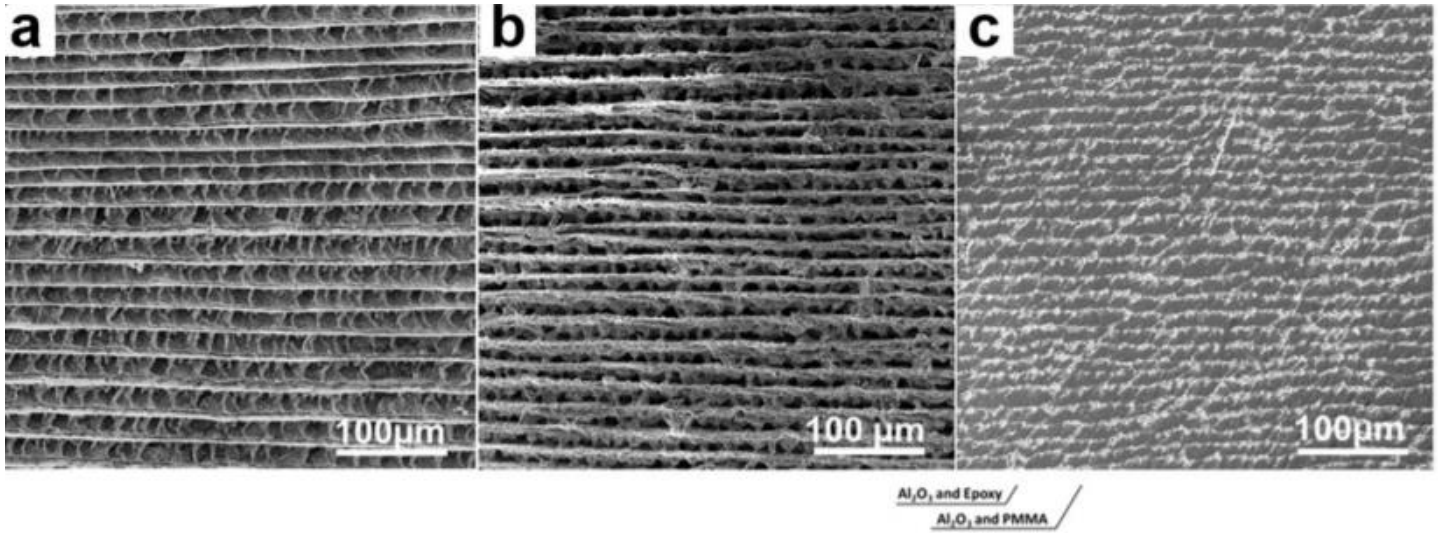

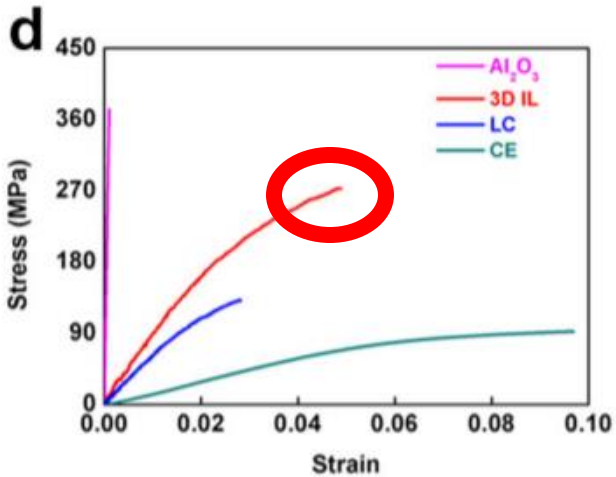

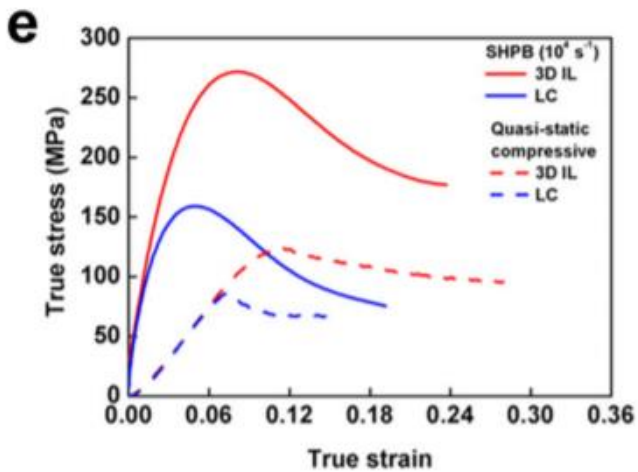

DOI 10.1038/s41427-018-0009-6

Nacre-inspired structures

High content Alumina (98%) + silica-calcia glassy phase

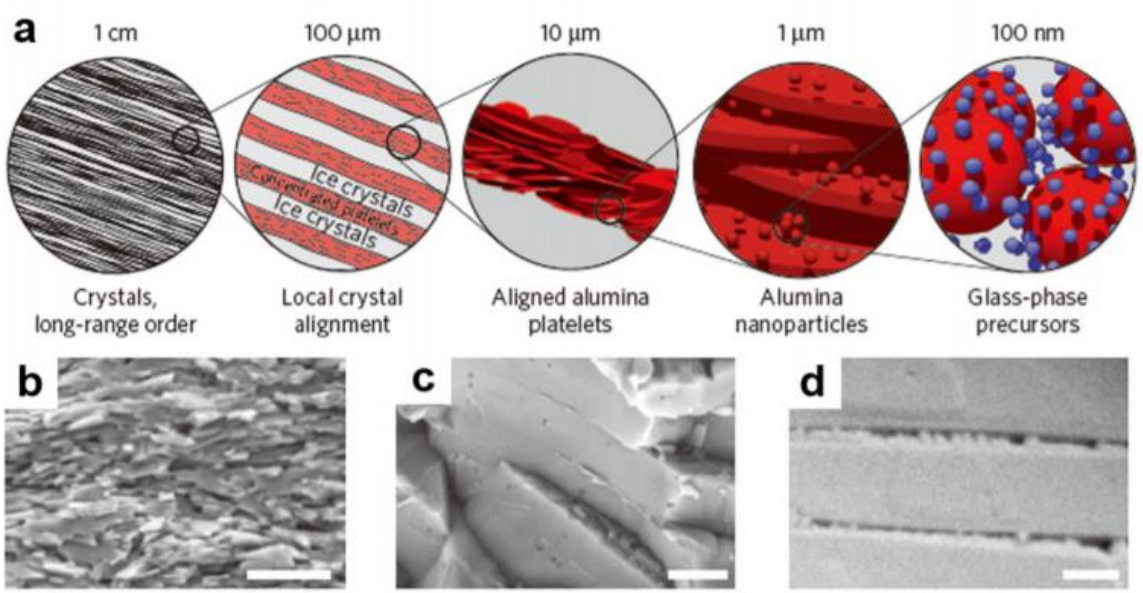

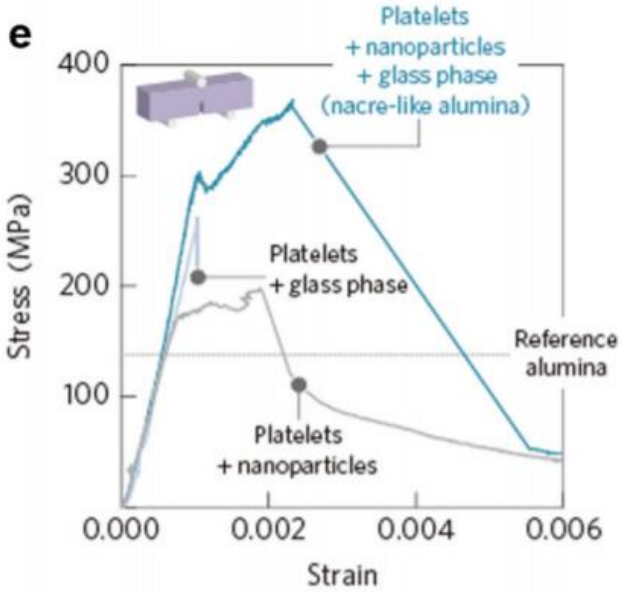

High strength (480 MPa) and high fracture toughness (22 MPa $m^{0.5}$)

DOI 10.1038/s41427-018-0009-6

Nacre-inspired structures

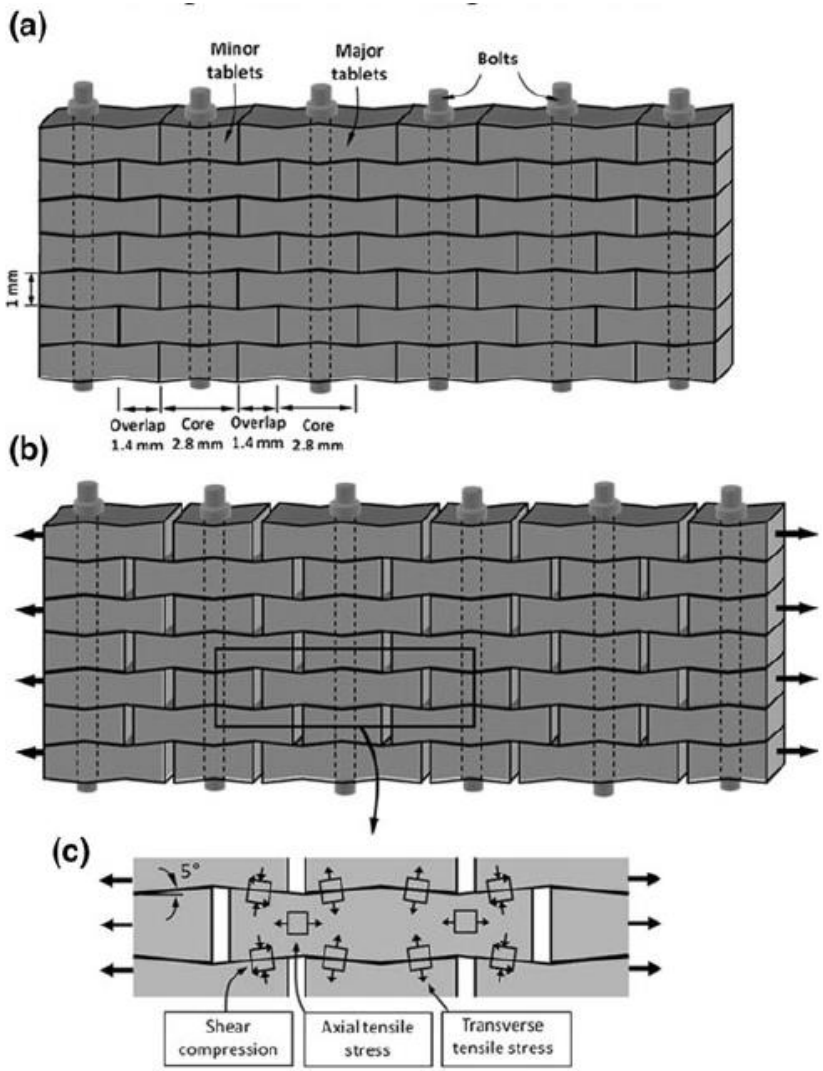

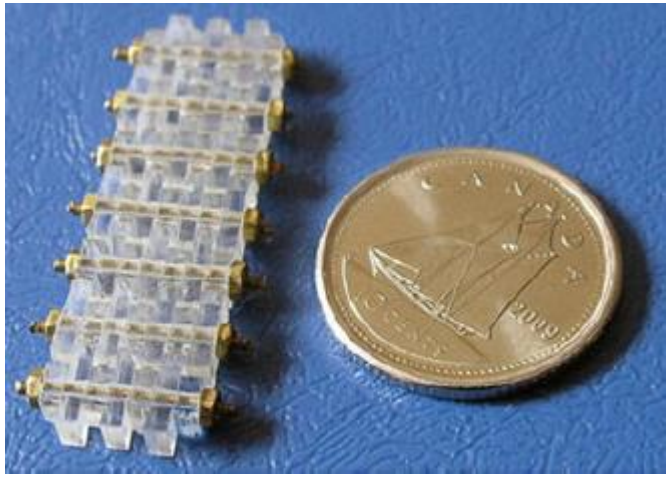

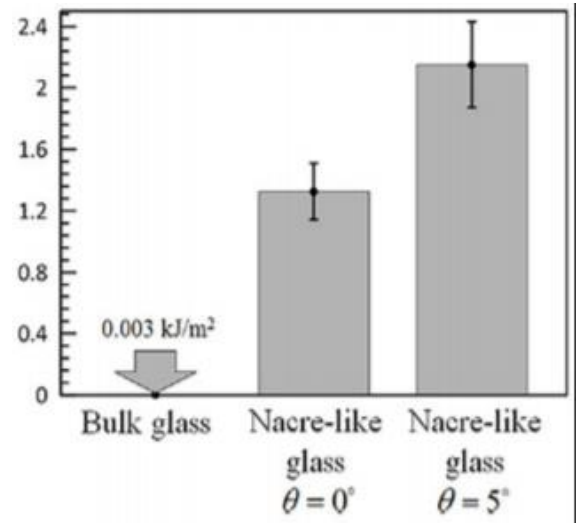

Nacre-inspired structures

Bioinspired nacre structural materials	Scale	Fracture toughness (MPa $\sqrt{m}$)
Al/Al–Si	μm	5.5–10
Al_2O_3/Al–Si	μm	40
Al_2O_3/PMMA[a]	μm	30
Al_2O_3/TiO_2	mm	12
$SiC/Al_2O_3–Y_2O_3$	mm	14
Si_3N_4/BN	mm	28

Fabrication of nacre-like materials

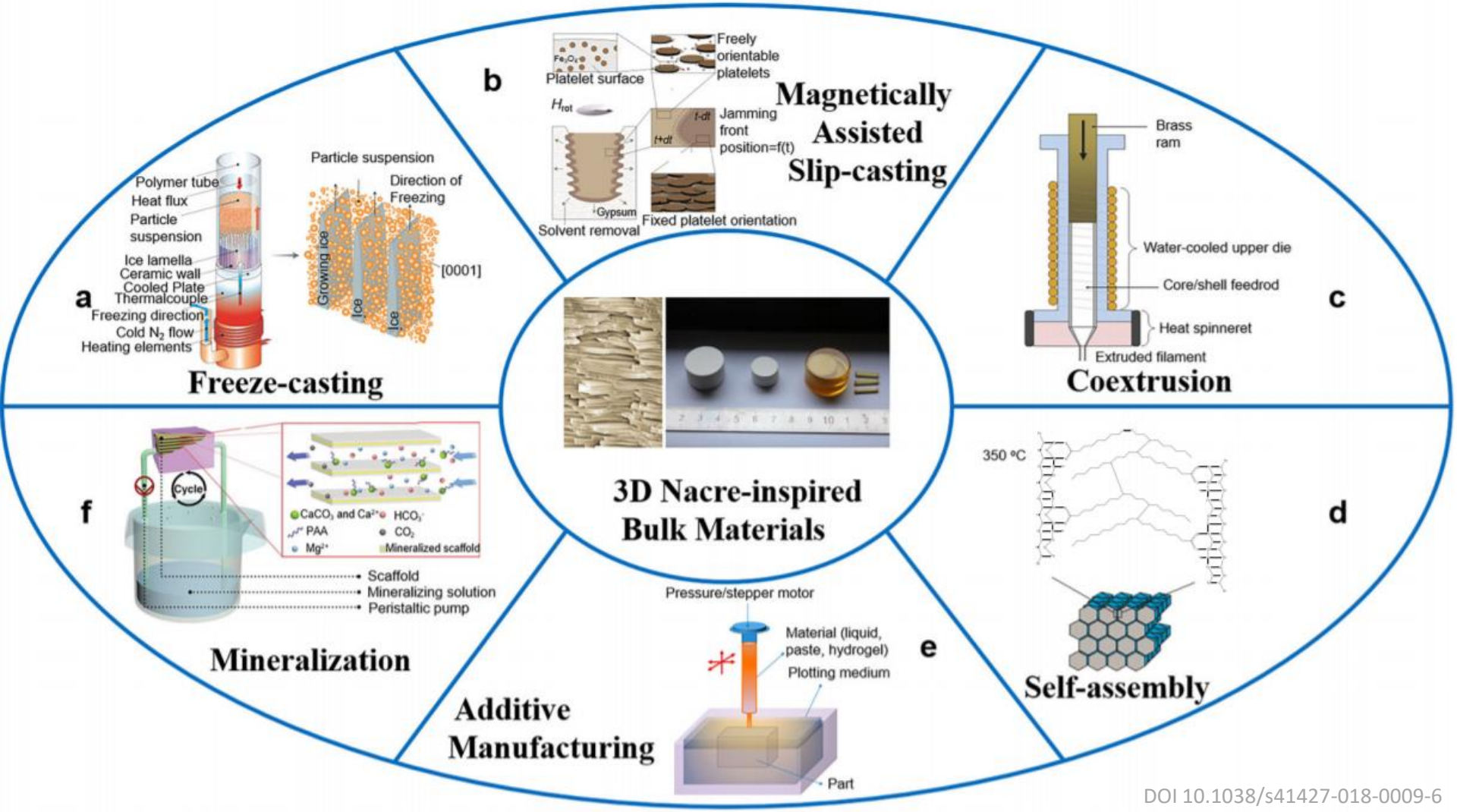

DOI 10.1038/s41427-018-0009-6

Fabrication of nacre-like materials

An example of scalable fabrication process

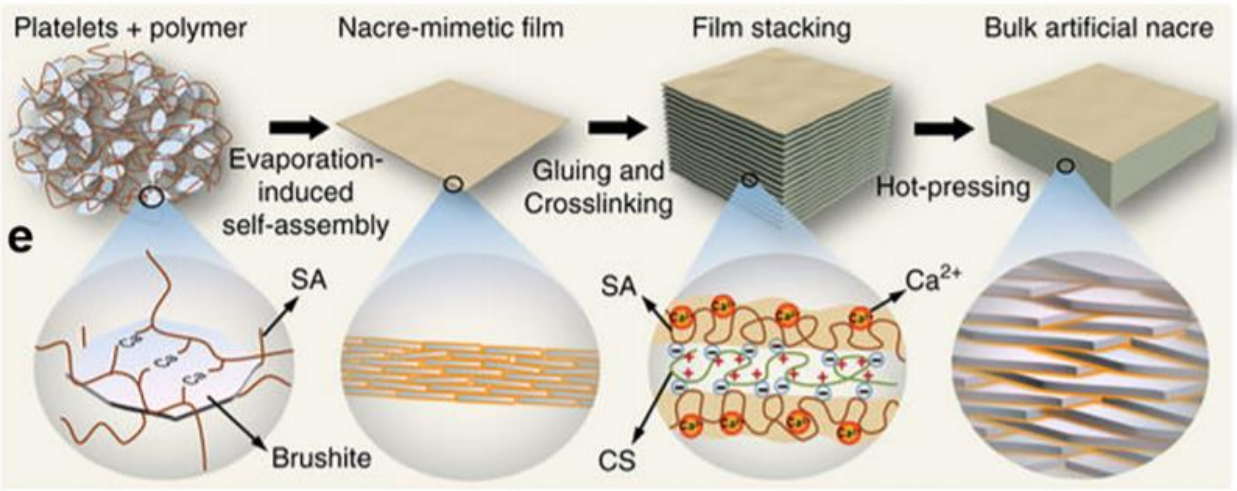

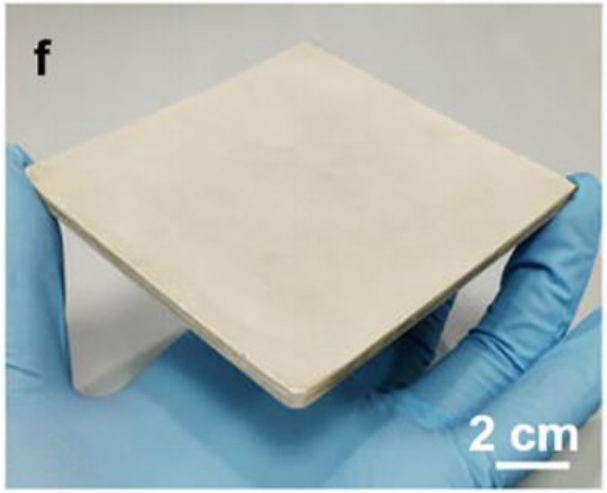

DOI 10.1038/s41427-018-0009-6

Fabrication of nacre-like materials

Freeze casting

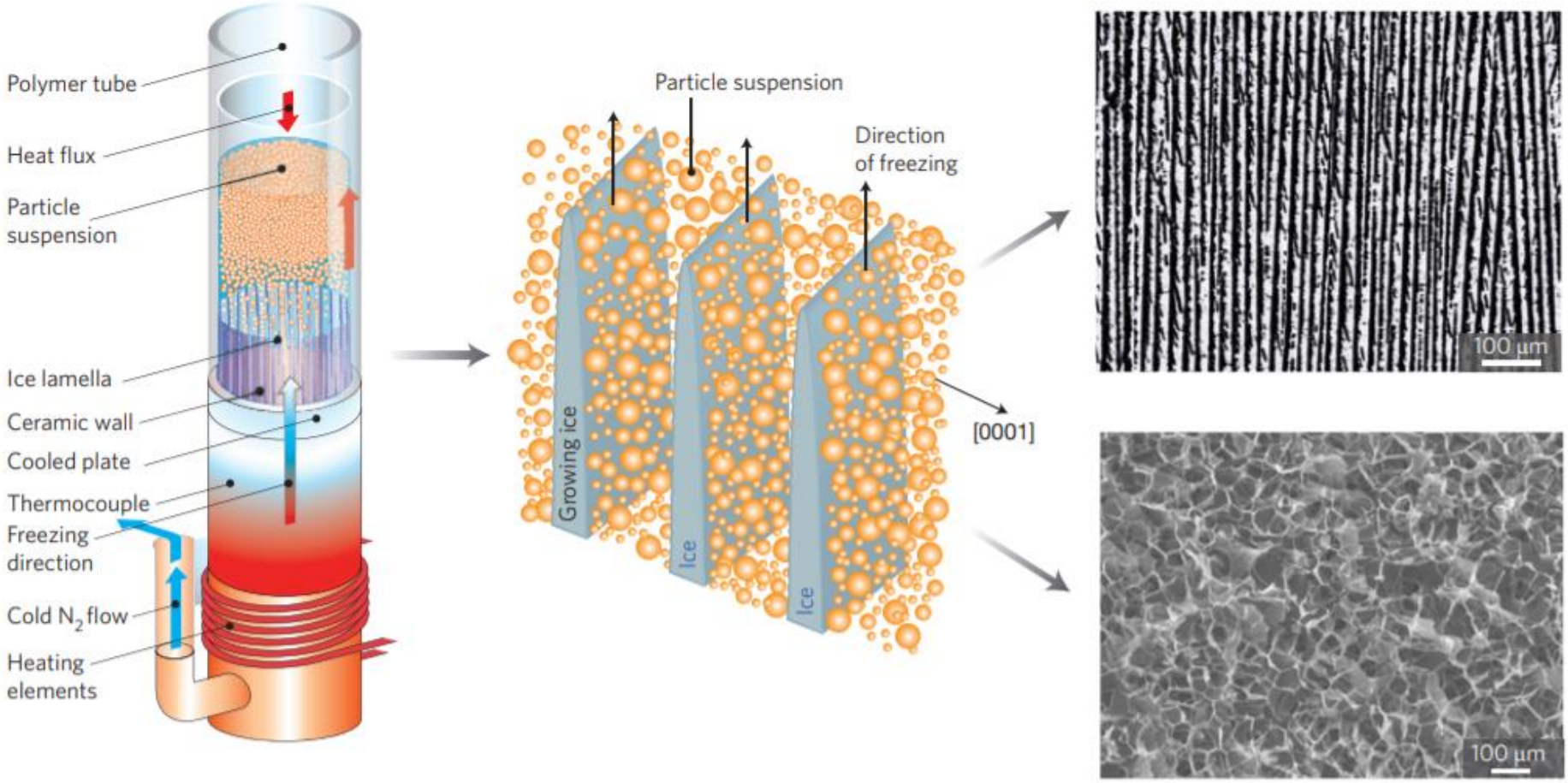

DOI: 10.1038/NMAT4089

Fabrication of complex, hybrid hierarchical structures

Additive manufacturing

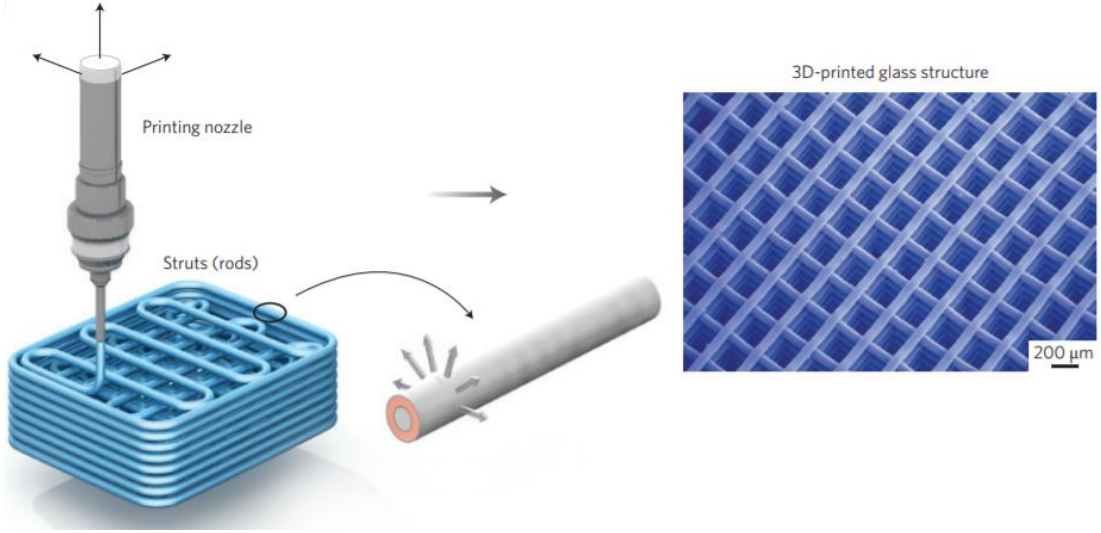

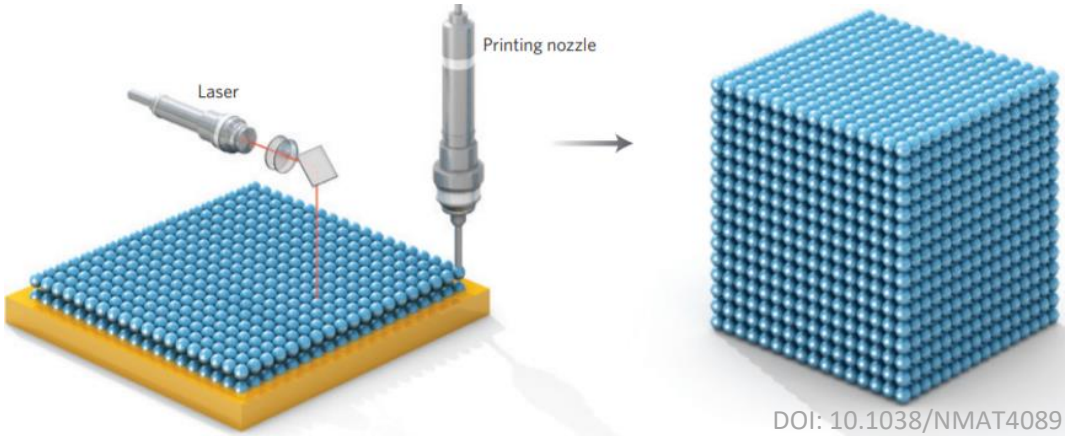

DOI: 10.1038/NMAT4089

Applications

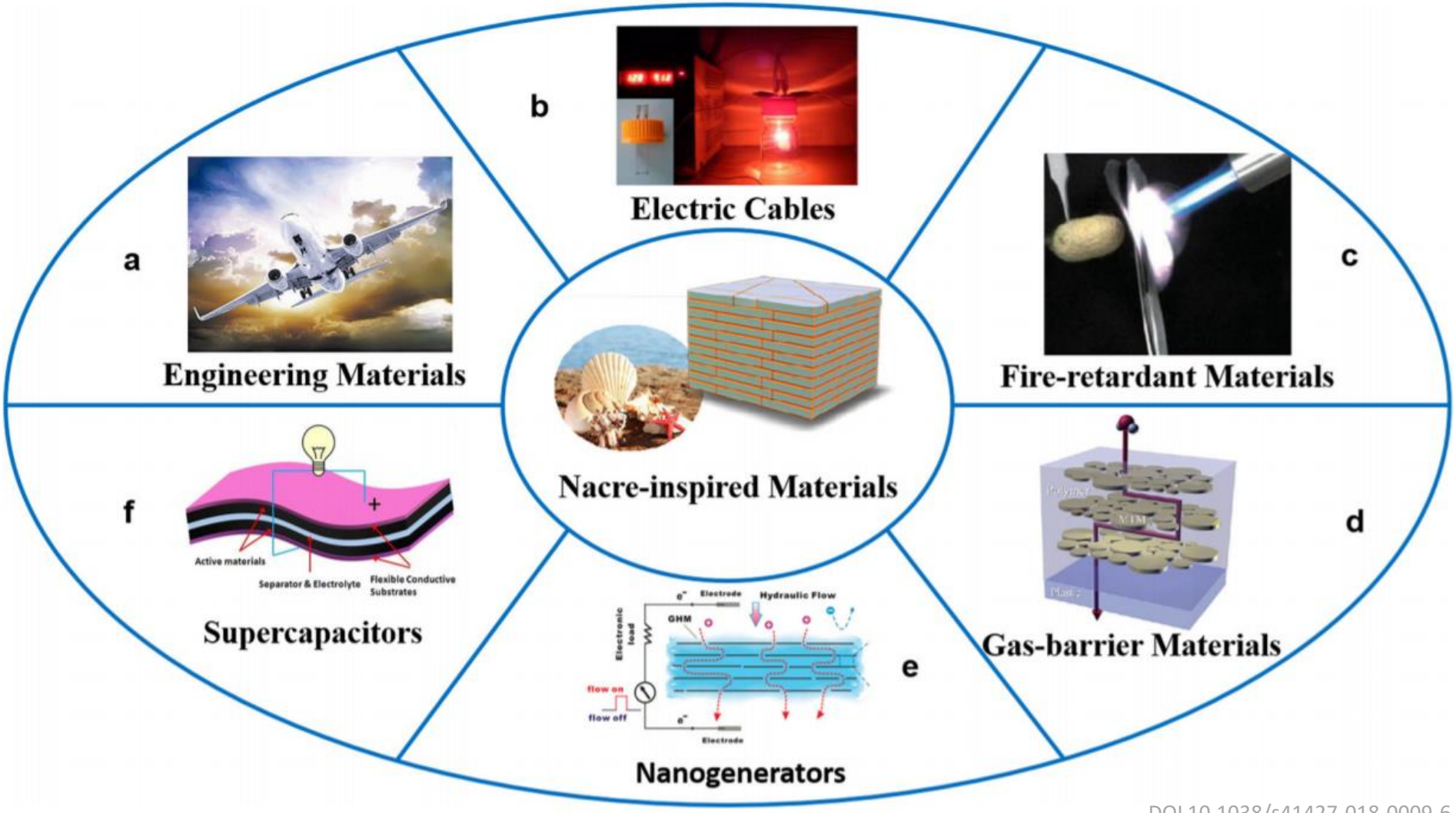

DOI 10.1038/s41427-018-0009-6

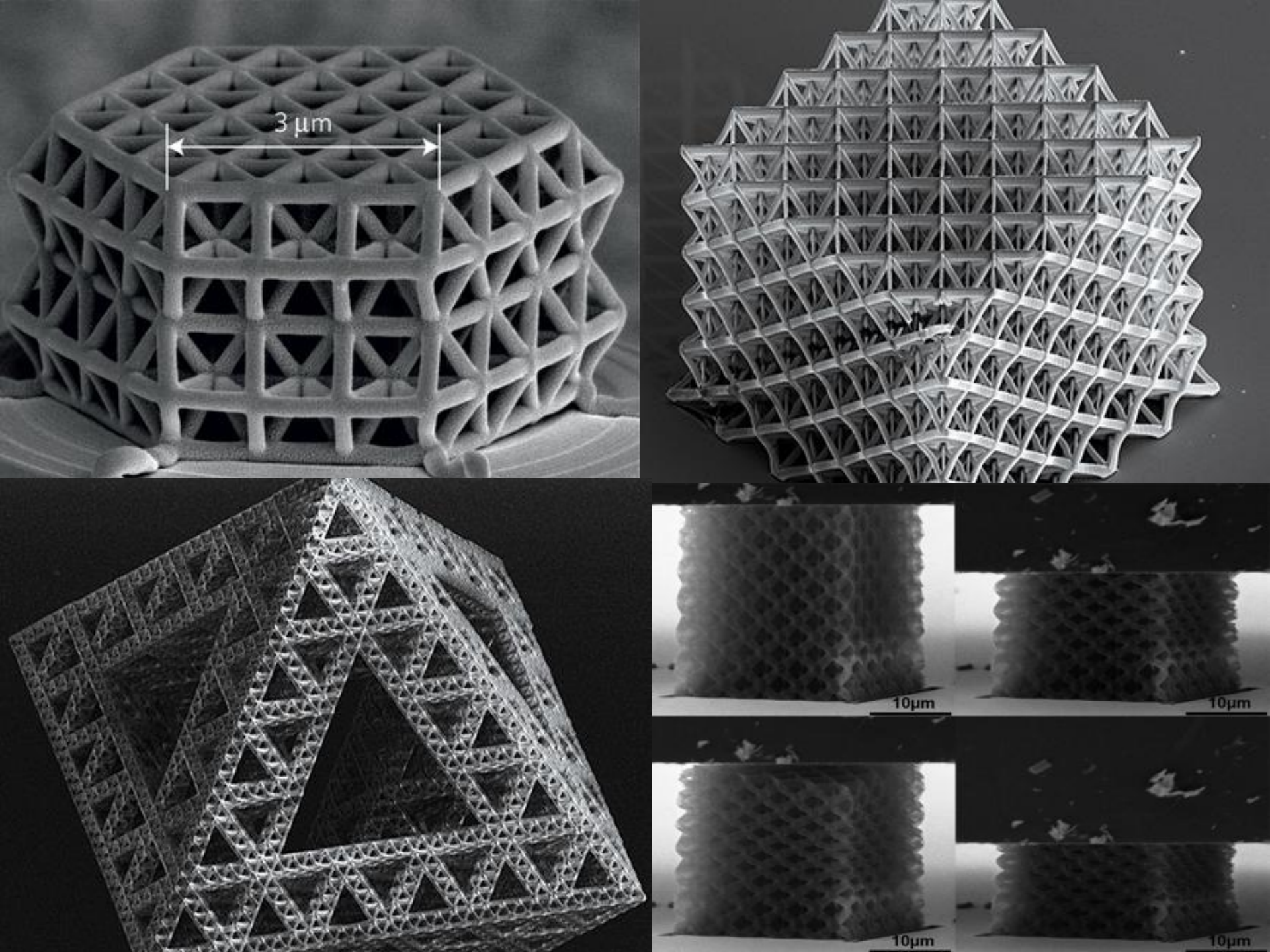
3 µm
10µm
10µm
10µm
10µm

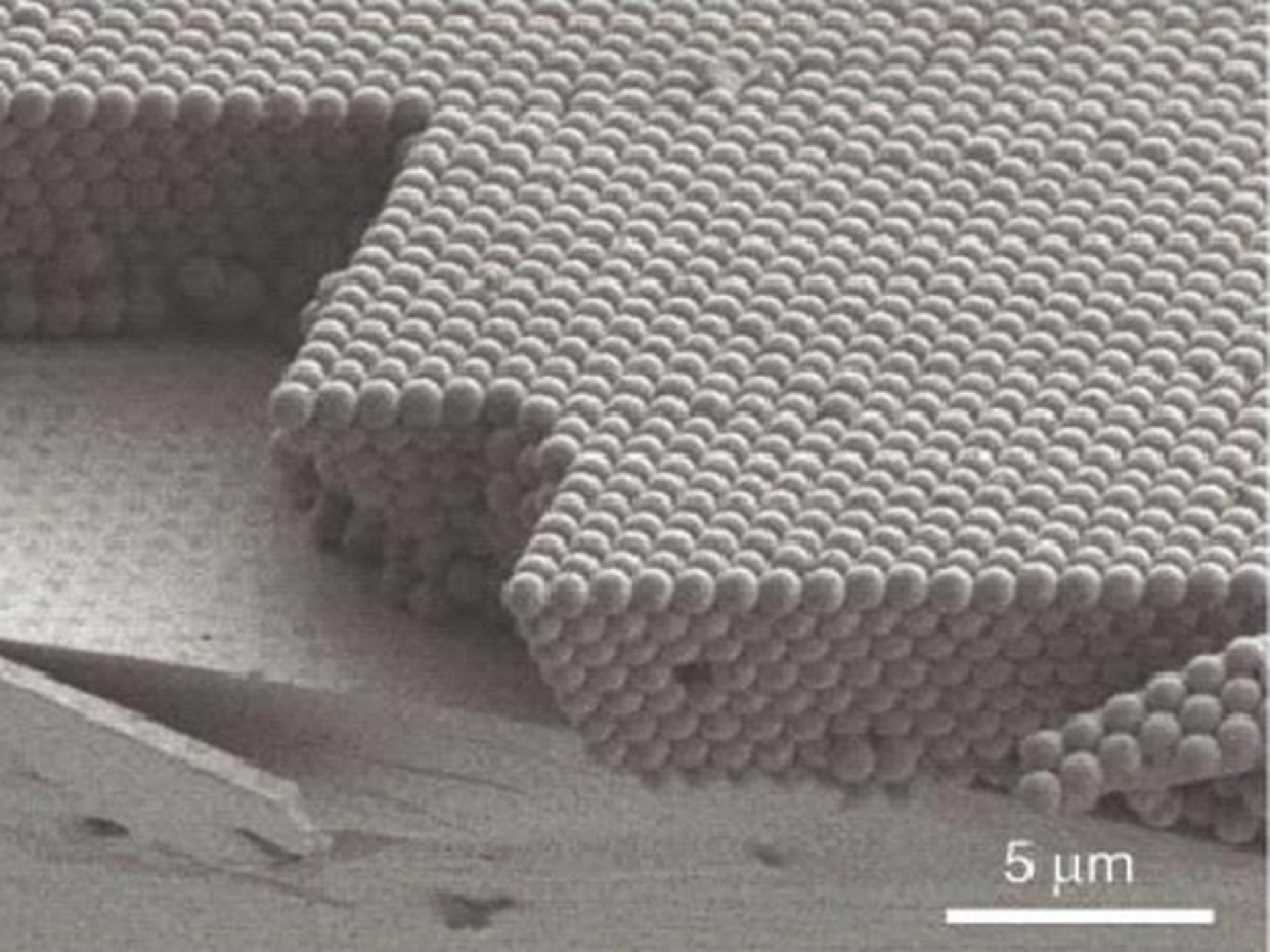
5 µm

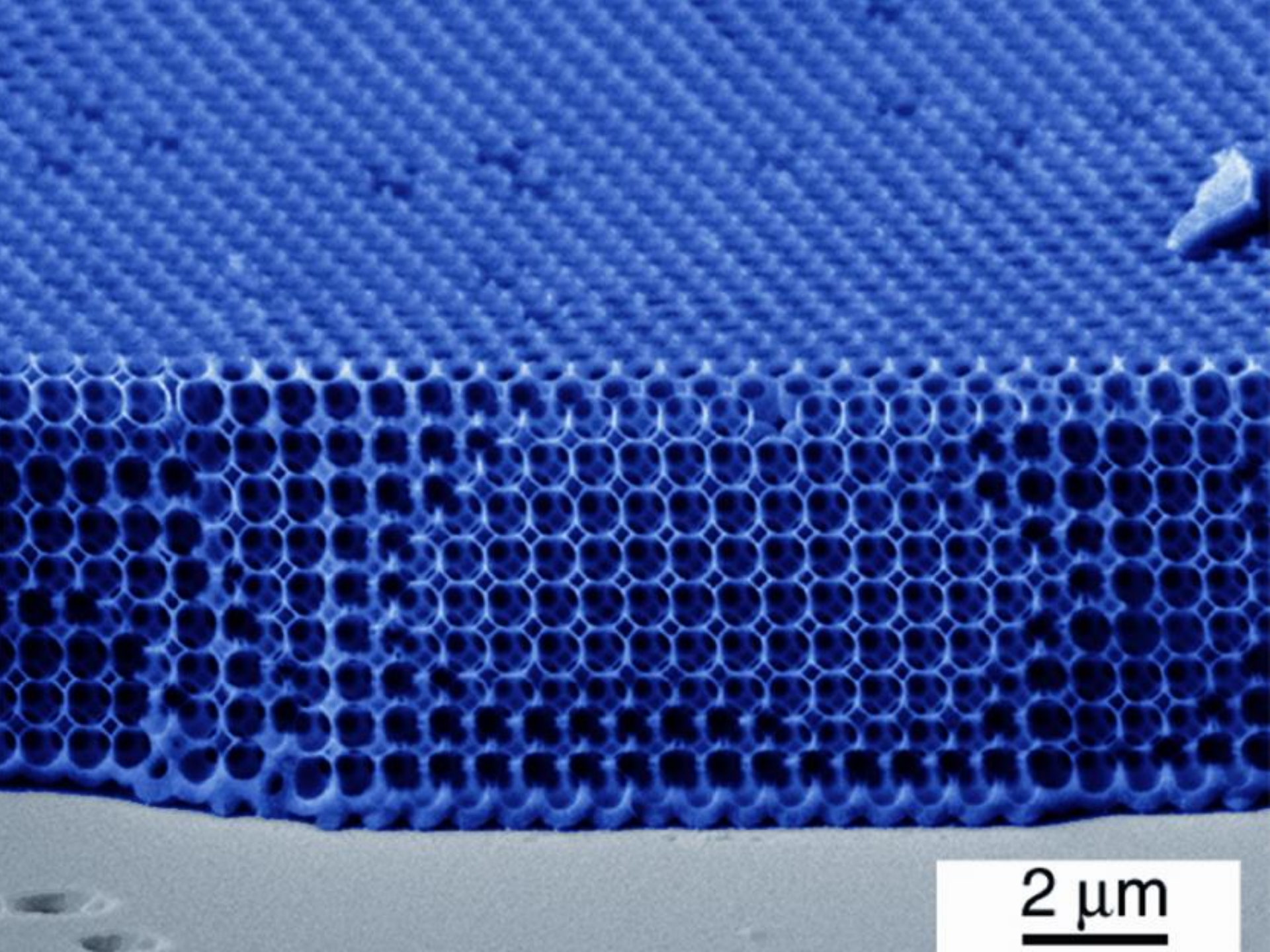
2 μm

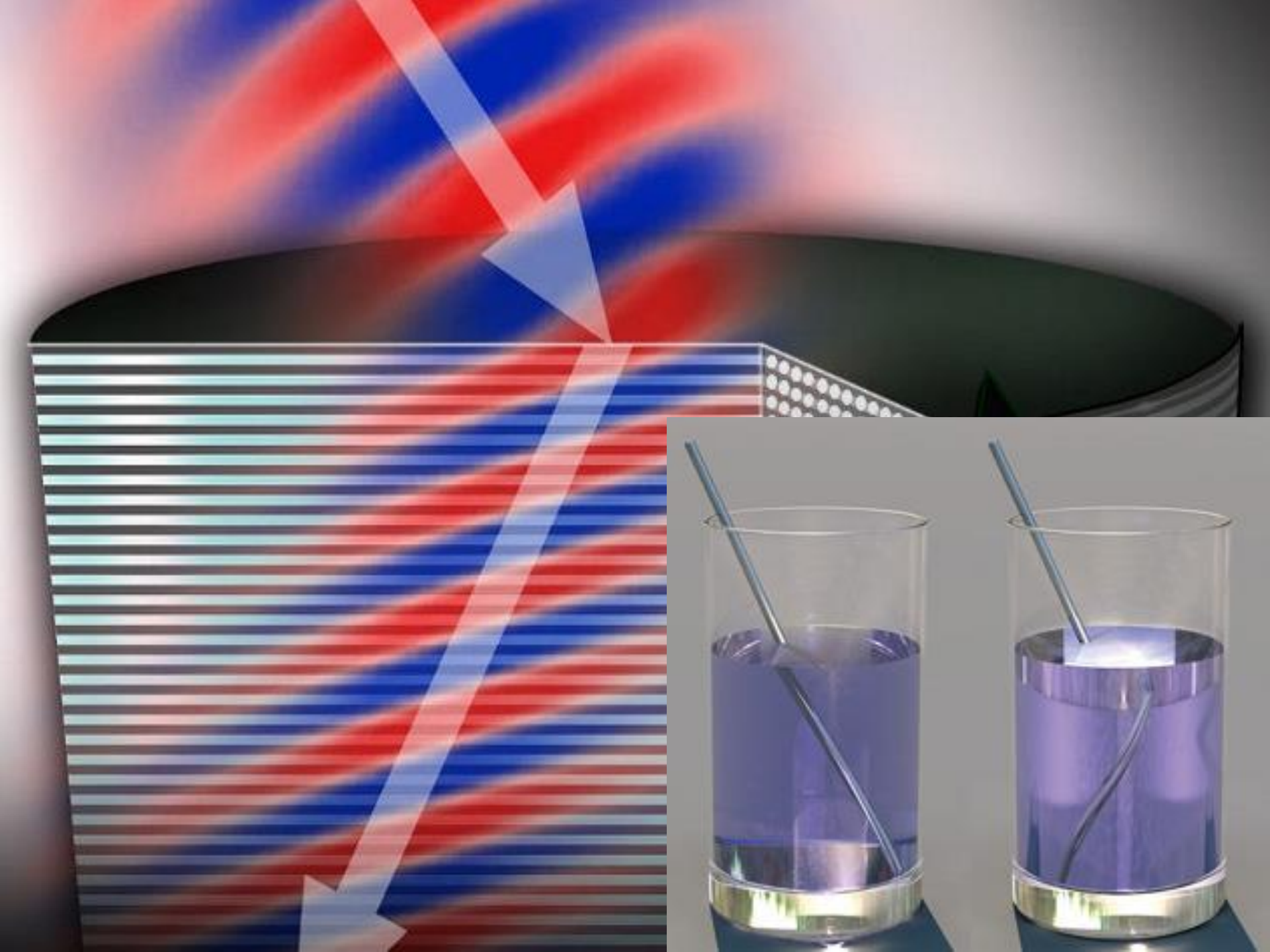

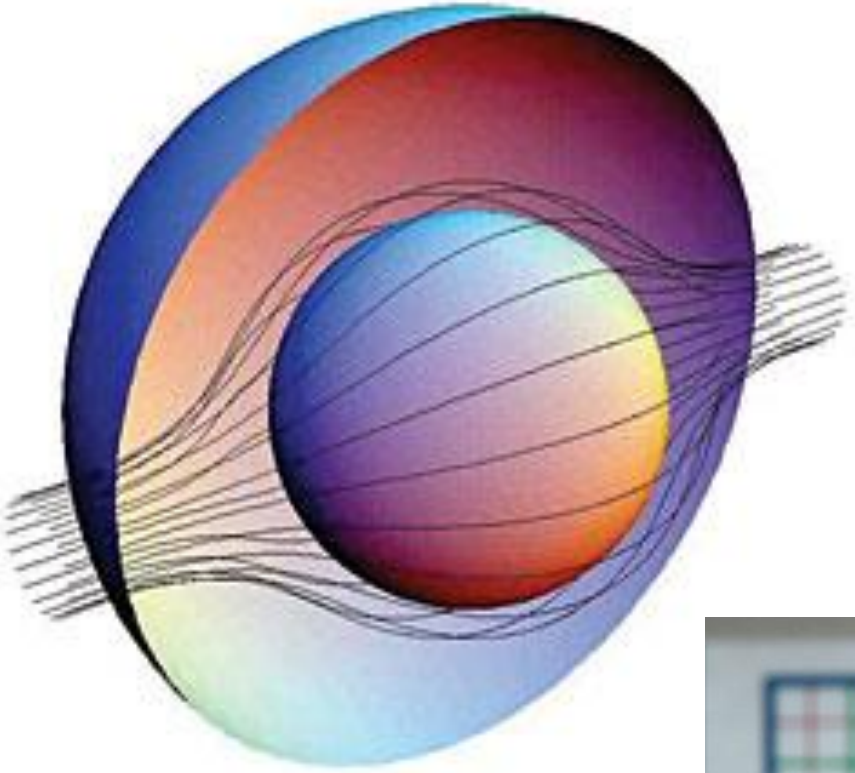

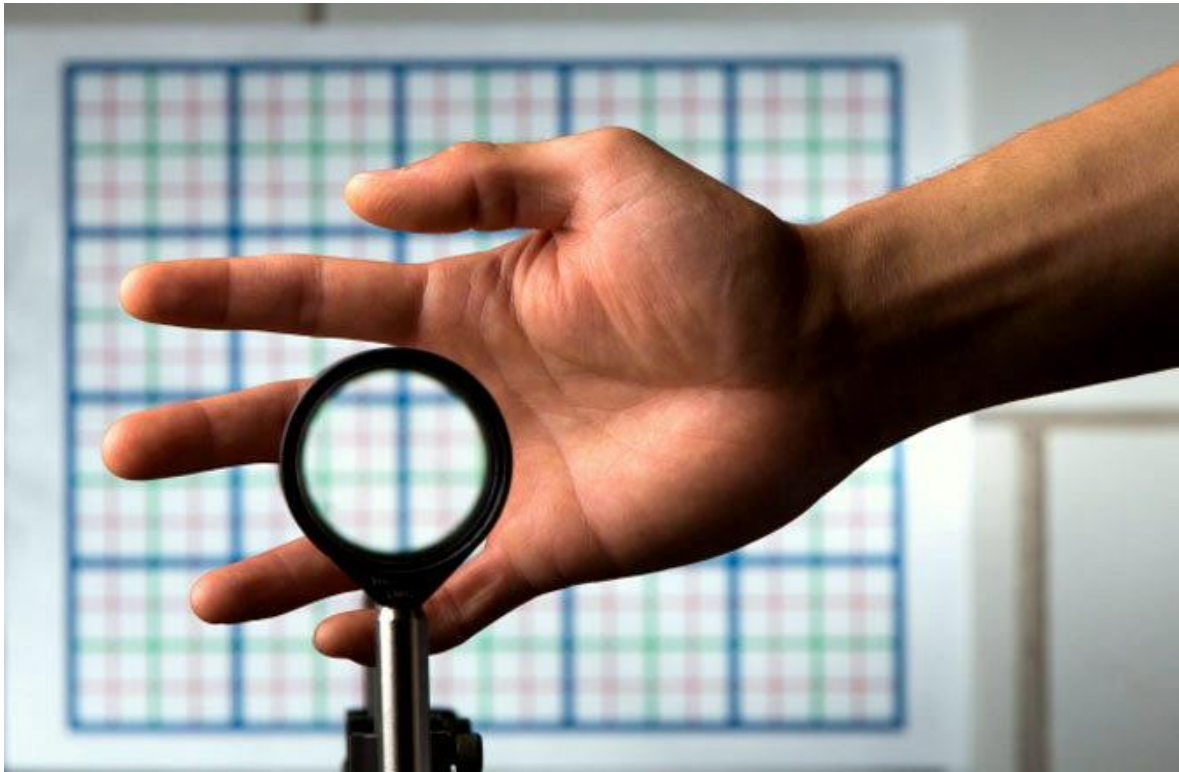

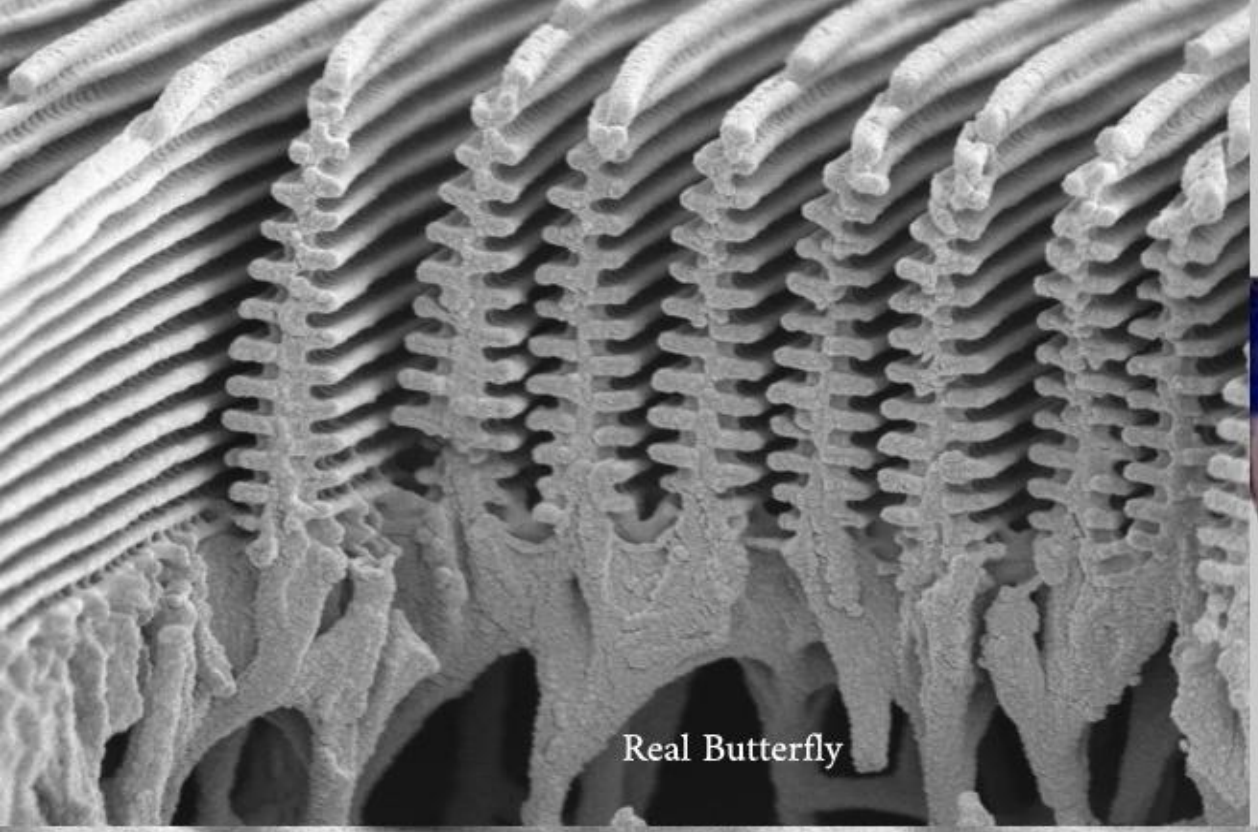

Real Butterfly

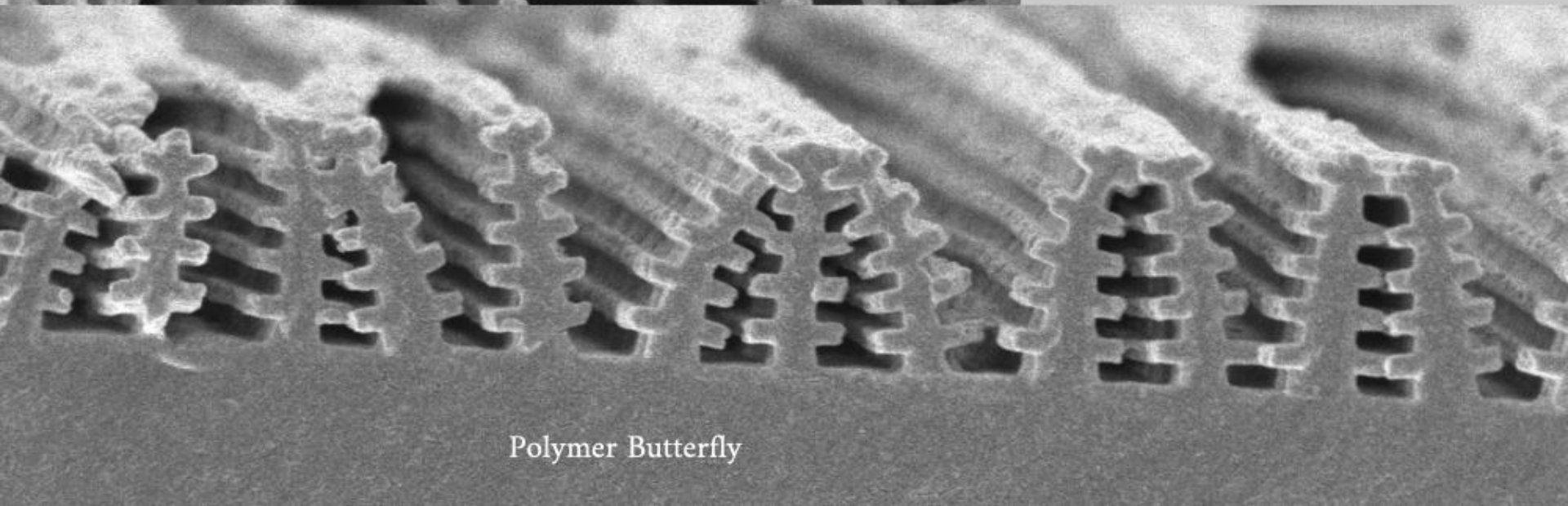

Polymer Butterfly

December 2017 Vol. 42 No. 12
www.mrs.org/bulletin

MRS Bulletin

MRS MATERIALS RESEARCH SOCIETY®
Advancing materials. Improving the quality of life.

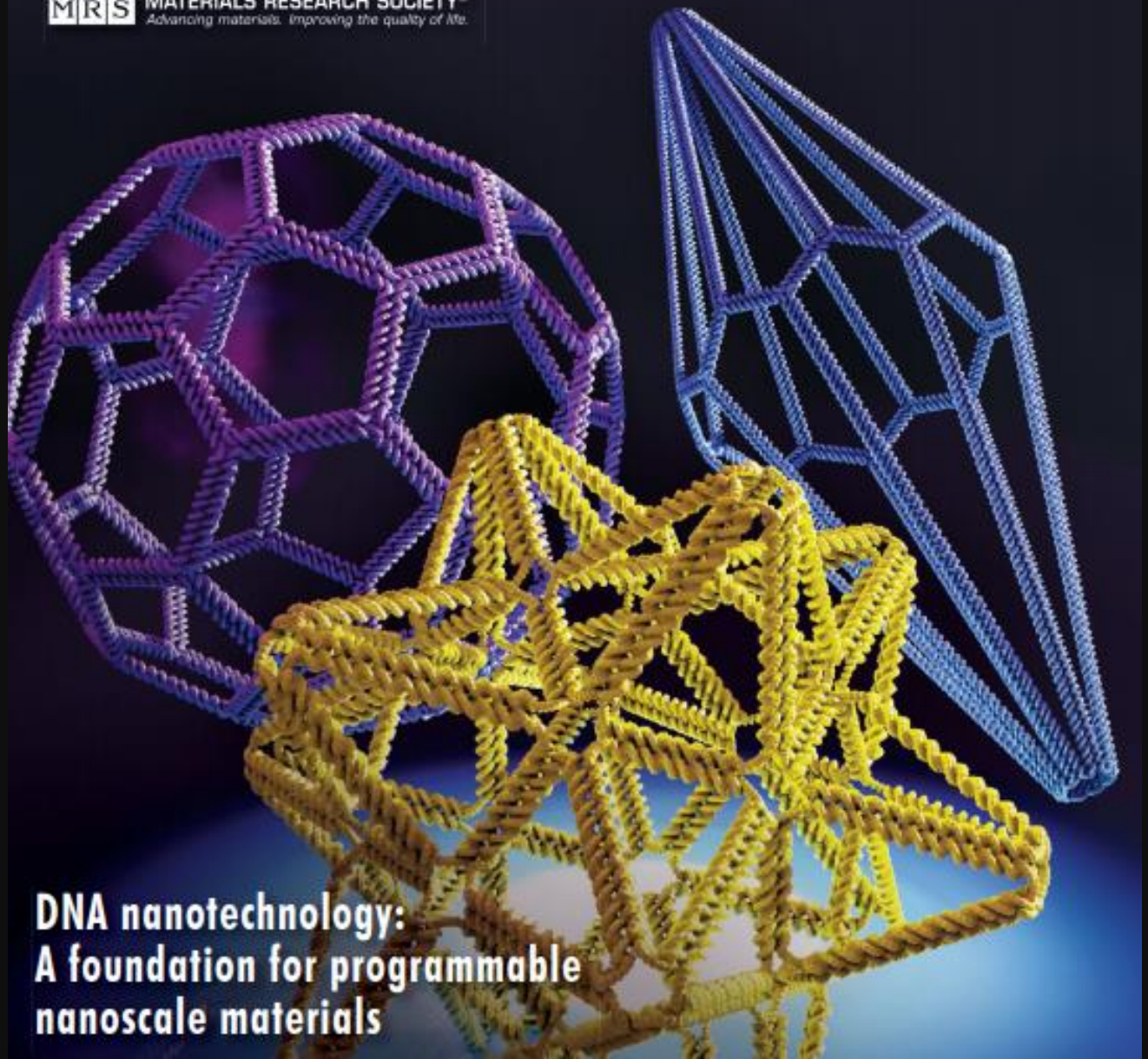

DNA nanotechnology: A foundation for programmable nanoscale materials

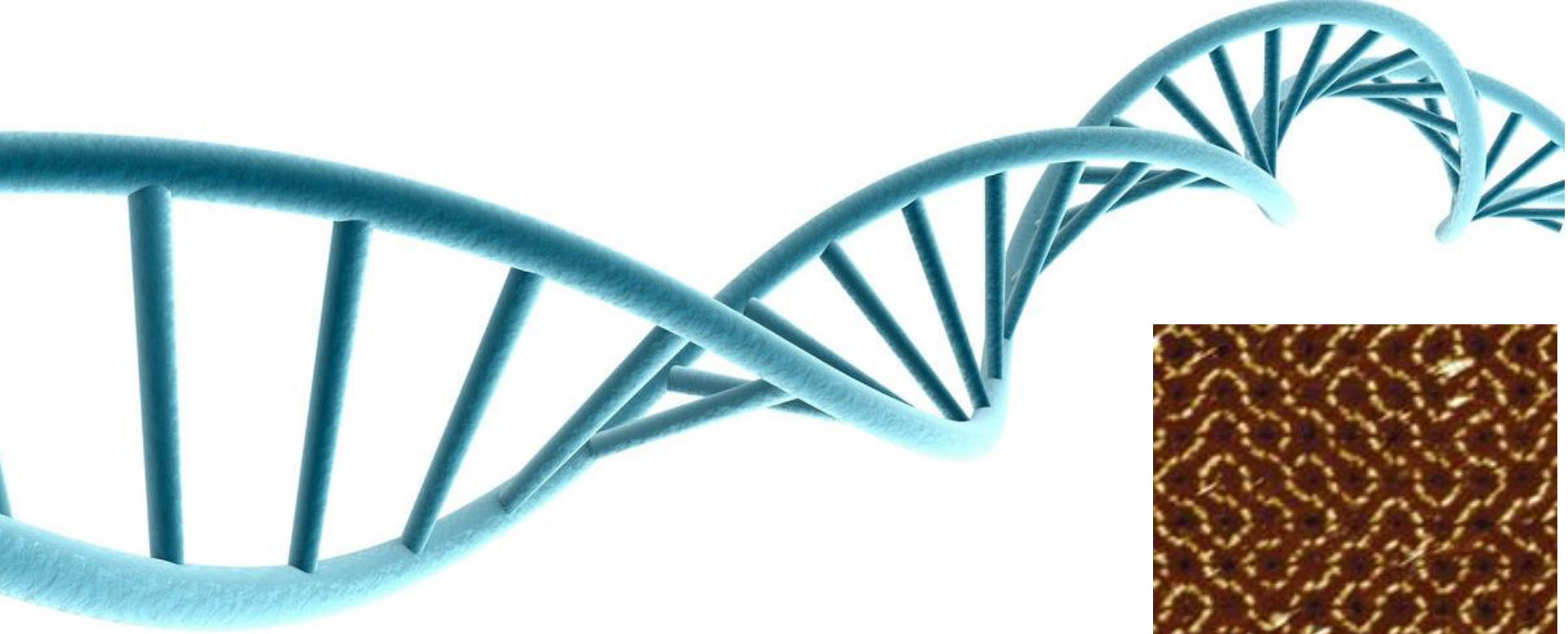

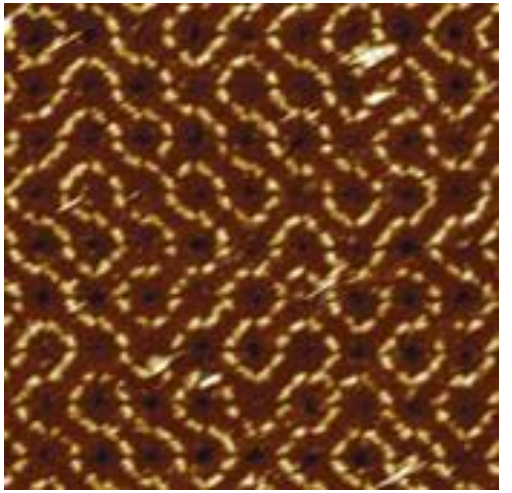

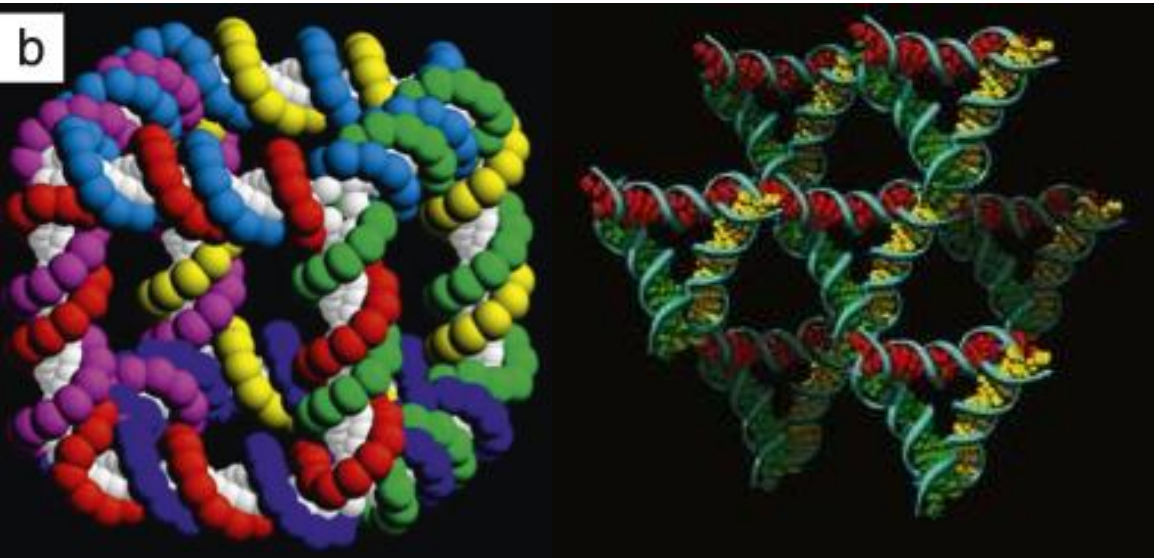
b

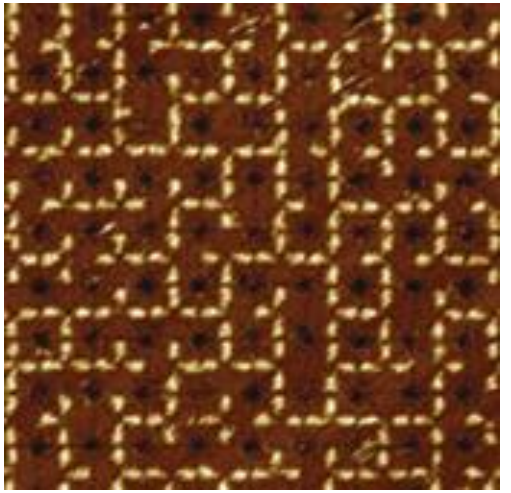

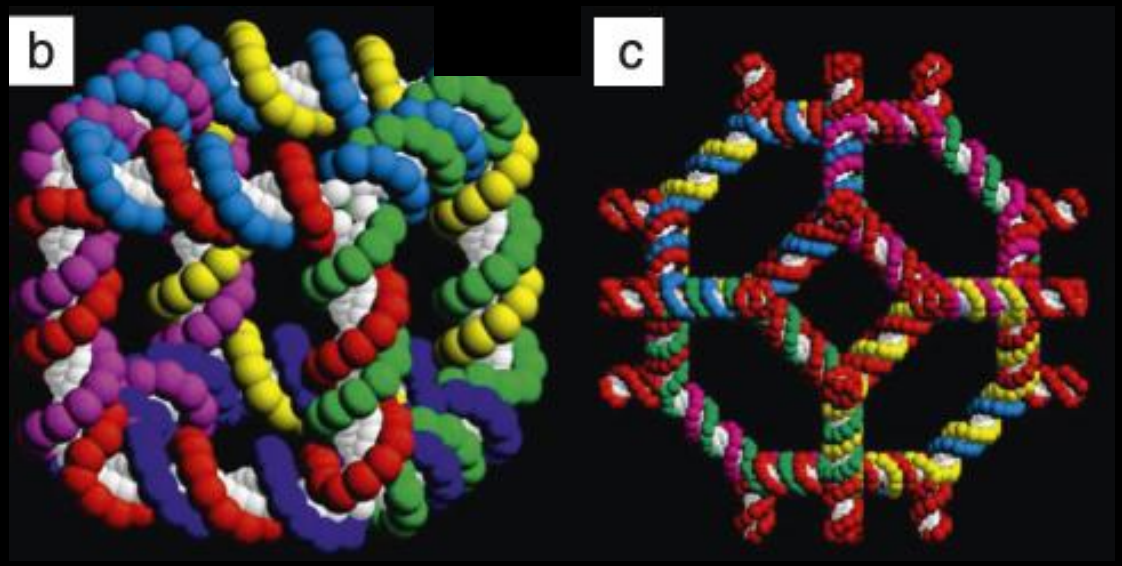

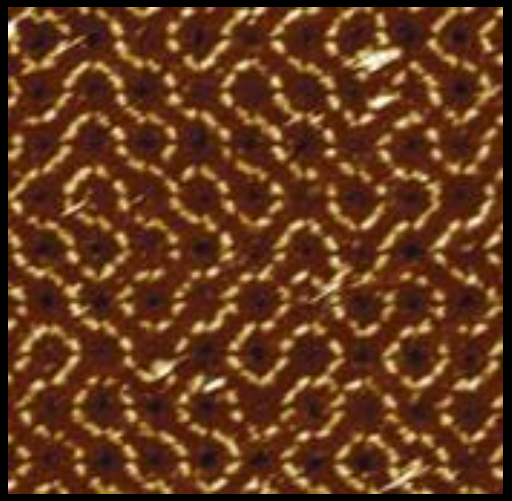

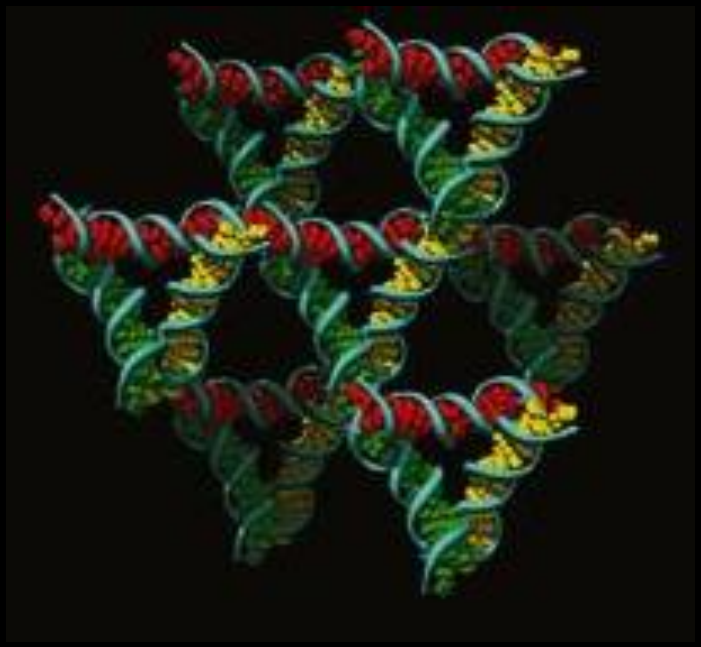

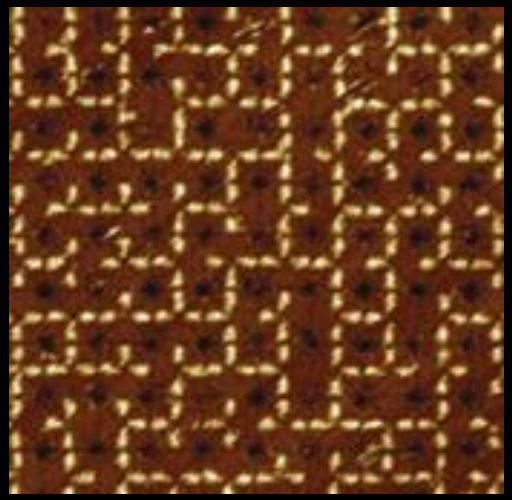

MRS Bulletin 42 (2017)